Coordination Chemistry Reviews, 121 (1992) 43–130
Elsevier Science Publishers B.V., Amsterdam

Thio-oxalates: their ligand properties and coordination chemistry

Wolfgang Dietzsch, Peter Strauch and Eberhard Hoyer
Department of Chemistry, University of Leipzig, D/O-7010 Leipzig (FRG)

(Received 20 December 1991)

CONTENTS

A. INTRODUCTION

Oxalates occurring in nature, as well as man made, belong to the classics of chemistry and especially of coordination chemistry. As early as 1868 the German

---

Correspondence to: E. Hoyer, Department of Chemistry, University of Leipzig, D/O-7010 Leipzig, FRG.

0010-8545/92/$15.00 © 1992 Elsevier Science Publishers B.V. All rights reserved.

chemist Hermann Kolbe succeeded in the condensation of two C_1 building blocks to form $C_2O_4^{2-}$ by passing CO_2 over molten sodium [1] according to the reaction

$$2Na_{liq} \xrightarrow[360°C]{CO_2} Na_2C_2O_4 \tag{1}$$

Of course, he extended the experiment also to CS_2 in an effort to get tetrathio-oxalate, but failed.

The first paper on a thio-oxalate, namely 1,2-dithio-oxalate (dto) (and diphenyl-dithio-oxalate), had already appeared in 1909, dealing with its ligand properties towards Ni(II) and also other metal ions [2]. The authors isolated a Ni(II) bis-complex as a dipotassium salt and proposed the ligand for the analytical determination of nickel, cobalt and iron (the X-ray structure of $K_2[Ni(dto)_2]$ had already been published in 1935; Ni(II) is square-planar S_4-chelated, and the corresponding Pd(II) and Pt(II) compounds are isomorphous [3]).

Oxalate and its thio-homologues, as compounds with a C_2 backbone, belong principally to organic chemistry and are thus included in comprehensive works such as Beilstein (*Handbook of Organic Chemistry*) or Houben-Weyl (*Methoden der Organischen Chemie*). The Gmelin (*Handbook of Inorganic Chemistry*), however, also records oxalate and its coordination chemistry but not thio-oxalates. Lacking a single hydrogen atom directly connected to carbon, all thio-oxalates are strictly speaking inorganic as well. In this review we exclude most of the organic chemistry aspects of thio-oxalates, unless they are of key importance for synthesis or for structure and ligand properties in connection with coordination compounds. We direct the reader's attention to two reviews in which most of organic chemistry of thio-oxalate derivatives is summarized [4,5].

This review is divided into three main parts. After an overview on the topology and synthesis of thio-oxalates and the structures of the isolated alkali and onium salts (Sect. B), facts on the modes of ligation follow as Sect. C. Section D is devoted to the five individual thio-oxalates, and contains most knowledge up to the beginning of 1991. Papers on thio-oxalates which are mainly physically oriented are also included here, e.g. spectroscopy of all kinds and wavelengths, magnetic behaviour, electrical conductivity in the solid state, crystal chemistry, and kinetics of ligand substitution. As well as the references, a second bibliography is arranged by metal (heterobimetallic chelates are indexed twice; see Tables 4, 6 and 7).

B. TOPOLOGY, SYNTHESES AND STRUCTURES OF NON-COORDINATED THIO-OXALATES

Oxalate and its sulphur analogues are the smallest (composed of only six atoms) four-ligator atom ligands which provide possibilities for both low-strained five-membered (side-on) or four-membered (end-on) chelate rings for purely topological reasons. The possible alternatives (bridging or non-bridging) are obvious. The number of possible coordination modes is dependent on the number of sulphur atoms introduced instead of oxygen. In addition, further variation is introduced by the different torsion angles of the two carboxylate halves of the ligands (between 0° and 90° for mto, *i*-dto, trto and tto or between 0° and 180° for dto). The principal topologies of the five thio-oxalate dianions are depicted in Fig. 1 together with the common nomenclature and abbreviations used.

There are X-ray crystal and molecular structure analyses from all but one of the dianionic representatives isolated as alkali or "onium" salts; three monomethylated monoanions and diseleno-oxalate are incorporated in Table 1. The data are self-explanatory.

The C–C bond length has the expected value for carbon–carbon single bonds with an apparently slight multiple bond contribution related more or less systematically to the number of sulphur atoms in the thio-oxalate dianion. The series oxalate→1,2-dithio-oxalate→tetrathio-oxalate shows a stepwise shortening of the C–C bond length: 1.574→1.516→1.461 Å.

As in oxalates, the dihedral distortion of the molecule along the C–C bond in ionic thio-oxalates is obviously connected with packing effects, although values near 90° are favoured, thereby minimizing the charge repulsion, maximizing electron delocalization and, in a way, "non-bond" sulphur–sulphur interaction.

Unfortunately, the precision of determination of the carbon–chalcogen bond lengths (C–Y) is normally not sufficient for answering the question whether there are two different C–Y bonds in a CY_2 moiety (as found for free oxalic acid dihydrate [14] with symmetric H-bridges;) i.e. different "carbonyl" C=O and "hydroxy" C–O bond lengths.

With the exception of tetrathio-oxalate, the syntheses of the different thio-

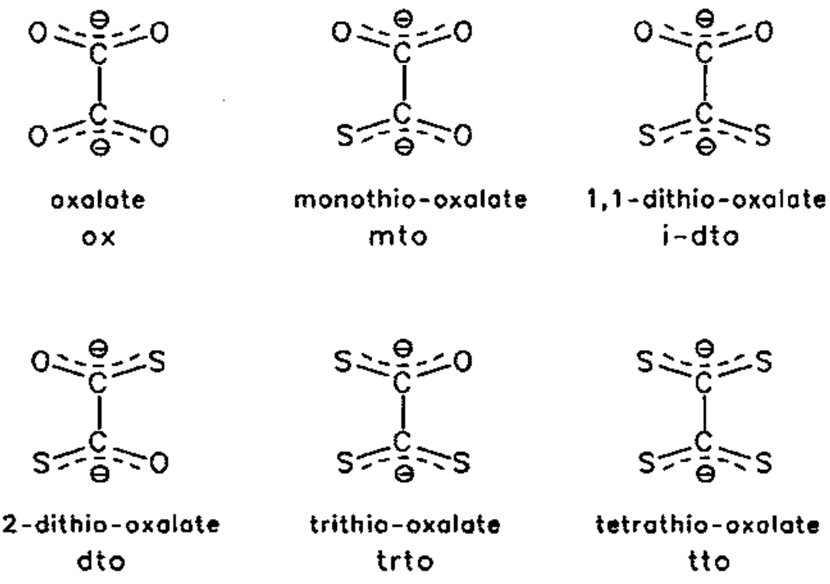

oxalate
ox

monothio-oxalate
mto

1,1-dithio-oxalate
i-dto

1,2-dithio-oxalate
dto

trithio-oxalate
trto

tetrathio-oxalate
tto

Fig. 1. Topology of thio-oxalates (also oxalate) and abbreviations used.

TABLE 1

Structural data of oxalate, thio-oxalates and seleno-oxalates

Compound	C—C (Å)	Torsion angle about C—C (°)	Ref.
$K_2[O_2C{-}CO_2]\cdot H_2O$[a]	1.574(2)	0	6
$Cs_2[S_2C{-}CO_2]\cdot CsCl\cdot H_2O$	1.50(2)	90	7
$K_2[SOC{-}COS]$	1.516(3)	103.5[b]	8
$K_2[S_2C{-}COS]\cdot KCl$[c]	1.52(3)	85.7	9
	1.51(3)	89.7	
$(Ph_4P)_2[S_2C{-}CS_2]\cdot 6H_2O$	1.461(19)	79.5(1.0)	10
$K[O_2C{-}COOCH_3]$	1.546(6)	1.2	11
$K[O_2C{-}COSCH_3]$	1.572(6)	12.5	11
$K[SOC{-}COSCH_3]$	1.562(9)	9.9[b]	12
$K_2[SeOC{-}COSe]$	1.59(2)	*trans*-planar	13

[a] "Trans-planar"; hydrogen bonds to only two oxygens of $C_2O_4^{2-}$.

[b] Referred to a planar *cis*-configuration.

[c] Two independent $C_2S_3O^{2-}$ anions are present.

oxalates (and diseleno-oxalate) are standard organic chemistry work starting with synthons in which the C_2 backbone is already present and ready for nucleophilic attack by HS^- or $S(e)^{2-}$ (as alkali salts), namely oxalic acid diethyl ester for monothio-oxalate, trichloroacetic acid for 1,1-dithio-oxalate, oxalyl chloride (via dialkyl- or diphenyl-dithio-oxalic acid ester) for 1,2-dithio-oxalate (diphenyl oxalic ester for diseleno-oxalate) and trichloroacetic acid phenyl ester for trithio-oxalate. The long-sought tetrathio-oxalate can be made by reductive electrodimerization of carbon disulphide in acetonitrile in the presence of a supporting electrolyte with a cation which precipitates the tetrathio-oxalate, thus preventing follow-up reactions. Table 2 summarizes all preparative opportunities.

TABLE 2

Synthetic ways to thio-oxalate dianions

Isolated compound	Starting compound	S-Nucleophile	Ref.
$K_2[SOC{-}CO_2]\cdot H_2O$	$HOOC{-}COOC_6H_5$	KHS	15
	$H_5C_2OOC{-}COOC_2H_5$	KHS	16
$K_2[S_2C{-}CO_2]$	$Cl_3C{-}COOH$	K_2S	15
$K_2[SOC{-}COS]$	$ClOC{-}COCl$ (via $RSOC{-}COSR$)	KHS	2,17
$K_2[S_2C{-}COS]$	$Cl_3C{-}COOC_6H_5$	KHS	15
$K_2[S_2C{-}COS]\cdot KCl\cdot H_2O$		K_2S/KHS	9
$A_2[S_2C{-}CS_2]$[a]	CS_2 electroreduction		10,18
$K_2[SeOC{-}COSe]$	$H_5C_6OOC{-}COOC_6H_5$	K_2Se	13

[a] A = K, Me_4N, Et_4N.

C. MODES OF LIGATION IN THIO-OXALATE COMPLEXES

For purely topological reasons the modes of coordination shown in Fig. 2 have to be taken into consideration.

Taking into account the chalcogeno atom make-up of the ligands, the variation in number and geometry is remarkably large. It turns out, however, that side-on coordination is preferred no matter whether the chalcogen is oxygen or sulphur. The only authentic example of an end-on coordination was reported recently in $[(Ph_3P)_2Ag(trto)Ag(PPh_3)_2]$, where trithio-oxalate links a side-on bound silver ion with an end-on bound silver ion [19(c)]. The end-on coordination of oxalate to Co^{2+} (also end-on bridging oxalate between two Co^{2+}) within the cavity of the macrocyclic ligand 1,4,10,13,16,22-hexaaza-7,19-dioxacyclotetracosane, proposed by Martell and Motekaitis recently [20], has not been confirmed up to now by X-ray structure analysis. Further apparent exceptions belong either to "ethenetetrachalcogenolates" ($[Fe_4(CO)_{12}(C_2S_4)]$, see below) or oxalates where four metal atoms are bound by just one bridging ligand ($Cs_6[Mo_4O_6S_2(C_2O_4)_5]\cdot H_2O$ [21]; $K_6[Mo_4O_6S_2(C_2O_4)_5]\cdot 10H_2O$ [22]). It should be added, however, that an end-on mode is found with oxalate in two binuclear complexes containing tin(IV) or VO(II), but it turns out that the "carboxylate" side is only monodentate in both these cases [23,24] (see Fig. 3).

The same coordination type was found for bridging dto in a binuclear manga-

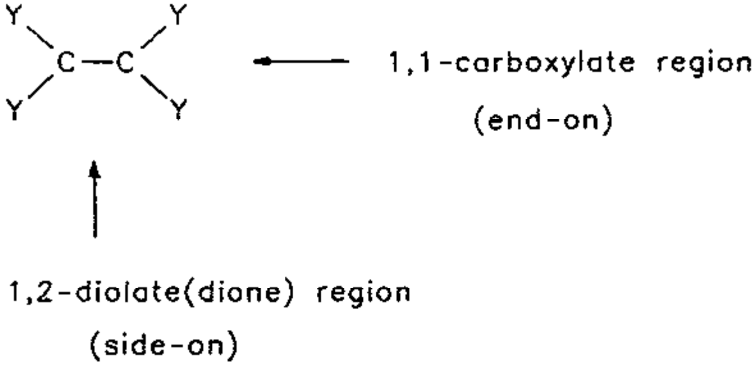

Fig. 2. Principal ligating functions of thio-oxalates.

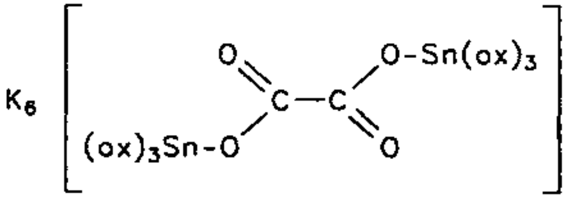

Fig. 3. Monodentate oxalate bridging $[Sn(ox)_3]^{2-}$ units [23].

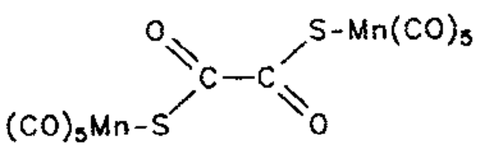

Fig. 4. Monodentate 1,2-dithio-oxalate bridging $[Mn(CO)_5]^+$ units [25].

nese(I) compound [25] (see Fig. 4) and is postulated also for $Cs_4[Re_2(dto)_3(CO)_6]$ [26].

For stoichiometric reasons of charge, mononuclear chelates are anionic. In these cases the choice of the donor atom set is governed by "hard/soft" relationships between metal ion and ligator. This holds also for the linking of two different metal ions by (side-on bound) thio-oxalates. In addition, because the bridging ligand 1,2-dithio-oxalate is usually planar, linkage isomers can be observed [27]. Some possible cases of ligation are depicted for dto in Fig. 5. Besides X-ray evidence there are other spectroscopic means from which the coordination mode can be concluded, mainly infrared data. A representative IR treatment is given by Coucouvanis and his group in [16] for mto and in [27–29] for dto on the basis of normal coordinate analyses carried out by Nakamoto and co-workers, who also published Raman and resonance Raman spectra of dto complexes [30,31] (see also Sect. D.(iii)(e)).

Ligand "flipping" from *S,S*-chelation to *O,O*-chelation is observed with dto in $K_3[Fe(S_2C_2O_2)_3]$ (dissolved in CH_2Cl_2) during the reaction of the latter with $[Ag(PPh_3)_2]^+$ (see Fig. 6). The C—O stretching frequency drops from 1561 cm^{-1} in the starting material to 1380 cm^{-1} in the resulting bimetallic tetranuclear chelate $\{Fe[(O_2C_2S_2)Ag(PPh_3)_2]_3\}$ [27]; for an X-ray structure of this compound, see [32].

A similar change in only one of three ligands of the compound $K_2[Sn(S_2C_2O_2)_3]$ (C—O stretching frequency 1598 cm^{-1} [29]) was found after reaction with $[Cu(PTol_3)_2]^+$ (Tol = tolyl, C_7H_7) giving $K\{(dto)_2Sn[(O_2C_2S_2)Cu(PTol_3)_2]\}\cdot(acetone)_2$(C—O stretching frequencies 1627 and 1371 cm^{-1}; for X-ray structure see [33]); see Fig. 7.

In some cases also, changes in coordination modes of mto [16] or dto [27] in solution can be followed by IR spectrometry: the complexes $\{Cr[(S_2C_2O_2)M(PPh_3)_2]_3\}$ (M = Cu(I) or Ag(I)), for instance, slowly undergo a kinetically controlled linkage isomerization in CH_2Cl_2 yielding $\{Cr[(O_2C_2S_2)M(PPh_3)_2]_3\}$ via $\{Cr[(SOC_2SO)M(PPh_3)_2]_3\}$, as shown in Fig. 8.

D. SYSTEMATICS OF THIO-OXALATE COMPLEXES

In the following section, all reported thio-oxalate complexes (mostly chelates) up to the beginning of 1991 are collected under the heading of the individual thio-oxalates. After discussion of interesting properties, the complexes are grouped roughly following the Periodic Table, starting with the representative elements.

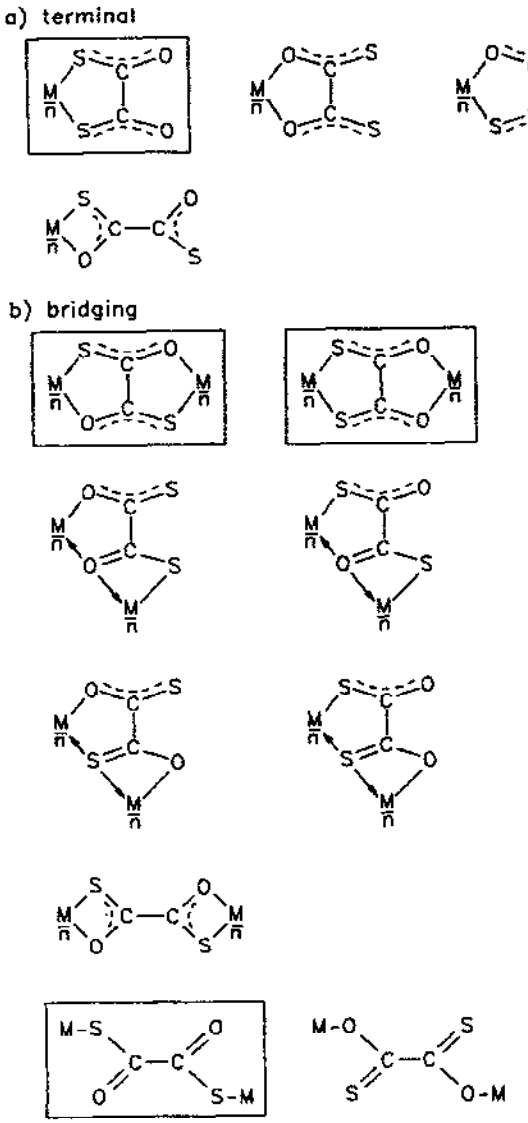

Fig. 5. Some ligation possibilities depicted for dto (outlined cases have been confirmed by X-ray structures).

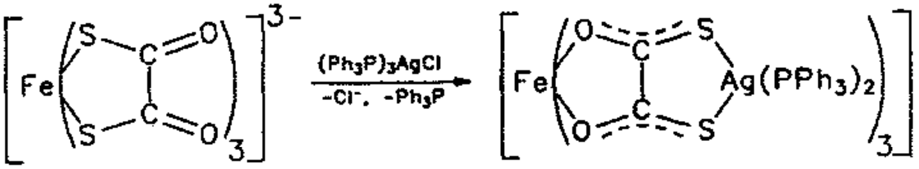

Fig. 6. Ligand "flipping" from *S,S*- to *O,O*-chelation [27].

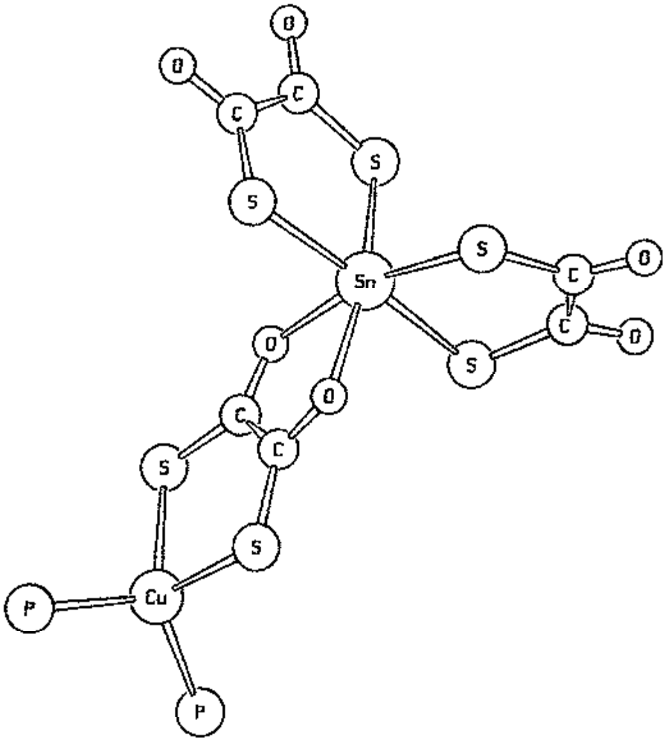

Fig. 7. Structure of the anion in K{(dto)$_2$Sn[(O$_2$C$_2$S$_2$)Cu(PTol$_3$)$_2$]}·(acetone)$_2$[33].

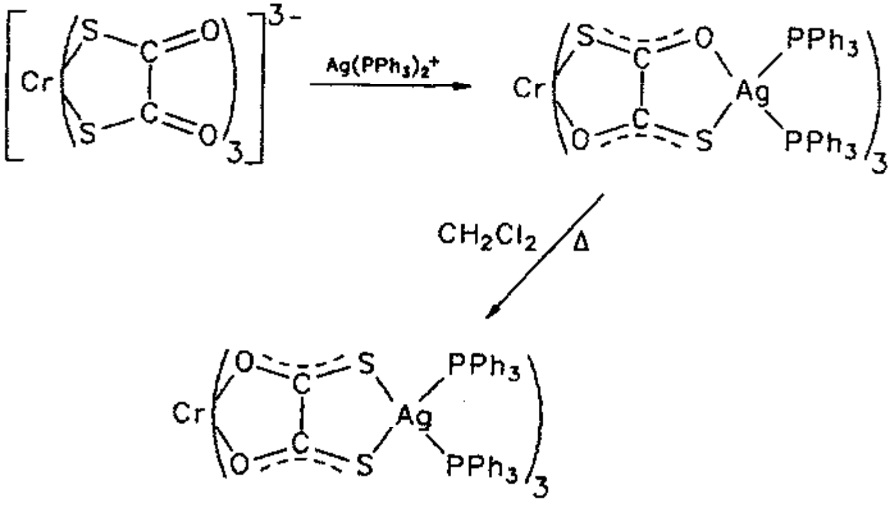

Fig. 8. Linkage isomerization in {Cr[(dto)Ag(PPh$_3$)$_2$]$_3$} [27].

(i) Monothio-oxalate $[O_2C{-}COS]^{2-}$, mto

There are as many as 27 published complexes containing monothio-oxalate as ligand. They are described in 10 papers which deal mainly with the synthesis, properties and structure of mto and its complexes. Besides introducing the ligand as the alkali salt there are two special ways of preparation. In the complex $[Cr(mto)(en)_2]^+$ or $[Co(mto)(en)_2]^+$ the ligand is formed by selective oxidation of coordinated mercaptoacetate (thioglycolate) through Ce(IV), Np(VI), *N*-chlorosuccinimide in *N*,*N*-dimethylformamide or excess acetic anhydride in dimethyl sulphoxide [34–37]

$$[M(en)_2(SCH_2CO_2)]^+ \xrightarrow{\text{oxidation}} [M(en)_2(SCOCO_2)]^+ \qquad (M = Cr, Co) \qquad (2)$$

The other method was found by chance: treating $Cs_2[Mo_2O_4(C_2O_4)_2(H_2O)_2]\cdot 2H_2O$ with Cs_2dto in the presence of O_2 forms the monothio-oxalate compound $Cs_2[MoO(S_2)_2(SOC_2O_2)]$ besides other products [21,38,39].

$[Co(en)_2(mto)]Cl\cdot H_2O$ has been found to undergo photoredox decomposition in concentrated HCl, $HClO_4$ or water when irradiated in the near UV region (Xe arc lamp, $NiSO_4$ or $CoSO_4$ solution filter) giving Co(II), H_2S, S_8 and oxalate $C_2O_4{}^{2-}$ as products [40].

Like other thio-oxalates mto complexes are mainly concentrated round the middle and late members of the first transition metal series. Because of the presence of two different side-on positions (*O*,*S* or *O*,*O*), mto can act both as a semi-soft and as a hard sided ligand. Examples of the latter (*O*,*O*) action are mono- or tetranuclear complexes of aluminium and gallium. Evidence for the *O*,*O*-chelate structure of these compounds was given by IR spectra [16,41]. Discussions on the IR assignments can be found under the heading "1,2-dithio-oxalate". Very recent work deals with electron paramagnetic resonance (EPR) investigations of aqueous solutions containing different vanadyl/mto species [42]. There are three X-ray structures, of two compounds containing the complex unit $[(en)_2Co(mto)]^+$ and of the Mo(VI) compound mentioned above. Besides the unusually short C–O bond length involving the oxygen of the CO_2 part which is not bound to the molybdenum (1.09(7)Å, compared with 1.230(3) and 1.228(7) Å in the Co(III) compounds) there are no other interesting details in the structures. It should be mentioned that mto is almost planar in the cobalt complex, the dihedral angle being 15.8° (torsion about the C–C bond) in $Cs_2[MoO(S_2)_2(mto)]$ (see Table 3). Table 4 collects all the individual monothio-oxalates.

(ii) 1,1-Dithio-oxalate $[O_2C{-}CS_2]^{2-}$, i-dto

1,1-Dithio-oxalate is the thio-oxalate with the unique constitution of carbon-coupled CS_2 and CO_2 entities. Interestingly, its coordination chemistry is very scanty.

TABLE 3

Structural data of the monothio-oxalate ligand in its complexes

Compound	Distances in Å							
	M–S	M–O	C–S (ligator atoms)	C–O	C–C	C–O (–COS)	C–O ($-CO_2$)	Ref.
$[Co(mto)(en)_2]Cl \cdot H_2O$[a]	2.241(1)	1.920(2)	1.723(3)	1.281(3)	1.546(4)	1.211(4)	1.230(3)	37
$[Co(mto)(en)_2]_2(S_2O_6) \cdot 2H_2O$[a]	2.237(2)	1.904(4)	1.702(6)	1.269(7)	1.560(11)	1.217(8)	1.228(7)	36
$Cs_2[MoO(S_2)_2(mto)]$[b]	2.53(2)	2.32(4)	1.61(6)	1.29(7)	1.53(8)	1.22(7)	1.09(7)	39

[a] Torsion angle in mto near 0°.

[b] Torsion angle in mto 15.8°.

TABLE 4

Monothio-oxalate complexes

M	No.	Compound	M.p. (°C)	Colour (solid state)	Magnetism (μ_B)	IR ($\bar{\nu}_{C-O}$)	Electronic spectra ($\bar{\nu}_{max} \times 10^{-3}$ cm^{-1} (ε_0))	Ref.
K	see compound 19							
Cs	see compound 18							
Ca	see compound 19							
Ba	1	Ba(mto)[a]						
Al	2	$(Ph_4P)_3[Al(mto)_3]\cdot CH_2Cl_2$	183–5	Yellow	Diam.	1671s 1422s 1319s		16
Al	3	$\{Al[(mto)Cu(PPh_3)_2]_3\}$	191–3	Yellow	Diam.	1668s 1460s	27.8 (9700)	16
Al	4	$\{Al[(mto)Ag(PPh_3)_2]_3\}\cdot CH_2Cl_2$	177–9	Yellow	Diam.	1671s 1456s 1353s		16
Ga	5	$(Ph_4As)_3[Ga(mto)_3]$[b]			Diam.	1670s 1420 1315		41
Ga	6	$\{Ga[(mto)Ag(PPh_3)_2]_3\}$	173dec	Light green	Diam.	1660s 1460s 1330s		41
In	7	$(Ph_4As)_4[In_2(mto)_5]$	158dec	Colourless	Diam.	1660s 1620s 1560m 1520m 1380m 1320m		41
Pb	8	Pb(mto)[a]						43
Cu	9	$(BzPh_3P)_2[Cu(mto)_2]$	117–8	Green	1.89(2)	1631s 1588s 1325s	16.7 (233) 29.4 (7600)	16
Cu	10	$(BzPh_3P)_2[Cu(mto)_2]\cdot 2H_2O$	105–6	Violet	1.80(2)	1645s 1590s	16.7 (265) 18.3 (236)	16

TABLE 4 (*continued*)

M	No.	Compound	M.p. (°C)	Colour (solid state)	Magnetism (μ_B)	IR ($\bar{\nu}_{C-O}$)	Electronic spectra ($\bar{\nu}_{max} \times 10^{-3}$ cm^{-1} (ε_0))	Ref.
						1316s	26.3 (6800)	
Cu	see also compounds 3,14,15,20,23							
Ag	see compounds 4,6,21							
Zn	11	$(BzPh_3P)_2[Zn(mto)_2]$	181	White	Diam.	1640s 1586s 1330s		16
V	12	$(Ph_4As)_2[VO(mto)_2]$	163–7	Grey	EPR[c]: A = 170.7 g = 1.996	1675s 1640s 1310s	15.3sh(140) 17.3 (160) 20.8 (160) 23.1sh(180) 34.4 (5440)	44
Cr	13	$(BzPh_3P)_3[Cr(mto)_3]\cdot CH_2Cl_2$	144–5	Green	3.90(2)	1640s 1583s 1320s	16.4 (204)	16
Cr	14	$\{Cr[(mto)Cu(PPh_3)_2]_3\}\cdot CH_2Cl_2$ (Cr–SO isomer)	151–2	Green	3.84(2)	1613s 1548s 1364s	16.7(265)	16
Cr	15	$\{Cr[(mto)Cu(PPh_3)_2]_3\}\cdot CH_2Cl_2$ (Cr–OO isomer)	166–7	Yellow	Diam.[d]	1632s 1435s 1342s	17.3 (134) 28.6 (11000)	16
Cr	16	$[(en)_2Cr(mto)]Cl$[e]				1670 1630 1340		36
Cr	17	$[(en)_2Cr(mto)]I$						34
Mo	18	$Cs_2[MoO(S_2)_2(mto)]$		Deep red to black		1635vs 1590s 1570s		39

						1338s		
Fe	19	$KCa[Fe(mto)_3] \cdot 3H_2O$	350	Red	5.74(2)	1639m 1592s 1302s		16
Fe	20	$\{Fe[(mto)Cu(PPh_3)_2]_3\}$	147	Violet	5.69(2)	1632s 1421s 1333s	18.5 (3500)	16
Fe	21	$\{Fe[(mto)Ag(PPh_3)_2]_3\}$	121–3	Orange	4.71(2)	1629s 1428s 1317s	31.5 (17000)	16
Co	22	$(BzPh_3P)_3[Co(mto)_3] \cdot CH_2Cl_2$	126–8	Green	Diam.	1632s 1578s 1332s	16.1 (319)	16
Co	23	$\{Co[(mto)Cu(PPh_3)_2]_3\} \cdot CH_2Cl_2$	154–6	Green	Diam.	1615s 1555s 1380s	16.1 (82)	16
Co	24	$[(en)_2Co(mto)]_2(S_2O_6) \cdot 2H_2O$				1660	19.5 (156)	36
Co	25	$[(en)_2Co(mto)]Cl \cdot H_2O$				1625	36.6 (15600)	37
Co	26	$[(en)_2Co(mto)]ClO_4$				1340	46.5 (16000)	37
Ni	27	$(BzPh_3P)_2[Ni(mto)_2]$	181–2	Brown	Diam.	1651s 1610s 1302s	19.2 (171) 24.1 (2800)	16

---

[a] Mentioned in ref. 43 without details.

[b] No pure sample.

[c] In frozen pyridine solution.

[d] Seems likely to be erroneous.

[e] Only mentioned in ref. 36.

The first authentic example exhibiting a composition $\{[(Ph_3P)_2Ag]_2(i\text{-dto})\}$ is mentioned in ref. 45. Very recently, the structure of the analogous binuclear Cu(I) compound could be confirmed by X-ray analysis [19(d)]. Figure 9 shows the arrangement of the bridging 1,1-dithio-oxalate ligand linking two Cu(I) ions (see also Table 15).

A series of heterobimetallic *i*-dto complexes has also been isolated and characterized [19(f),(g)] (see Table 5). The EPR spectrum of $[(Ph_3P)_2Cu^I(i\text{-dto})Cu^{II}(i\text{-dto})Cu^I(PPh_3)_2]$ confirms the $Cu^{II}S_2O_2$ central entity. Preliminary EPR results for vanadyl *i*-dto species in solution have been published [42].

The title of a paper on "(1,1-dithio-oxalato-S,S′)bis-(μ_3-sulphido)-2,2,3,3-tetrakis(trimethylphosphine)-triangulo-tripalladium(II)" is misleading because the starting ligand, as well as the ligand found in the complex, is in fact 1,2-dithio-oxalate [46(b)].

(iii) 1,2-Dithio-oxalate $[SOC–COS]^{2-}$, dto

Dto is the thio-oxalate with the most extended coordination chemistry reported. There are more than 70 papers on its transition metal as well as its non-transition metal complexes starting as early as 1909 [2] with Ni(II), Co(III) and Fe(III). The ligand can even be purchased commercially as the dipotassium salt K_2dto (CAS registry number 20267–56–5) at a reasonable price (1986), about 50 times more expensive than potassium oxalate but only half the price of toluene-3,4-dithiole, another important 1,2-dithio ligand. Its synthesis runs from oxalyl chloride via the corresponding dithio-oxalic ester and the solvolytic cleavage with KHS. The standard

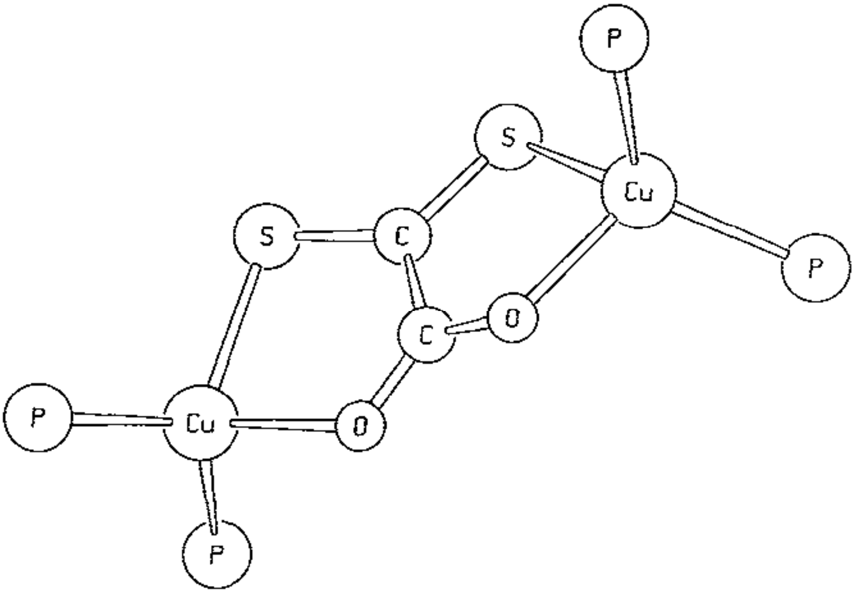

Fig. 9. Molecular structure of $[(Ph_3P)_2Cu(i\text{-dto})Cu(PPh_3)_2]$ (phenyl rings omitted) [19].

TABLE 5

1,1-Dithio-oxalate complexes

Compound	M.p. (°C)	Colour	Electronic spectra ($\bar{\nu}_{max} \times 10^3$ cm^{-1} (ε_0))	Ref.
$\{[(Ph_3P)_2Cu]_2(i\text{-dto})\}$	193–4	Brown	22.4 (11700)	19(e),(f),(g)
$\{[(Ph_3P)_2Ag]_2(i\text{-dto})\}$	140–3	Light brown	26.2 (4100) 21.5 (2900)	19(e),(f),(g)
$\{Cu[(i\text{-dto})Cu(PPh_3)_2]_2\}$	145–8(dec.)	Dark brown	22.0 (13500)	19(f),(g)
$\{Ni[(i\text{-dto})Cu(PPh_3)_2]_2\}$	168–71(dec.)	Dark brown	27.2 (10300) 23.6 (13000) 16.7 (2900) 15.3 (3200)	19(f),(g)
$\{Zn[(i\text{-dto})Cu(PPh_3)_2]_2\}$	181–3(dec.)	Brown	26.6 (10300) 22.3 (15300)	19(f),(g)
$\{Cu[(i\text{-dto})Ag(PPh_3)_2]_2\}$	167–9(dec.)	Dark brown	22.7 (4100)	19(f),(g)

method of preparing complexes starts with the alkali salts of dto, which are water soluble and fairly stable (see below).

The common feature of thio-oxalates, namely the ability to extend the coordination of binary complexes to further metal-containing species yielding definite multinuclear arrangements, is especially evident, and has indeed been widely investigated with dto itself. Important contributions to this subject were given by Coucouvanis and his group in a series of papers and summarized by himself in a conference volume [47].

(a) Solid-state structure characteristics of dto complexes

Table 6 allows a comparison of selected bond distances and angles in complexes containing terminal or bridging dithio-oxalate ligands as well as a few non-complex dithio-oxalate compounds.

Mononuclear complexes. For mononuclear chelates of dto, the structural characteristics of $K_2[Ni(dto)_2]$ are representative in several respects. Its structure has been examined three times by different authors, Cox et al. in 1935 [3], Coucouvanis et al. in 1973 [28], and Gleizes et al. in 1979 [60]. Curiously enough, in the last structural study the authors found a second polymorphic "black" form. By treating the normal "red" form with $K_2Cr_2O_7$ in aqueous solution, and after evaporation, a blend of "red" and "black" crystals is obtained with similar but different unit cells. In the "red" form (C2/c; "black" form $P2_1/n$) the $S_2C_2O_2$ moieties and the KO_2 units are nearly coplanar; however, both dto planes are twisted, causing a dihedral angle of 9°. In contrast to the "red" form, the "black" one exhibits a linear stacking of planar $[Ni(dto)_2]^{2-}$ anions, which are tilted with respect to the stacking axis (see Fig. 10). Similarly, this holds also for $Li_2[Ni(dto)_2]\cdot 2H_2O$ and $Na_2[Ni(dto)_2]\cdot 2H_2O$ [59]. Alkali and alkaline-earth counter ions influence the molecular structures of the negatively charged dto complex ions. This is because these cations are coordinated by the dto oxygens (compare also $Ba[Ni(dto)_2]\cdot 6H_2O$ [62]). Strictly speaking, dto acts as bridging ligand in the former complexes. For quantitative reasons, however, we record the compounds with alkali and alkaline-earth cations under the heading "mononuclear". In corresponding complexes with organic "onium" cations (e.g. pyridinium) [73,74(a),76] or ethylenediammonium [75] this interaction is lacking.

There are two copper bis-complexes differing only in the oxidation number (and of course in the number of cations) [51,52]. Whereas the Cu(II) bis-dto chelate was investigated as the $[K(18\text{-crown-}6)]^+$ salt, the Cu(III) bis-dto chelate could be isolated and crystallographically characterized as the $[(Ph_3P)_2N]^+$ salt. In the case of $(TTF^{\cdot +})[Cu(dto)_2]$ (TTF = tetrathiafulvalene), decomposition occurs when the complex is exposed to X-rays, preventing the resolution of the crystal structure [77(a)]. Both $[Cu(dto)_2]^{2-}$ and $[Cu(dto)_2]^-$ anions are planar and located on the centres of symmetry. Crown ether chelated K^+ ions are bound further to the alpha-diketone sides of the $[Cu(dto)_2]^{2-}$ complex. The major differences between the

TABLE 6

Comparison of selected bond distances (Å) and angles (°) in complexes containing terminal or bridging dithio-oxalate ligands (completed by some non-complex derivatives)

M	No.	Compound	M–S	M–O	C–S	C–O	C–C	Intraligand		Torsion angle along	Ref.
								S–M–S	O–M–O	S–C–C–S	
–	1	S,S'-Et$_2$dto (–60°C)			1.749	1.209	1.533			*Trans*-planar	48
–	2	S,S'-(3-Cl-Ph)$_2$dto			1.753(3)	1.195(3)	1.541(3)			*Trans*-planar	49
Li	see compound 22										
Na	see compounds 23,41										
K	3	K[SOC–COSMe]			1.743(6)	1.213(7)	1.562(9)			O–C–C–O	12
					COSMe	COSMe				9.9(*cis*)	
					1.688(6)	1.224(8)					
K	4	K$_2$dto	3.306– 3.492	2.730– 2.939	1.704(3)	1.233(4)	1.516(9)			76.5(*trans*)	8
K	see also compounds 7,8,20,21,24,25,56,62										
Cs	see compounds 13,14,18										
Ca	see compounds 21,26,27										
Ba	see compound 28										
Al	5	{Al[(dto)Ag(PPh$_3$)$_2$]$_3$}^{a}	Ag–S	Al–O				S–Ag–S	O–Al–O		32
			2.589(3)	1.889(8)	1.66(1)	1.28(1)	1.55(2)	83.2(1)	82.5(4)	13.1	
In	6	(Ph$_4$As)$_4$[(dto)$_2$In(dto)In(dto)$_2$]	2.551(3)		1.724(12)	1.210(15)	1.547(16)	85.49(9)		15 and 45	50
			μ-dto								
			2.638(4)	2.334(7)	1.705(11)	1.238(14)	1.545(16)			*Trans*-planar	
Sn	7	K{(dto)$_2$Sn[(dto)Cu(PTol$_3$)$_2$]}·(acetone)$_2$^{b}	Sn–S	K–O							33
			2.462(2)	2.715(6)– 3.137(6)	1.732(8)	1.207(8)	1.539(11)	89.44(8)		4.5	
			2.477(2)		1.734(7)	1.207(8)	1.562(10)	88.19(8)		12.5	
		μ-dto	Cu–S	Sn–O					O–Sn–O		
			2.321(2)	2.158(4)	1.661(6)	1.275(6)	1.540(8)		74.47(17)		
Sn	see also compounds 29,30										

TABLE 6 (*continued*)

M	No.	Compound	M–S	M–O	C–S	C–O	C–C	Intraligand		Torsion angle along	Ref.
								S–M–S	O–M–O	S–C–C–S	
Cu	8	K(18-crown-6)]$_2$[Cu(dto)$_2$]·DMF		K–O							51,52
			2.268(2) 2.253(2)	2.777(4)	1.703(5)	1.222(6)	1.545(7)	88.85(7)		Planar	
Cu	9	[(Ph$_3$P)$_2$N][Cu(dto)$_2$]	2.164(1) 2.178(1)		1.730(5)	1.217(6) 1.186(6)	1.524(7)	87.48(5)		Planar	51,52
Cu	10	[CuMn(dto)$_2$(H$_2$O)$_3$]·4.5H$_2$O^c	2.274(6)	2.31(1)	1.70(2)	1.26(2)	1.51(2)	91.7(2)	69.2(5)	Nearly planar	53
Cu		see also compound 7									
Ag	11	{[(Ph$_3$P)$_2$Ag]$_2$(dto)}	2.513(2)	2.510(6)	1.717(8)	1.213(9)	1.561(11)			*Trans*-planar	45
Ag		see also compounds 5,19									
Zn	12	(Ph$_4$As)$_2$[Zn(dto)$_2$]^d	2.311(2) 2.322(2)		1.728(7) 1.741(7)	1.203(9) 1.218(8)	1.566(11) 1.531(10)	95.6(1) 95.2(1)		31.7(2) 43.3(2)	54
Zn		see also compound 50									
Y, La, Ce, Nd, Sm, Eu, Gd, Dy, Er, Yb		see compounds 31–46									
Th		see compound 47									
Mo	13	Cs$_2${[MoO(dto)]$_2$S$_2$}		Mo=O							21
			2.42(3)	1.70(4)	1.65(5)	1.28(7)	1.62(8)	79.0(9)		Planar	
Mo	14	Cs$_2$[MoO(dto)$_2$]·H$_2$O		Mo=O							39
			2.407(2)	1.660(8)	1.725(10)	1.22(1)	1.54(1)	85.3(1)		2.0, 15.1	
Mn	15	{[(CO)$_5$Mn]$_2$(dto)}	2.379		1.737	1.209	1.555			*Trans*-planar	25
Mn		see also compounds 10,48,61,65									
Tc	16a	(Ph$_4$As)$_2$[TcN(dto)$_2$]^e		Tc≡N							55
			2.387(2)	1.613(4)	1.727(5)	1.213(10)	1.549(12)	86.2(1)			
Tc	16b		2.394(2)	1.606(7)	1.740(6)	1.211(8)	1.558(9)	86.2(1)			56
Tc	17	Ph$_4$As[TcO(dto)$_2$]		Tc=O							55
			2.329(1)	1.646(4)	1.758(6)	1.199(7)	1.528(10)	86.8(1)			

Re	18	Cs[ReO(dto)$_2$]			Re=O							26
				2.334(3)	1.674(7)	1.743(10)	1.209(14)	1.539(15)	87.0(1)			
Fe	19	{Fe[(dto)Ag(PPh$_3$)$_2$]$_3$}^{a}		Ag–S	Fe–O				S–Ag–S	O–Fe–O		32
				2.587(2)	2.003(6)	1.68(1)	1.28(1)	1.52(1)	83.3(1)	77.8(3)	11.6	
Fe	20	{K$_2$[Fe(dto)$_2$NO]·H$_2$O}$_2$		2.282(1)		1.714(3)	1.226(4)	1.536(4)	88.7(1)			57
				2.255(1)				1.546(4)				
				2.275(1)								
				2.263(1)								
Co	21	KCa(+)$_{589}$–[Co(dto)$_3$]·4H$_2$O^f			Ca–O							58
			(1)	2.250(4)	2.485(9)	1.721(14)	1.207(14)	1.539(18)	89.30(14)		7.8	
				2.259(4)	2.573(10)	1.689(15)	1.246(15)					
			(2)	2.230(4)	2.531(9)	1.707(13)	1.228(15)	1.493(17)	89.90(15)		1.5	
				2.230(4)	2.442(10)	1.724(13)	1.224(14)					
			(3)	2.256(4)	2.476(9)	1.658(14)	1.220(13)	1.603(16)	89.84(15)		4.1	
				2.237(4)	2.733(10)	1.672(14)	1.231(14)					
					K–O							
					3.322(12)							
					2.784(10)							
					2.791(11)							
					3.017(11)							
Ni	22	Li$_2$[Ni(dto)$_2$]·2H$_2$O^g			Li–O							59
				2.189(1)	1.989–	1.693(2)	1.240(2)	1.527(2)	92.42(4)		Planar	
					2.077(4)							
Ni	23	Na$_2$[Ni(dto)$_2$]·2H$_2$O			Na–O							59
				2.178(1)	2.352–	1.696(3)	1.239(3)	1.521(4)	92.02(3)		Planar	
					2.455(3)							
Ni	24	K$_2$[Ni(dto)$_2$]^h		2.30		1.83					Planar	3
					K–O							28
				2.180(3)	2.769(6)	1.750(9)	1.207(10)	1.544(10)	92.9(1)			
Ni	25	K$_2$[Ni(dto)$_2$]^i			K–O							60
		"black form"		2.1826(5)	2.798(2)	1.707(2)	1.234(2)	1.540(3)	92.09(2)		Planar	
Ni	26	[Ca(H$_2$O)$_4$][Ni(dto)$_2$]·2H$_2$O^j			Ca–O							
				2.25(1)	2.49(4)	1.73(5)	1.17(5)	1.61(7)	89.1(5)	64.1		61

TABLE 6 (*continued*)

M	No.	Compound		M–S	M–O	C–S	C–O	C–C	Intraligand		Torsion angle along	Ref.
									S–M–S	O–M–O	S–C–C–S	
				2.14(1)	2.48(3)	1.70(5)	1.26(5)	1.52(6)	94.4(5)			
Ni	27	$[Ca_3(H_2O)_8(C_2O_4)][Ni(dto)_2]_2 \cdot 6H_2O^j$		2.174(4)	2.468(9)	1.68(1)	1.26(1)	1.51(2)	92.2(1)	64.6(3)		61
				2.174(4)	2.500(9)	1.70(1)	1.25(1)		87.8(1)	78.4(4)		
Ni	28	$Ba[Ni(dto)_2] \cdot 6H_2O^k$			Ba–O							62
				2.177(3)	2.772– 3.045(6)	1.713(9)	1.226(10)	1.548(12)	92.0(2)			
Ni	29	$(BzPh_3P)_2[(dto)Ni(dtoSnCl_4)]$		dto								28
				2.156(9)		1.76(2)	1.17(3)	1.61(3)	91.7(3)		Planar	
				2.136(7)		1.78(2)	1.13(3)					
				μ-dto	Sn–O							
				2.171(8)	2.168(16)	1.77(3)	1.19(3)	1.48(3)	91.2(3)			
				2.159(8)	2.154(13)	1.78(2)	1.20(3)					
Ni	30	$(BzPh_3P)_2[Ni(dtoSnCl_4)_2]$			Sn–O							28
				2.183(2)	2.212(5)	1.670(8)	1.264(9)	1.513(10)	92.6(1)		Planar	
Ni	31	$[(RE)_2(H_2O)_{2n}][Ni(dto)_2]_3 \cdot xH_2O$	Eu	Ni(1)–S	Eu–O		"terminal dto's"			O–Eu–O		63,64
	–40			2.185(2)		1.719(7)	1.206(9)	1.498(9)	91.69(7)			
				2.174(2)		1.706(7)	1.216(8)				Nearly planar	
		RE = Y, La, Ce, Nd, Sm, *Eu*, Gd, Dy, Er, *Yb*^{l}		2.199(2)	2.544(4)	1.697(6)	1.250(7)	1.524(1)	91.93(7)	62.66		
				2.174(2)	2.484(5)	1.697(6)	1.239(8)			63.47		
				Ni(2)–S	2.482(5)							
				2.182(2)	2.533(4)	1.680(6)	1.259(8)	1.501(9)	87.45(6)			
				2.174(2)		1.686(6)	1.267(7)					
			Yb	Ni(1)–S	Yb–O		"terminal dto's"			O–Yb–O		
				2.177(2)		1.709(6)	1.234(7)	1.542(7)	91.75(6)			
				2.170(2)		1.703(6)	1.223(7)					
				2.196(2)	2.359(4)	1.674(6)	1.251(7)	1.528(7)	92.93(7)	67.33		
				2.189(2)	2.329(4)	1.684(6)	1.248(7)			66.30		
				Ni(2)–S	2.341(4)							
				2.188(2)	2.395(4)	1.679(6)	1.256(7)	1.521(8)	92.79(6)			
				2.182(2)		1.690(5)	1.238(6)					

Ni	41	$Na[La(C_2O_4)(H_2O)_4][Ni(dto)_2]\cdot 4.2H_2O^{m,n}$									65
Ni	42	$[La(H_2O)_4(glycine)]_2[Ni(dto)_2]_3\cdot glycine\cdot 7H_2O^{n,o}$									66
Ni	43	$[Yb(C_2O_4)][Ni(dto)_2(H_3O)]\cdot 1.5H_2O^{n,p}$									65
Ni	44	$[Yb(H_2O)_2(glycine)_2]_2[Ni(dto)_2]_3\cdot 8H_2O^{n,q}$									66
Ni	45	$[Ce_2(H_2O)_{10}(C_4O_4)][Ni(dto)_2]_2\cdot 5.2H_2O^{n,r}$									67
Ni	46	$\{[Ce(H_2O)_3(\beta\text{-alanine})]_2(C_2O_4)\}[Ni(dto)_2]_2\cdot 6H_2O^{n,s}$									68
Ni	47	$[Th(H_2O)_6][Ni(dto)_2]_2\cdot 6.5H_2O^{t}$		Th—O							69
			2.19(2)	2.58(3)	1.74(5)	1.26(7)	1.41(8)	91.9(7)			
			μ-dto								
			2.20(2)		1.63(4)	1.30(4)	1.50(7)	92.4(5)			
Ni	48	$[NiMn(dto)_2(H_2O)_3]\cdot 4.5H_2O^{c}$		Mn—O					O—Mn—O		53,70
			2.174(5)	2.33(1)	1.68(2)	1.27(2)	1.50(2)	92.4(2)	69.2(4)		
Ni	49	$[(en)_2Ni(dto)Ni(dto)]$		Ni—O					O—Ni—O		71
			2.170(8)	2.15(1)	1.71(2)	1.23(3)	1.50(4)	92.5(3)	77.5(5)		
			2.185(8)				1.53(4)	92.1(3)			
Ni	50	$[ZnNi(dto)_2(H_2O)_{2.08}]^{u}_{\infty}$		Ni—O					O—Zn—O		72
			2.182(2)	2.00(18)	1.676(5)	1.245(5)	1.529(10)	92.48(9)	79.1(2)		
				Zn—O							
				2.077(3)							
Ni	51	$(NC_4H_4NH)_2[Ni(dto)_2]$	2.178(1)		1.715(4)	1.221(5)	1.545(5)	92.02(4)		1.9	73
Ni	52	$[(4\text{-}MeC_5H_4NH)_2[Ni(dto)_2]$	2.180(1)		1.719(5)	1.227(6)	1.530(7)	92.7(1)		0.7	73,74a
Ni	53	$[H_3N(CH_2)_2NH_3][Ni(dto)_2]$	2.178(0)		1.718(2)	1.227(2)	1.530(3)	92.42(2)		Planar	75
			2.165(0)		1.709(2)	1.237(2)					
Ni	54	$[C_{12}N_2H_{12}][Ni(dto)_2]^{v}$	2.167(2)–		1.719(9)–	1.21(1)–	1.51(1)			5(2),6(2)	76
			2.176(2)		1.744(7)	1.23(1)					
Ni	55	$(C_5H_6N)_2[Ni(dto)_2]^{u,w}$	2.182(2)		1.713(7)	1.239(9)	1.545(9)	92.6(1)		Planar	74a
			2.176(2)		1.744(7)	1.23(1)					
Pd	56	$K_2[Pd(dto)_2]^{b,n}$	2.44								3
Pd	57	$(Ph_4As)_2[Pd(dto)_2]$	2.300(3)		1.721(8)	1.23(1)	1.53(1)	89.3(3)			74b
Pd	58	$(TTF)_2[Pd(dto)_2]^{x}$	2.306(1)		1.732(3)	1.214(4)	1.556(4)	88.66(2)		y	77
Pd	59	$[Pd(dto)(Me_3P)_2]$	2.334(1)		1.724(4)	1.215(5)	1.544(5)	87.9(0)		Nearly planar	46b
Pd	60	$\{[(Me_3P)_2Pd]_2(\mu_3\text{-}S)_2Pd(dto)\}$	2.300(2)		1.714(10)	1.22(1)	1.56(1)	89.6(1)			46b
Pd	61	$[PdMn(dto)_2(H_2O)_3]\cdot 4.5H_2O^{c,n}$									53,78

TABLE 6 (*continued*)

M	No.	Compound	M–S	M–O	C–S	C–O	C–C	Intraligand		Torsion angle along	Ref.
								S–M–S	O–M–O	S–C–C–S	
Pt	62	$K_2[Pt(dto)_2]$[h,n]									3
Pt	63	$(TTF)_2[Pt(dto)_2]$[n,z]									77
Pt	64	$(TTF)_3[Pt(dto)_2]$*	2.311(2)		1.735(8)	1.232(10)	1.550(9)	89.57(6)		Planar	77
Pt	65	$[PtMn(dto)_2(H_2O)_3]\cdot 4.5H_2O$[c]		Mn–O					O–Mn–O		53
			2.295(11)	2.30(3)	1.70(4)	1.30(4)	1.45(5)	90.3(4)	68.6(10)	Planar	

[a] Compounds $\{M[(dto)Ag(PPh_3)_2]_3\}$ (M = Al, Fe) are isomorphous.

[b] "Bridging" dto ligand between Sn and K, *S,S*-bound to Sn; two different kinds of dto ligands: one chelates the potassium, while the other one acts additionally as a monodentate ligand for another K.

[c] Compounds $[AMn(dto)_2(H_2O)_3]\cdot 4.5H_2O$ (A = Cu, Ni, Pd, Pt) are isostructural. Bimetallic one-dimensional compounds with dto; infinite zigzag chain molecules $\{[Mn(H_2O)_3](O_2C_2S_2)A(S_2C_2O_2)\}$ stacked chains; each layer of stacked chains is separated from the next one by intervening water molcules.

[d] Two different dto ligands, tetrahedral angle = 86.8°.

[e] Two different modifications (unit cells) are reported.

[f] Three different ligands (1), (2), (3).

[g] Compounds $M_2[Ni(dto)_2]\cdot 2H_2O$ (M = Li, Na) are isostructural.

[h] Compounds $K_2[M(dto)_2]$ (M = Ni, Pd, Pt) are isomorphous; in $K_2[Ni(dto)_2]$ there is twisting of the ligands by 9° relative to each other.

[i] Formed from the "normal red form" by reaction with $K_2Cr_2O_7$. Totally planar $Ni(dto)_2$ units stack along the *b* direction. There is a straightforward relationship between the structures of "red" and "black" form.

[j] "$[Ca_3Ni_2]$" results from "[CaNi]" in aqueous medium, where the dto is partly transformed into oxalate; both structures are built of zigzag chains of nickel atoms and either tetrahydrated or dihydrated calcium atoms with dto as bridging ligands. These chains are stacked into layers: in "[CaNi]" the layers are weakly bonded to each other by a few intervening H_2O molecules. In contrast, in "$[Ca_3Ni_2]$" the layers are firmly bridged by oxalate anions at the Ca atoms.

[k] It is of one-dimensional type, consisting of flat $[Ni(dto)_2]^{2-}$ anions stacked in a zigzag way with Ba^{2+} and H_2O filling the tunnels between the anionic columns. The anionic stacking differs from the "roof-tile-like" type observed in the one-dimensional alkali derivatives of $[Ni(dto)_2]^{2-}$.

[l] The former part of the series (up to Dy) crystallizes in the monoclinic system ($P2_1/c$) and the latter part crystallizes in the triclinic system ($P1$). The monoclinic network exhibits channels running parallel to the direction [100] in which some water molecules are inserted. The triclinic structure can be described as a pseudo-lamellar structure, water molecules being inserted between the layers. There are two different Ni atoms in each heteropentanuclear entity.

[m] Infinite chains $\cdots La{-}O_2C_2O_2{-}La\cdots$, grafted on each La atom by a $[Ni(dto)_2]^{2-}$ group.

[n] No detailed structural data reported.

[o] Two La(III) atoms are bridged, in an infinite way, by one glycine with contacts La–La respectively equal to 6.204(1) and 6.248(1) Å.

[p] Cyclic tetramers $(YbO_2C_2O_2)_4$ are linked together by $[Ni(dto)_2]^{2-}$ forming infinite chains.

[q] Two Yb(III) atoms are twofold bridged, in an infinite way, by two glycine ligands thus forming a dinuclear entity with a short Yb–Yb distance of 4.734 Å.

[r] Bidimensional structure with layers of $[Ce_2(C_4O_4)]_\infty$ parallel to plane (001) and $[Ni(dto)_2]^{2-}$ anions branched on the cerium atoms.

[s] β-Alanine and oxalate bridge several positions of the cerium atom, and the $[Ni(dto)_2]^{2-}$ is branched on the cerium atom.

[t] Heterotrinuclear entity $Th(H_2O)_6Ni_2(dto)_4$.

[u] Bimetallic chain, ribbons $\cdots Ni(S_2C_2O_2)Zn(O_2C_2S_2)Ni\cdots$, Zn is octahedrally surrounded by six oxygen atoms (four from dto, two from water molecules; the remaining water molecules are bound to only 4% of all Ni atoms, giving non-stoichiometry).

[v] $C_{12}N_2H_{12}{}^{2+}$ = 6,7-dihydrodipyrido[1,2-*a*:2′,1′-*c*]pyrazinium.

[w] $C_5H_6N^+$ = pyridinium (some crystallographic data reported also for the 3-methylpyridinium, 3-ethylpyridinium, 4-methylpyridinium and 4-ethylpyridinium salts).

[x] The crystal structure consists of mixed stacks of donor $(TTF^{\cdot +})_2$ dimers and $[Pd(dto)_2]^{2-}$ acceptors.

[y] The anion possesses a "chair" conformation. The dihedral angle between the PdS_4 plane and the $S_2C_2O_2$ plane is ca. 8°.

[z] Compounds $(TTF)_2[M(dto)_2]$ (M = Pd, Pt) are isomorphous.

[*] Two different TTF species are present: $[(TTF^{\cdot +})_2(TTF^{\circ})][Pt(dto)_2]$.

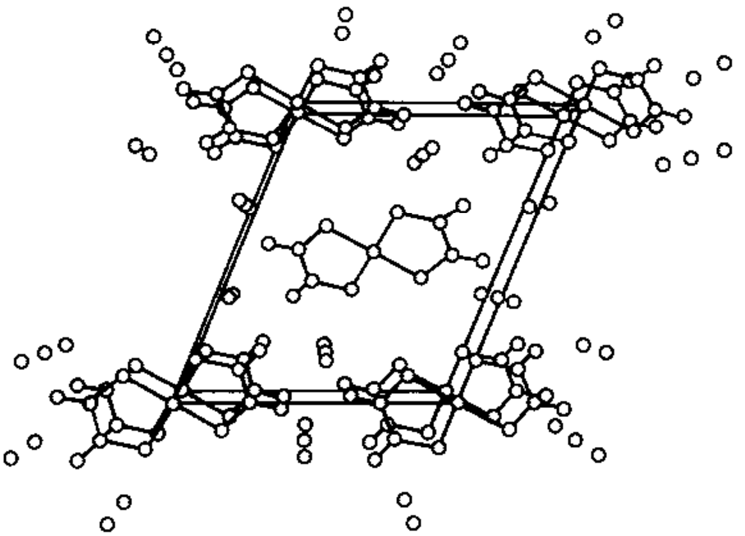

Fig. 10. View down the stacking axis of the unit cell of "black" $K_2[Ni(dto)_2]$ [60].

molecular structures of the $[Cu(dto)_2]^{-,2-}$ anions lie in the different mean Cu–S bond lengths: Cu(II)–S is 2.260 Å and Cu(III)–S 2.171 Å [52]. The latter value agrees very well with analogous distances in other Cu(III) dithiolates [79,80]. Shorter bonds in the "higher valent" metal complexes compared with longer ones for metal(II) are generally expected and are found also for other dithiolates [81,82]. Zn(II) forms a tetrahedral dto bis-complex $[(C_6H_5)_4As]_2[Zn(dto)_2]$ (dihedral angle 86.8°). In addition there are two different torsion angles between the two COS entities along the C–C axis in the two ligands: 31.7° and 43.3° [54].

In $KCa[Co(dto)_3]\cdot 4H_2O$ (the only "mononuclear" tris-chelate of dto for which the X-ray structure is known [58]), potassium and calcium ions influence the actual structure by coordinating the dto oxygens as in bis-chelates (see above).

The mononuclear mixed-ligand complex $[(PMe_3)_2Pd(dto)]$ contains one sulphur-bound dto and two phosphorus atoms in square-planar coordination geometry around the palladium [46(b)]. A significant lengthening of the Pd–P distances in this compound (2.301 Å) compared with 2.253 Å in the oxalate compound $[(PEt_3)_2Pd(C_2O_4)]$ suggests that the thio-oxalate ligand is a better *trans*-labilizing group than oxalate.

Mononuclear five-coordinated oxometal chelates of dto. As expected in the three mononuclear $MO(dto)_2$ complexes (M = Mo [39], Tc [55], Re [26] and in $[TcN(dto)_2]^{2-}$ [55,56], the coordination polyhedrons have roughly C_{4v} symmetry with the metals considerably above the S_4 base plane (see Fig. 11). However, this is due mainly to the mutual inclination of the two ligands. In the molybdenyl complex

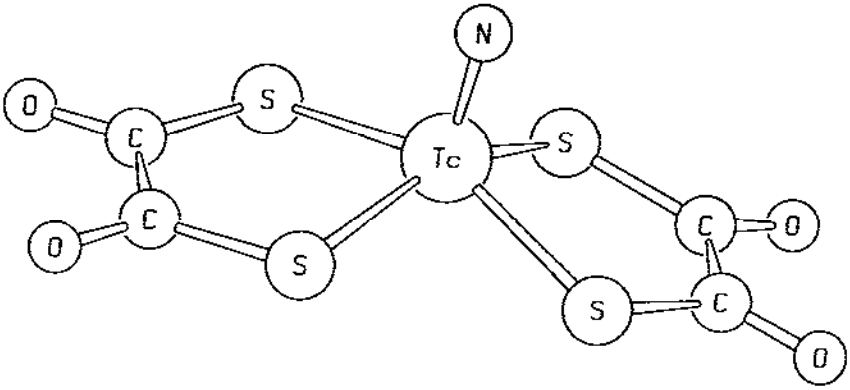

Fig. 11. Structure of the anion in $(Ph_4As)_2[TcN(dto)_2]$ [56].

the "bite" of the dto ligand is 3.260 Å, which is, according to the authors, the largest one ever reported.

Binuclear homometal dto complexes. At present, two symmetric binuclear dto chelates are known which differ in constitution (except the central bridging unit dto): $[(Ph_3P)_2Ag(\mu\text{-dto})Ag(PPh_3)_2]$ [45] and $(Ph_4As)_4[(dto)_2In(\mu\text{-dto})In(dto)_2]$ [50]. Thus, according to the X-ray structures, dto links two tetrahedrally coordinated silver(I) ions (Fig. 12) or two octahedrally coordinated indium(III) ions (Fig. 13). In both

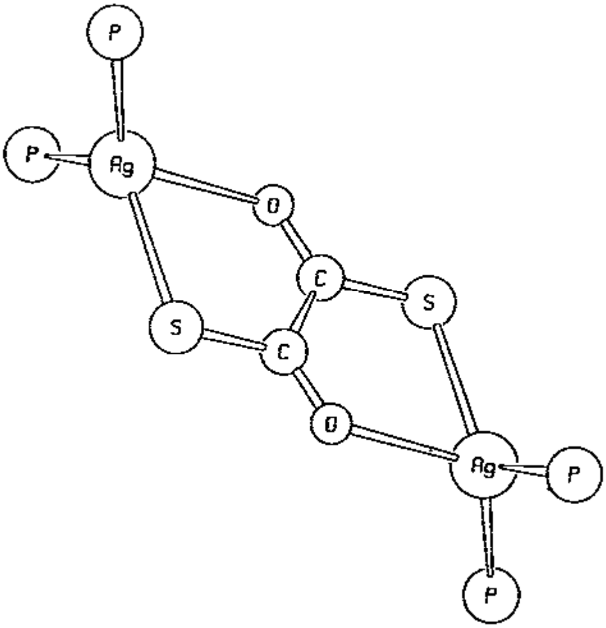

Fig. 12. Molecular structure of $[(Ph_3P)_2Ag(dto)Ag(PPh_3)_2]$ (phenyl rings omitted) [45].

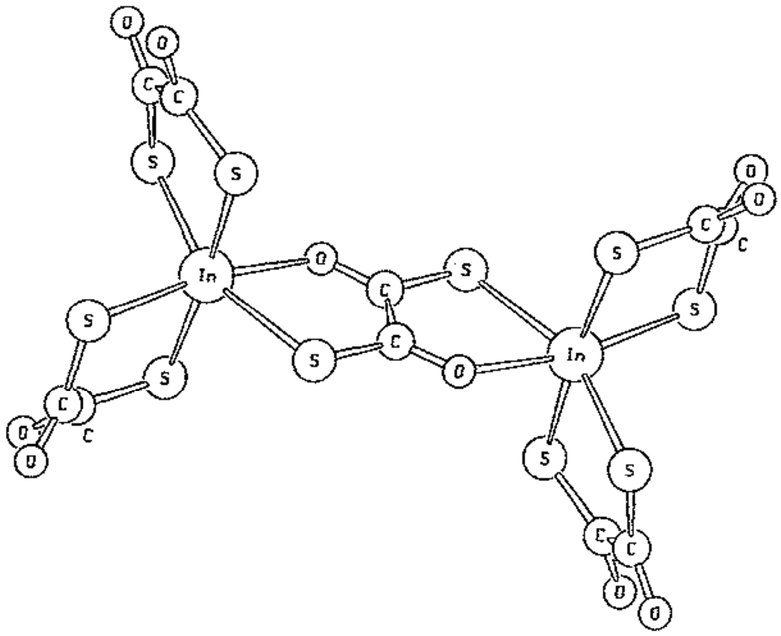

Fig. 13. Structure of the anion in $(Ph_4As)_4[(dto)_2In(dto)In(dto)_2]$ [50].

compounds the bridging ligand turns out to be planar, whereas in the indium compound the terminal dtos are twisted with different torsion angles: 15° or 45° (the anion possesses a centre of symmetry, space group $P\bar{1}$).

In a third binuclear ("homometal") complex $[(en)_2Ni(\mu\text{-}dto)Ni(dto)]$ the bridging dto links an octahedral N_4NiO_2 core with a planar NiS_4 core as shown in Fig. 14 [71].

$Cs_2[Mo_2O_2S_2(dto)_2]$ [21] is a homobinuclear compound without dto bridges but possessing μ-sulphido bridges (see Fig. 15).

As already mentioned, dto indeed links two $Mn(CO)_5$ entities in $[(CO)_5Mn(\mu\text{-}dto)Mn(CO)_5]$. The bridging ligand acts as monodentate, however, via sulphur to each manganese atom [25].

Binuclear heterometal dto complexes. The only genuine heterobimetallic dto complex is the binuclear $(BzPh_3P)_2[(dto)Ni(S_2C_2O_2)SnCl_4]$ [28], a typical "Coucouvanis complex", with dto linking a planar NiS_4 unit with an octahedral Sn(IV) (see Fig. 16). Another heterometallic dto chelate is strictly speaking trimetallic because the potassium is also coordinated by dto oxygens (see above under "mononuclear"): $K\{(dto)_2Sn[(O_2C_2S_2)Cu(PTol_3)_2]\}\cdot(acetone)_2$ (see Fig. 7) [33]. In the latter case dto links octahedral Sn(IV) with tetrahedral Cu(I).

Oligo- and polynuclear dto complexes. In $(BzPh_3P)_2[Ni(S_2C_2O_2SnCl_4)_2]$ the Ni(II) ions, square planar coordinated by four sulphur donor atoms, form the centres of

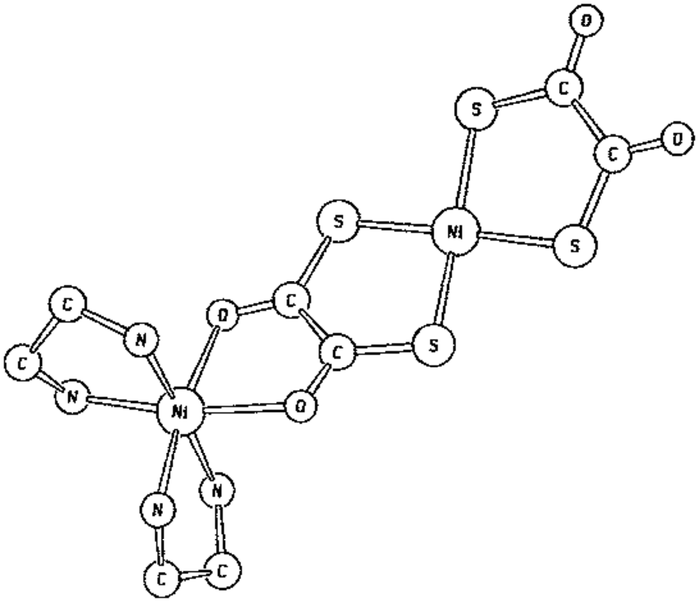

Fig. 14. Molecular structure of [(en)$_2$Ni(dto)Ni(dto)] [71].

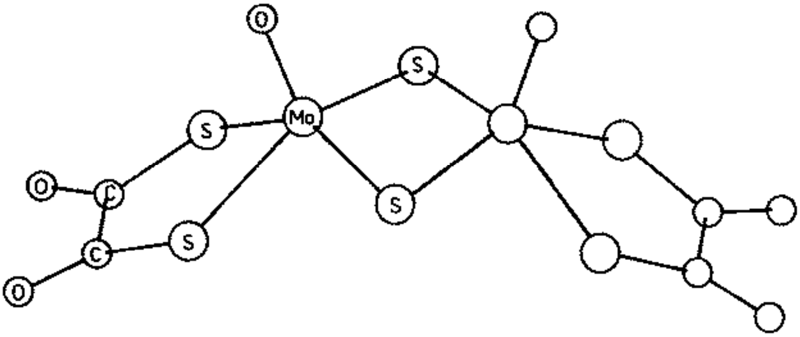

Fig. 15. Structure of the anion in Cs$_2$[(dto)MoO(μ-S)$_2$MoO(dto)] [21].

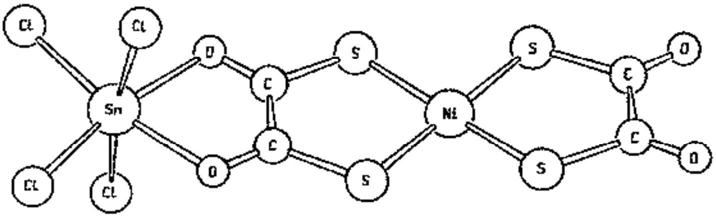

Fig. 16. Structure of the anion in (BzPh$_3$P)$_2$[(dto)Ni(dtoSnCl$_4$)] [28].

trinuclear complexes and are linked via two dto ligands with two hexa-coordinated tin atoms which themselves are in an O_2Cl_4 environment [28]. Infrared data and bond length changes reflect strong differences between the "parent" complexes and the "SnX_4 adducts" suggesting a predominance of resonance form B (see Fig. 17) in the valence bond (VB) description of these "adducts".

The Sn–O distances (mean 2.212 Å) are markedly longer than in cases with only one dto-$SnCl_4$ unit in the Ni, Sn binuclear complex mentioned above (2.161 Å). The Ni–S bonds are also slightly lengthened. Coucouvanis attributed this to different π-back-bonding effects.

In the other reported trinuclear dto complex, three Pd atoms are triangularly connected by two central μ_3-sulphides [46(b)]. There is, however, only one dto ligand terminally *S,S*-bound to one of the three palladium atoms, as can be seen from Fig. 18.

Iron(III) and aluminium(III) form tetranuclear heterobimetallic complexes with phosphine shielded Ag(I) in $\{M[(O_2C_2S_2)Ag(PPh_3)_2]_3\}$ [32].

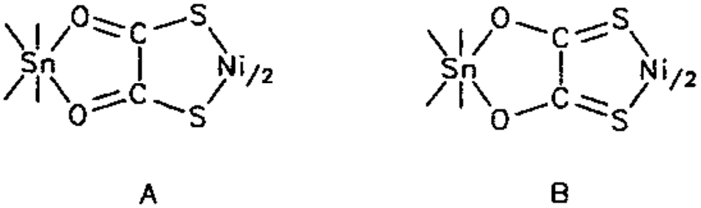

Fig. 17. Resonance forms of the Ni(dto)Sn cores [28].

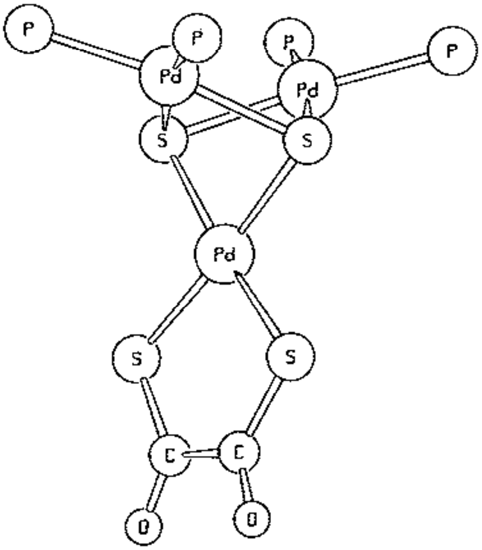

Fig. 18. Molecular structure of $\{(dto)Pd(\mu_3\text{-}S)_2[Pd(PMe_3)_2]_2\}$ (methyl groups omitted) [46(b)].

There is a great variety of polynuclear dto complexes which all consist of $\cdots(O_2C_2S_2)M(S_2C_2O_2)\cdots$ (M = Ni, Pd or Pt) units interconnected by "hard–hard" building blocks containing rare-earth [63–68], Ca [61], Ba [62], Zn [72], Th [69] or Mn [53,70,78] ions and water [53,61–70, 72,78], oxalate [65,68], squarate [67], glycine [66] or β-alanine [68] ligands. In the case of Mn, complexes with Ni, Pd, Pt, Cu or Mn(II) could be formed [53,70]. The general structural feature of that group of polynuclear complexes is the presence of infinite networks of chains, ribbons and layers giving rise to various stacks, columns or channels. The complexes can be obtained as crystals by co-precipitation of corresponding mixtures of the starting materials from aqueous solution.

Solid state conductivities and magnetism. Some compounds were studied with regard to their solid state conductivity behaviour. Although the conductivity behaviour is anisotropic the values do not reach the typical "organic metal" level as found in the classic TTF–TCNQ [62,69,77]. The solid state conductivity increases in the series $Ba[Ni(dto)_2]\cdot 6H_2O$ ($10^{-12}\,\Omega^{-1}\,cm^{-1}$) < non-1-D "red" $K_2[Ni(dto)_2]$ (4×10^{-11}) < 1-D "black" $K_2[Ni(dto)_2]$ (2×10^{-8}–5×10^{-9}) < $Na_2[Ni(dto)_2]\cdot 2H_2O$ (5×10^{-7}–5×10^{-8}) < $Li_2[Ni(dto)_2]\cdot 2H_2O$ (10^{-6}–10^{-7}). For a single crystal of the 1-D "black" $K_2[Ni(dto)_2]$ Λ is significantly higher (10^{-6}) along the stacking direction than is found for powder conditions. Thus, for a $Li_2[Ni(dto)_2]$ single crystal, values of about $10^{-4}\,\Omega^{-1}\,cm^{-1}$ could be expected in this direction. The temperature dependence of "black" $K_2[Ni(dto)_2]$ indicates a semiconductor behaviour.

The complexes $(TTF)_2[M(dto)_2]$ (M = Pd, Pt) have been found to be insulators, whereas the metal(III) compounds $TTF[M(dto)_2]$ (M = Ni, Cu) are semiconductors showing conductivities of 1.2×10^{-4} and $1.1\times10^{-6}\,\Omega^{-1}\,cm^{-1}$, respectively [77].

The compounds $[(RE)_2(H_2O)_{2n}][Ni(dto)_2]_3]\cdot xH_2O$ (RE = La, Ce, Nd, Sm, Eu, Gd, Y, Dy, Er, Yb) [63] and $[Th(H_2O)_6][Ni(dto)_2]_2\cdot 6.5H_2O$ [69] exhibit conductivities in the range 10^{-8}–$2\times10^{-7}\,\Omega^{-1}\,cm^{-1}$; a value of $10^{-6}\,\Omega^{-1}\,cm^{-1}$ was measured for the one-dimensional compound $[NH_3(CH_2)_2NH_3][Ni(dto)_2]$ [75].

The compound $[\{[Mn(H_2O)_3](O_2C_2S_2)Cu(S_2C_2O_2)\}\cdot 4.5H_2O]_n$ reveals another remarkable property. It is the first molecular "one-dimensional ferrimagnetic compound" to be reported in the literature, containing alternating Cu(II) 1/2 spins and Mn(II) 5/2 spins (see Fig. 19) antiferromagnetically coupled [53,70,78,83] (see also Sect. D(iii)(c)).

(b) Syntheses of dto complexes

In general, the complexes are formed by direct metathetical reaction between an alkali salt (mainly potassium or caesium) of the ligand, i.e. K_2dto or Cs_2dto, dissolved in a suitable solvent, generally water, and an appropriate metal compound [2]. Sometimes the complexes can be separated from the starting "parent" complex or the aqueous ligand solution by extraction into a halocarbon solvent, e.g. CH_2Cl_2 or $CHCl_3$, containing coordinatively unsaturated species (or large "onium" ions, like

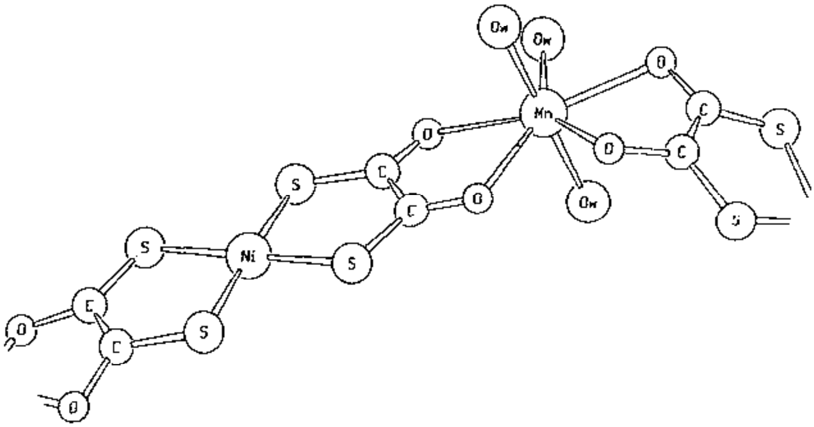

Fig. 19. Molecular structure of $\{[Mn(H_2O)_3](dto)M(dto)\cdot 4.5H_2O\}_n$ (M = Cu, Ni, Pd, Pt) [53].

Ph_4P^+ or Ph_4As^+). Representative examples are $\{M[(dto)M'(PR_3)_2]_3\}$ [27]. Large counter ions or special combinations of alkali with alkaline-earth or large ions can be used for precipitation of the complexes directly from the aqueous phase, e.g. $(BzPh_3P)_2[M(dto)_2]$ [28], $KBa[Co(dto)_3]\cdot 4H_2O$ [84] or $K(Me_3PhN)_2[Cr(dto)_3]\cdot H_2O$ [27]. All known dto compounds are listed in Table 7.

Several special syntheses should be emphasized:

SnX_4 "adducts" of some dto bis-chelates (e.g. $(BzPh_3P)_2[Ni(dtoSnCl_4)_2]$ [108] have been prepared by reaction of the parent bis-dithio-oxalates with the tin halides in acetone or CH_2Cl_2 [28] under anhydrous conditions.

Refluxing of violet $(Ph_4As)_3[Fe(dto)_3]\cdot 3CH_3NO_2$ in CH_2Cl_2 over 12 hours resulted in the formation of a brown product analyzed as $(Ph_4As)_4[Fe_2(dto)_5]$ [96] with EPR and IR spectra similar to those of the five-coordinate $(Ph_4P)_2[Fe(dto)_2X]$ complexes which are prepared by reaction of I_2, Br_2 or $FeCl_3$ with $[Fe(dto)_3]^{3-}$ in nitromethane, acetone or CH_2Cl_2 [96,98].

$(BzPh_3P)_2[Fe(dto)_2NO]$ has been isolated from a green solution as a crystalline product formed upon heating of violet $[Fe(dto)_3]^{3-}$ solution in the presence of either aqueous $NaNO_2$ or nitroalkanes (CH_3NO_2 or $C_2H_5NO_2$) [96].

Addition of polar solvents (e.g. DMF, CH_3CN, H_2O) or nucleophiles (e.g. Cl^-, Br^-, I^-, CN^- or SCN^-) turns the green colour of the CH_2Cl_2 solution of $[Cu(dtoSnCl_4)_2]^{2-}$ to violet, but only one compound could be isolated pure and crystallized, i.e. $(Ph_4As)_3P[Cu(dtoSnCl_4)_2Cl]$ [88]. Oxidation of $(BzPh_3P)_2[Cu(dto)_2]$ in CH_2Cl_2 in the dark with $FeCl_3\cdot 6H_2O$ as oxidant, dissolved in acetone, yielded the crystalline Cu(III) complex $BzPh_3P[Cu(dto)_2]\cdot CH_2Cl_2$, which can be transformed into the mixed ligand Cu(I) compound $BzPh_3P[Cu(dto)(PPh_3)_2]$ by Ph_3P in CH_2Cl_2 with COS being split off [51]. This complex is formed also via a compound described as "$(Ph_3P)_2Cu(S_2C_2O_2H)$" which was prepared by simultaneous reaction of $CuCl_2\cdot 2H_2O$ and Ph_3P with K_2dto in water–ethanol [29].

TABLE 7

1,2-Dithio-oxalate complexes

M	No.	Compound	M.p. (°C)	Colour (solid state)	Magnetism (μ_B)	IR (cm^{-1})					Electronic spectra ($\bar{\nu}_{max} \times 10^{-3}$ cm^{-1} (ε_0))		Ref.
						$\bar{\nu}_{C=O}$	$\bar{\nu}_{C-C+C-S}$	$\bar{\nu}_{C-S}$	$\bar{\nu}_{M-S(O)}$[y]	Others[y]			
Li	see compound 121												
Na	see compounds 122,123,168												
K	see compounds 2,7–9,21,27,45,48–50,56,69–72,78,83,91–93,96,97,102,111,113–115,118,124–126,187,210												
Cs	see compounds 57,60,65,66												
Ca	see compounds 49,51,92–94,111,112,144,145												
Sr	see compound 72												
Ba	see compounds 50,69–71,95,96,113–115,146,147,188												
Al	1	$(Ph_4As)_3[Al(dto)_3]$	110dec	Light brown	Diam.	1360s	1026s		370m				27
Al	2	$K_3[Al(dto)_3]$[a]											27
Al	3	$\{Al[(dto)Cu(PPh_3)_2]_3\}$	175dec	Brown	Diam.	1402s	1030s	607m			22.5	(11900)	27
								667sh					
Al	4	$\{Al[(dto)Ag(PPh_3)_2]_3\}$[b]	195dec	Light brown	Diam.	1395s	1025s	609m	366s		25.0	(3480)	27
								667sh			28.5	(10300)	
Ga	5	$\{Ga[(dto)Ag(PPh_3)_2]_3\}$	192dec	Olive green	Diam.	1390s							41
In	6	$(Ph_4As)_4[In_2(dto)_5]$	165dec	Yellow	Diam.	1610s							41
						1520s							
Sn	7	$K_2[Sn(dto)_3]$		Yellow		1598							29
Sn	8	$K\{Sn(dto)_2[(dto)Cu(PPh_3)_2]\}$		Orange		1371s			Sn–S				29
									332,323				
Sn	9	$K\{(dto)_2Sn[(dto)Cu(PTol_3)_2]\} \cdot (acetone)_2$				1627							33
						1371							
Sn	10–12	$\{XSn[(dto)Cu(PPh_3)_2]_3\}$[c,d]		Brown		1368			Sn–Cl				29
		X = Cl, Br, Me							350				
									Sn–Br				
									284				
Sn	13–15	$\{X_2Sn[(dto)Cu(PPh_3)_2]_2\}$[c,d]							Sn–Cl				29
		X-Cl and/or Me							350				

TABLE 7 (*continued*)

M	No.	Compound	M.p. (°C)	Colour (solid state)	Magnetism (μ_B)	IR (cm^{-1}) $\tilde{\nu}_{C=O}$	$\tilde{\nu}_{C-C+C-S}$	$\tilde{\nu}_{C-S}$	$\tilde{\nu}_{M-S(O)}$^{y}	Others^y	Electronic spectra ($\tilde{\nu}_{max}\times10^{-3}$ cm^{-1} (ε_0))		Ref.
Sn	16–18	BzPh$_3$P{X$_2$Cl$_2$Sn[(dto)Cu(PPh$_3$)$_2$]}^{c,d} X = Cl and/or Me				1402 1421 1447							29
Sn	19	{Sn$_2$Cl$_2$[(dto)Cu(Ph$_3$P)$_2$]$_2$}$_\infty$^{c}				1331			Sn–Cl 268				29
Sn	20	{Sn[(dto)Cu(PPh$_3$)$_2$]$_2$}^{c}											29
Sn	see also compounds 38,39,148–153,197–201,217,218												
Pb	see compound 154												
Cu	21	K$_2$[Cu(dto)$_2$]		Black	EPR								85,86, 87
Cu	22	(BzPh$_3$P)$_2$[Cu(dto)$_2$]	169–70	Brown	1.81(5)	1620s 1585s					24.6	(9130)	51,88
Cu	23	(Ph$_4$As)$_2$[Cu(dto)$_2$]^c			1.81								77(a),88
Cu	24	(Ph$_4$P)$_2$[Cu(dto)$_2$]^c									26.1	(11000)	51,87
Cu	25	(EtPh$_3$P)$_2$[Cu(dto)$_2$]^c									24.7	(8490)	51
Cu	26	(R$_4$N)$_2$[Cu(dto)$_2$] (R = Et, Bu)^c									25.0	(11400)	51,77(b)
Cu	27	[K(18-crown-6)]$_2$[Cu(dto)$_2$]·DMF^{c,e}		Dark green									51,52
Cu	28	[Mn(H$_2$O)$_3$][Cu(dto)$_2$]·4.5H$_2$O		Brown									53,78
Cu	29	[CuMn(dto)$_2$(H$_2$O)$_3$]^c		Black									53
Cu	30	[Cu(dto)(mnt)]$^{2-}$ ^{f}											86
Cu	31	BzPh$_3$P[Cu(dto)$_2$]·CH$_2$Cl$_2$O^g		Red	Diam.	1640 1590					16.3 26.2	(758) (22300)	51
Cu	32	Bu$_4$N[Cu(dto)$_2$]		Red							16.3 26.3	(614) (20000)	51
Cu	33	[(Ph$_3$P)$_2$N][Cu(dto)$_2$]^c		Red									52
Cu	34	TTF[Cu(dto)$_2$]		Dark green	EPR^h						12.4, 19.2 24.1^i		77

Cu	35	$\{[(Ph_3P)_2Cu]_2(dto)\}$	205–7	Orange	Diam.	1528s							27,88
Cu	36	$BzPh_3P[Cu(dto)(PPh_3)_2]^c$		Orange									29,51
Cu	37	$[(Ph_3P)_2Cu(dtoH)]$		Orange	Diam.	1536							29
Cu	38	$[(Ph_3P)_2N]_2[Cu(dtoSnCl_4)_2]$	169–72	Green	1.83(5)	1475s							88
Cu	39	$(Ph_4As)_3[Cu(dtoSnCl_4)_2Cl]$	161–2	Violet	Diam.								88
Cu	see also compounds 3,8–20,44,52,53,87,99,119,155												
Ag	40	$\{[(Ph_3P)_2Ag]_2(dto)\}$	168–70	Yellow brown	Diam.	1545s							27,45,
													88
Ag	see also compounds 4,5,54,55,88,100,101,156,157												
Au	41	$K[Au(dto)_2]$									31.0sh		89
											36.5	(16000)	
											41.5sh		
Au	42	$\{[(Ph_3P)Au]_2(dto)\}$	151	Light yellow									45
Zn	43	$(Ph_4As)_2[Zn(dto)_2]$	195–198	Light yellow	Diam.	1610s	1025		327m				27,54
Zn	44	$\{Zn[(dto)Cu(PPh_3)_2]_2\}$	150dec	Brown	Diam.	1475s					23.7	(7500)	27,59
Zn	45	$K_2[Zn(dto)_2]^a$											27
Zn	see also compound 177												
Y, La, Ce, Nd, Sm, Eu, Gd, Dy, Er, Yb see compounds 158–173													
Th	see compound 174												
Zr	46	$[Zr(dto)_4]^{4-\ a,c}$											27
V	47	$(Ph_4As)_2[VO(dto)_2]$	112–114	Dark green	EPR	1630s	1070s			V–O	16.8	(140)	42,90
						1580s	915m			1010s	26.8	(1440)	
											31.3	(4790)	
											34.3	(7690)	
Cr	48	$K(Me_3PhN)[Cr(dto)_3]\cdot H_2O$	180dec	Dark green	3.85(3)	1570s	1050s		325s		17.0	(433)	27
											21.9	(1060)	
Cr	49	$d,l\text{-}KCa[Cr(dto)_3]\cdot 6H_2O$		Dark green	3.74						17.0	(435)	91,92,
											21.9	(1028)	93
											34.7	(26900)	
Cr	50	$KBa[Cr(dto)_3]\cdot 4H_2O$			3.89								91,92
Cr	51	$Ca[Co(en)_2(NO_2)_2][Cr(dto)_3]\cdot 2H_2O^{c,k}$		Green									92
Cr	52	$\{Cr[(dto)Cu(PPh_3)_2]_3\}^l$	175dec	Brown	3.86(3)	1508s	1050s	594w	339s		24.4	(14200)	27
Cr	53	$\{Cr[(dto)Cu(PPh_3)_2]_3\}^m$	190dec	Brown	3.79(3)	1372s	1120w	663m	370s		21.7	(14700)	27

TABLE 7 (*continued*)

M	No.	Compound	M.p. (°C)	Colour (solid state)	Magnetism (μ_B)	IR (cm^{-1})					Electronic spectra ($\tilde{\nu}_{max} \times 10^{-3}$ cm^{-1} (ε_0))		Ref.
						$\tilde{\nu}_{C=O}$	$\tilde{\nu}_{C-C+C-S}$	$\tilde{\nu}_{C-S}$	$\tilde{\nu}_{M-S(O)}$[y]	Others[y]			
Cr	54	$\{Cr[(dto)Ag(PPh_3)_2]_3\}$[l]	131dec	Light brown	3.86(5)	1622m 1440s 1572s			325s 370s		16.7 20.8 31.3	(456) (1910) (29900)	27
Cr	55	$\{Cr[(dto)Ag(PPh_3)_2]_3\}$[m]	174–177 dec	Light brown	3.95(5)	1370s	1120w	663m	375s		17.2 22.2 32.8	(365) (3500) (47800)	27
Cr	56	$K_3[Cr(dto)_3]$[a]											27
Mo	57	$Cs_2[Mo_2O_2S_2(dto)_2]$		Olive green		1638vs 1620vs	1070s			Mo–O$_t$ 952 919			21
Mo	58	$(Ph_4P)_2[Mo_2O_2S_2(dto)_2]$				1631s 1637s			Mo=O 960s Mo–S$_b$ 452w		330sh 290sh 266sh		94
Mo	59	$(Ph_4P)_2[Mo_2O_2S_4(dto)]$				1630s			Mo=O 942m 956s Mo–S$_b$ 466		462br 330sh 290sh 265sh		94
Mo	60	$Cs_2[MoO(dto)_2]\cdot H_2O$		Red[n]		1612 1590	1045	920		Mo–O$_t$ 949			39
Mn	61	$\{[Mn(CO)_5]_2(dto)\}$[e]											25
Mn	see also compounds 28,29,175,202,219[o]												
Tc	62a	$(Ph_4As)_2[TcN(dto)_2]$	215dec	Pale purple		1612	1079			Tc–N 1071m			55
Tc	62b	different modification	142–144	Violet		1620				1045			56

Tc	63	$Bu_4N[TcO(dto)_2]$	126–127	Burgundy	0.34/0.17^p				Tc–O$_t$	20.0sh		95
				Maroon					972	20.8	(275)	
										24.4sh		
										26.7	(3400)	
										33.6	(14700)	
Tc	64	$Ph_4As[TcO(dto)_2]$		Red brown					Tc–O$_t$	19.6sh		55,95
									980	20.8	(275)	
										24.4sh		
										26.7	(3310)	
										33.7	(14600)	
Re	65	$Cs_4\{[Re(CO)_3(dto)]_2(dto)$		Red		1590s	1065m	935w, 542m				26
						1559vs		818s, 512m				
Re	66	$Cs[ReO(dto)_2]$		Brown red		1665vs	1060vs	548m	Re–O$_t$			26
						1640vs			915m			
Re	67	$Bu_4N[ReO(dto)_2]$	137–138	Red brown	1.46/0.99^p				Re–O$_t$	19.2sh		95
									990	21.1	(340)	
										22.3	(330)	
										23.9	(480)	
										29.4sh		
										34.3	(18460)	
Re	68	$Ph_3MeAs[ReO(dto)_2]$							Re–O$_t$	19.2sh		95
									991	21.0	(300)	
										23.9	(430)	
										34.0	(18300)	
Fe	69	$KBa[Fe(dto)_3]\cdot 3H_2O$	180dec		2.35(5)	1550s						96
						1516s						
Fe	70	$KBa[Fe(dto)_3]\cdot 4H_2O$		Dark brown	2.95							92
Fe	71	$KBa[Fe(dto)_3]\cdot 6H_2O$			2.28					13.0sh	(124)	91
										18.3	(2605)	
										20.9	(2455)	
					2.36	1553						97
						1520						
Fe	72	$KSr[Fe(dto)_3]\cdot H_2O$			2.21	1562						97
						1520						

TABLE 7 (*continued*)

M	No.	Compound	M.p. (°C)	Colour (solid state)	Magnetism (μ_B)	IR (cm^{-1}) $\bar{\nu}_{C=O}$	$\bar{\nu}_{C-C+C-S}$	$\bar{\nu}_{C-S}$	$\bar{\nu}_{M-S(O)}$[y]	Others[y]	Electronic spectra ($\bar{\nu}_{max} \times 10^{-3}$ cm^{-1} (ε_0))	Ref.
Fe	73	$(Ph_4P)_3[Fe(dto)_3]$[c]										87,98
Fe	74	$(Ph_4As)_3[Fe(dto)_3]\cdot 3CH_3NO_2$	104–107	Violet	2.30(5)	1622sh	1046		300			27,96
						1561s						
					2.93	1630						97
						1560						
Fe	75	$(PhNH_3)_3[Fe(dto)_3]\cdot H_2O$		Black	2.61	1580						97
						1510						
Fe	76	$[Co(en)_3][Fe(dto)_3]$			2.35							92
Fe	77	$[Co(en)_3][Fe(dto)_3]\cdot H_2O$			2.34	1575						97
						1518						
Fe	78	$K_3[Fe(dto)_3]$[c]										27,87
Fe	79	$(Ph_4As)_4[Fe_2(dto)_5]$	127–130	Brown	3.5(2)	1615s, br						96
Fe	80	$(Ph_4P)_2[Fe(dto)_2I]$	230dec		4.03	1615s						96,98
Fe	81	$(Ph_4P)_2[Fe(dto)_2X]$			EPR							98
	82	X = Cl, Br										
Fe	83	$\{K_2[Fe(dto)_2NO]\cdot H_2O\}_2$		Black						N–O		57
										1665		
Fe	84	$(BzPh_3P)_2[Fe(dto)_2NO]$	158–161	Green	2.22(5)	1585s, br				N–O		96,99,
										1685		100
Fe	85	$(Et_4N)_2[Fe(dto)_2NO]$			2.24	1558				N–O		97
										1688		
Fe	86	$(Bu_4N)_2[Fe(dto)_2NO]$			2.30	1590						97
Fe	87	$\{Fe[(dto)Cu(PPh_3)_2]_3\}$	135–136	Black	5.93(5)	1382s		604m	312s			27,96,
								650m				97,101
Fe	88	$\{Fe[(dto)Ag(PPh_3)_2]_3\}$	145–147	Black	5.81(5)	1380s		603m	314s, br			27,96
								653m				97,101
Fe	89	$(PhNH_3)_2[Fe(dto)_2]\cdot H_2O$[q]		Brown red								84

Ru	90	$(Ph_4As)_3[Ru(dto)_3]^c$			EPR						102
Co	91	$K_3[Co(dto)_3]\cdot 2H_2O^c$		Dark brown							27,84
Co	92	$KCa[Co(dto)_3]\cdot 6H_2O$		Dark brown	Diam.				17.7	(1263)	91,103
									22.0	(4725)	
Co	93	$(+)_{589}$-$KCa[Co(dto)_3]^c$		Burgundy							58
Co	94	$Ca[Co(en)_2(NO_2)_2][Co(dto)_3]\cdot H_2O^{c,k}$									92
Co	95	$KBa[Co(dto)_3]\cdot 4H_2O$ or $2H_2O^c$		Reddish brown							84
Co	96	*d*- and *l*-$KBa[Co(dto)_2]\cdot 5H_2O$		Dark brown							92
		$(+)_{546}$-$KBa[Co(dto)_3]\cdot 5H_2O$							35.5	(29500)	93
Co	97	$K(Me_3PhN)_2[Co(dto)_3]$	245dec	Brown	Diam.				17.7	(680)	27
									21.9	(2950)	
Co	98	$(PhNH_3)_3[Co(dto)_3]^c$		Dark brown							84
Co	99	$\{Co[(dto)Cu(PPh_3)_2]_3\}$	161–164	Brown	Diam.	1498s	1100s	344m	20.4	(7500)	27
			dec						27.0	(25500)	
Co	100	$\{Co[(dto)Ag(PPh_3)_2]_3\}$	130dec	Light brown	Diam.	1608w	1081sh	343s, br	17.2	(912)	27
						1530s			20.4	(2870)	
Co	101	$\{Co[(dto)Ag(PPh_3)_4]_3\}$	159dec	Dark brown	Diam.	1583s	1045^q	329m			27
						1527s					
Co	102	$A_2[Co(dto)_2]^q$ A = K, Ph_4P									87
Co	103	$[Co(en)_2(dto)]Cl\cdot 2H_2O$				1600	1070				93
Co	104	$[Co(en)_2(dto)]Cl$		Brown		1569	1055		19.7	(224)	36,93
									26.8	(1340)	
									35.9	(16400)	
									40.0	(18500)	
Co	105–110	$[Co(phen)_2(dto)]X\cdot nH_2O$	>190dec	Orange, red		≈1600	≈1070		≈19.0		104
		X = Cl(n = 2), Br(1), I(1),		or brown					≈27.8		
		NO_3(1), ClO_4(0), CH_3COO(3)							≈33.3sh		
Co	see also compounds 51,76,77,94,112										
Rh	111	$KCa[Rh(dto)_3]\cdot 4H_2O$		Yellow							92
Rh	112	$Ca[Co(en)_2(NO_2)_2[Rh(dto)_3]\cdot H_2O^{c,k}$		Yellow							92
Rh	113	$KBa[Rh(dto)_3]\cdot 4H_2O^c$		Intense yellow							84
Rh	114	*d*- and *l*-$KBa[Rh(dto)_3]\cdot 6H_2O^c$									92
Rh	115	$(+)_{546}$-$KBa[Rh(dto)_3]\cdot 6H_2O^c$									93

TABLE 7 (*continued*)

M	No.	Compound	M.p. (°C)	Colour (solid state)	Magnetism (μ_B)	IR (cm^{-1})					Electronic spectra ($\tilde{\nu}_{max} \times 10^{-3}$ cm^{-1} (ε_0))		Ref.
						$\tilde{\nu}_{C=O}$	$\tilde{\nu}_{C-C+C-S}$	$\tilde{\nu}_{C-S}$	$\tilde{\nu}_{M-S(O)}{}^y$	Others^y			
Rh	116	$(PhNH_3)_3[Rh(dto)_3]\cdot H_2O^c$		Intense yellow									84
Rh	117	$(Ph_4As)_3[Rh(dto)_3]\cdot 3CH_3NO_2$	104dec	Brown	Diam.	1558s	1043m		307m				27
									290m				
Rh	118	$K_3[Rh(dto)_3]^a$											27
Rh	119	$\{Rh[(dto)Cu(PPh_3)_2]_3\}$	170dec	Brown	Diam.	1503s	1098s		321m				27
Ni	120	"$H_2[Ni(dto)_2]$"^{r}											84
Ni	121	$Li_2[Ni(dto)_2]\cdot 2H_2O^e$											59
Ni	122	$Na_2[Ni(dto)_2]\cdot 2H_2O^e$											59
Ni	123	$Na_2[Ni(dto)_2]\cdot 2.5H_2O^c$		Black									84
Ni	124	$K_2[Ni(dto)_2]$"red form"		Dark red	Diam.	1602	1084		362		≈17.7		2,3,
				to black		1585					≈19.8		31,60,
													84,86,
													105,106
Ni	125	$K_2[Ni(dto)_2]$"black form"		Black		1505	1144		374				31,60
						1490							
Ni	126	$K_2[Ni(dto)_2I]^f$		(Blue)							≈16.5		60
Ni	127	$(NH_4)_2[Ni(dto)_2]\cdot 4H_2O^c$		Black									84
Ni	128	$(Et_4N)_2[Ni(dto)_2]^c$											77b
Ni	129	$(Bu_4N)_2[Ni(dto)_2]$									17.7sh	(1300)	89
											19.9	(3700)	
											33.4	(24000)	
											38.6	(18800)	
											44.4	(16700)	
Ni	130	$(PhNH_3)_2[Ni(dto)_2]^c$		Reddish brown									84
Ni	131	$(NC_4H_4NH)_2[Ni(dto)_2]^{c,a}$		Black									73
Ni	132	$(C_5H_5NH)_2[Ni(dto)_2]^a$		Black		1575vs	1090vs	535w	368s				74a
									410m				

Ni	133	$(3\text{-Me-}C_5H_4NH)_2[Ni(dto)_2]^{a}$		Black		1560s	1090vs	530w	365s 415m				74a
Ni	134	$(3\text{-Et-}C_5H_4NH)_2[Ni(dto)_2]^{a}$		Black		1575vs	1087s	575w	360s 415m				74a
Ni	135	$(4\text{-Me-}C_5H_4NH)_2[Ni(dto)_2]^{a,b}$		Black		1590vs	1090vs	525m	365vs 409m				73,74a
Ni	136	$(4\text{-Et-}C_5H_4NH)_2[Ni(dto)_2]^{a}$		Black		1595vs	1090s	535s	360vs 414m				74a
Ni	137	$[H_3N(CH_2)_2NH_3][Ni(dto)_2]^{a,b}$		Brown–red									75
Ni	138	$[C_{12}N_2H_{12}][Ni(dto)_2]^{a,e}$		Dark red									76
Ni	139	$(Ph_4P)_2[Ni(dto)_2]^{a}$											87
Ni	140	$(Ph_4P)_2[Ni(dto)_2]\cdot CH_3NO_2$	285										107
Ni	141	$(BzPh_3P)_2[Ni(dto)_2]$	255–256	Dark red	Diam.	1605s 1588s	1050s	614m	349s		17.8sh 19.9 32.7	(2300) (3500) (18500)	28
Ni	142	$(Ph_4As)_2[Ni(dto)_2]$				1605s 1588s	1050s	614m	349s		17.8 19.9 32.7	(2300) (3500) (18500)	27
Ni	143	$TTF[Ni(dto)_2]^{c,d}$		Dark blue									77b
Ni	144	$[Ca(H_2O)_4][Ni(dto)_2]\cdot 2H_2O^{e}$		Red									61
Ni	145	$[Ca_3(H_2O)_8(C_2O_4)][Ni(dto)_2]_2\cdot 6H_2O^{e}$		Black									61
Ni	146	$Ba[Ni(dto)_2]\cdot 4H_2O^{c}$		Black									84
Ni	147	$Ba[Ni(dto)_2]\cdot 6H_2O^{c}$		Black									62
Ni	148	$(BzPh_3P)_2[Ni(dto)(dtoSnF_4)]^{f}$	185–186	Blue	Diam.	1640s 1625s 1460s	1050m 1025w	649w 615sh	378m 365m	Sn–X 600s 581s 537 327 240 212			28
Ni	149	$(BzPh_3P)_2[Ni(dto)(dtoSnCl_4)]\cdot H_2O^{f,g,h}$	163–164	Blue	Diam.	1640s 1613s 1445s	1052m 1025w	645w 614m	385m	363s 328br 221s 184s 160s	15.2 15.9 18.2sh 33.2sh	(3200) (3200)	28,108

TABLE 7 (*continued*)

M	No.	Compound	M.p. (°C)	Colour (solid state)	Magnetism (μ_B)	IR (cm^{-1}) $\tilde{\nu}_{C=O}$	$\tilde{\nu}_{C=C+C-S}$	$\tilde{\nu}_{C=S}$	$\tilde{\nu}_{M-S(O)}{}^{y}$	Others^{y}	Electronic spectra ($\tilde{\nu}_{max}\times10^{-3}$ cm^{-1} (ε_0))		Ref.
Ni	150	$(Ph_4P)_2[Ni(dto)(dtoSnCl_4)]^{t}$	204		Diam.								107
Ni	151	$(BzPh_3P)_2[Ni(dtoSnCl_4)_2]^{u}$	219–220	Blue	Diam.	1469s	1150m	628m	378s	362s	16.0	(6900)	28,108
										353s	17.2	(4900)	
										333s	18.5	(3300)	
										218s	32.5	(49000)	
										173s			
										156s			
Ni	152	$(BzPh_3P)_2[Ni(dtoSnBr_4)_2]^{v}$	196–197	Blue	Diam.	1460s	1143m	626m	375s	246s	16.0	(6200)	28
										235s	17.2	(4200)	
										227sh	18.6	(2800)	
										176s	27.8	(16500)	
										131s	32.3	(37000)	
										98s			
Ni	153	$(BzPh_3P)_2[Ni(dtoSnI_4)_2]$	135–136	Green	Diam.	1470s	1140m	626m	375s	196s	15.9	(5300)	28,30
										186s	18.5	(2800)	
										180s	27.9	(17500)	
										132s	33.0	(41500)	
										105s			
Ni	154	$Pb[Ni(dto)_2]\cdot2H_2O^{c}$											84
Ni	155	$\{Ni[(dto)Cu(PPh_3)_2]_2\}$	176dec	Violet	Diam.	1528s	1102s		371s		16.5	(5690)	27
											17.7	(5910)	
											19.1	(5970)	
Ni	156	$\{Ni[(dto)Ag(PPh_3)_2]_2\}$	165dec	Red	Diam.	1653s	1034s		345s		20.1	(3000)	27
						1628s							
Ni	157	$\{Ni[(dto)Ag(PPh_3)_4]_2\}$	170dec	Red	Diam.	1603s,br	1051s		348				27

Ni	158–167	$[RE(H_2O)_n]_2[Ni(dto)_2]_3 \cdot xH_2O^e$		Black								63,64,
		$n=5$: RE = Y, La, Ce, Nd,										65
		Sm, Eu, Gd, Dy										
		$n=4$: RE = Er, Yb										
		$9.5 < x < 11.5$										
Ni	168	$Na[La(H_2O)_4(C_2O_4)[Ni(dto)_2]_2 \cdot 4.2H_2O^e$		Black								65
Ni	169	$[Yb(C_2O_4)(H_2O)][Ni(dto)_2] \cdot 1.5H_2O^e$		Black								65
Ni	170	$[Ce_2(H_2O)_{10}(C_4O_4)][Ni(dto)_2]_2 \cdot 5.2H_2O^e$		Black								67
Ni	171	$[La(H_2O)_4(glycine)]_2$-$[Ni(dto)_2]_3$ glycine$\cdot 7H_2O^e$										66
Ni	172	$[Yb(H_2O)_2(glycine)_2]_2$-$[Ni(dto)_2]_3 \cdot 8H_2O^e$										66
Ni	173	$\{[Ce(H_2O)_3(\beta\text{-alanine})]_2(C_2O_4)\}$-$[Ni(dto)_2]_2 \cdot 6H_2O^e$		Black								68
Ni	174	$[Th(H_2O)_6][Ni(dto)_2]_2 \cdot 6.5H_2O^e$		Black								69
Ni	175	$[Mn(H_2O)_3][Ni(dto)_2] \cdot 4.5H_2O$		Dark red	Diam.							53,70
Ni	176	$[(en)_2Ni(dto)Ni(dto)]$		Purple	2.08	1605						71
						1588						
Ni	177	$Zn[Ni(dto)_2] \cdot 2.08H_2O$		Black	1.02							72
Ni	178	$[Ni(dto)(Et_2PCH_2CH_2PEt_2)]^w$	296	Yellow		1640						46b
Ni	179	$[Ni(dto)(Ph_2PCH_2CH_2PPh_2)]^w$				1638						46b,109
Ni	180	$[Ni(dto)(PMe_3)_2]$		Red–brown		1630						46b
Ni	181	$[Ni(dto)(CH_3OCH_2CH_2OCH_3)]^c$										46b
Ni	182–185	$[Ni(dto)L]^{2-}$										86
		L = cdc, *i*-mnt, cpd, mnt^{a,x}										
Ni	186	$[Ni(dto)(CN)_2]^{2-}$ ^{a}										110,111
Pd	187	$K_2[Pd(dto)_2]^c$		Orange								3,53
				Yellow								84,87,
												105,106
Pd	188	$Ba[Pd(dto)_2] \cdot 3H_2O^c$		Orange								84
Pd	189	$(PhNH_3)_2[Pd(dto)_2]^c$		Yellow								84
Pd	190	$[Et_4N)_2[Pd(dto)_2]^c$		Dark blue								77
Pd	191	$[Bu_4N)_2[Pd(dto)_2]$								25.1	(7200)	89
										36.4	(42000)	
										41.3	(17000)	
Pd	192	$(BzPh_3P)_2[Pd(dto)_2]$	243–4	Yellow	Diam.	1618s	1048m	614m	317s	25.1	(7200)	28
						1590s				36.4	(42000)	

TABLE 7 (*continued*)

M	No.	Compound	M.p. (°C)	Colour (solid state)	Magnetism (μ_B)	IR (cm^{-1})					Electronic spectra ($\tilde{\nu}_{max} \times 10^{-3}$ cm^{-1} (ε_0))		Ref.
						$\tilde{\nu}_{C=O}$	$\tilde{\nu}_{C-C+C-S}$	$\tilde{\nu}_{C-S}$	$\tilde{\nu}_{M-S(O)}$^{y}	Others^{y}			
											41.3	(17000)	
Pd	193	$(Ph_4As)_2[Pd(dto)_2]$		Yellow									74b
Pd	194	$(Ph_4P)_2[Pd(dto)_2]^{c}$											87
Pd	195	$(Ph_4P)_2[Pd(dto)_2]\cdot CH_3NO_2$	227										107
Pd	196	$(TTF)_2[Pd(dto)_2]^{e}$		Dark brown	EPR^{h}						12.4,19.2, 25.6^{e}		77
Pd	197	$(BzPh_3P)_2[Pd(dto)(dtoSnCl_4)]^{t,y}$	168–169	Orange	Diam.	1635s 1612s 1448s	1050m	642m 628m	261m 267m	Sn–X 355s 331s 219s 168s 155s	22.5 23.5 27.0	(5300) (5200) (3600)	28,108
Pd	198	$(Ph_4As)_2[Pd(dto)(dtoSnCl_4)]$	201–202		Diam.	1623s 1580m 1480s 1450s					22.5 23.5 27.0	(5300) (5200) (3600)	108
Pd	199	$(BzPh_3P)_2[Pd(dtoSnCl_4)_2]^{t,y}$	219–221	Orange	Diam.	1465s	1150s	628m		355s 327s 216s 169s 156s	22.2sh 24.1 27.4sh	(7800) (12800) (8200)	28,108
Pd	200	$(BzPh_3P)_2[Pd(dtoSnBr_4)_2]$	209–210	Orange-red	Diam.	1460s	1143m	626w	331s	248s 234s 178s 131s 98s	22.2sh 23.8 26.2sh	(8600) (13200) (9100)	28

Pd	201	$(BzPh_3P)_2[Pd(dtoSnI_4)_2]$	152–153	Red	Diam.	1455s	1144m	625w	329s	194s 188s 180s 131s 104s	22.0 27.6	(2700) (5100)	28
Pd	202	$[Mn(H_2O)_3][Pd(dto)_2]\cdot4.5H_2O$		Orange	Diam.								53,78
Pd	203	$[Pd(dto)(Et_2PCH_2CH_2PEt_2)]^m$		Yellow		1632							46b
Pd	204	$[Pd(dto)(Ph_2PCH_2CH_2PPh_2)]$				1632							46b
Pd	205	$[Pd(dto)(PMe_3)_2]$		Yellow		1636							46b
Pd	206	$[Pd_3(\mu_3\text{-}S)_2(dto)(PMe_3)_4]^c$		Orange									46b
Pd	207–208	$[Pd(dto)L]^{2-}$ L = ned, *i*-mnt^{a,c}											112
Pd	209	$[Pd(dto)(CN)_2]^{2-\ a}$											112
Pt	210	$K_2[Pt(dto)_2]^c$		Dark red									3,53, 87,105, 106
Pt	211	$(Et_4N)_2[Pt(dto)_2]^c$											77
Pt	212	$(Bu_4N)_2[Pt(dto)_2]$									21.6 23.1sh 23.4 30.0 41.7 45.5	(2500) (8500) (1000) (26000) (25000)	89
Pt	213	$(Ph_4P)_2[Pt(dto)_2]^c$											87
Pt	214	$(Ph_4P)_3[Pt(dto)_2]\cdot2CH_3NO_2$	219										107
Pt	215	$(TTF)_2[Pt(dto)_2]^e$		Dark brown	EPR^b	–					12.4, 19.2, 24.1^e		77
Pt	216	$(TTF)_3[Pt(dto)_2]^e$		Black	EPR^b	–					12.4, 19.2, 24.1^e		77
Pt	217	$[Pt(dto)(dtoSnCl_4)]^{2-\ a,c}$											107
Pt	218	$[Pt(dtoSnCl_4)_2]^{2-\ a,c}$											107
Pt	219	$[Mn(H_2O)_3][Pt(dto)_2]\cdot4.5H_2O$		Black									53
Pt	220	$[Pt(dto)(Et_2PCH_2CH_2PEt_2)]^m$				1635							46b
Pt	221	$[Pt(dto)(Ph_2PCH_2CH_2PPh_2)]^m$				1638							46b
Pt	222	$[Pt(dto)(PMe_3)_2]^m$				1639							46b

TABLE 7 (*continued*)

---

[a] Not isolated in the solid state.

[b] Reported as also containing two molecules of $CHCl_3$.

[c] No further data reported.

[d] Some IR absorptions are given.

[e] Only X-ray structure.

[f] Detailed susceptibility and magnetization studies: quasi-one-dimensional ferrimagnetic chain; M^T vs. T presents a minimum at 130 K and a maximum at 7.5 K. Magnetization data at 1.3 and 4.2 K in the field range 0–5 T are consistent with an antiferromagnetic interaction between Cu(II) and Mn(II) through the dto bridge [83].

[g] First by mistake reported as $BzPh_3P[Cu(dto)(COS)_2]\cdot CH_2Cl_2$; also as the Ph_4As^+ salt [88].

[h] Weak narrow signal with a g value of ca. 2.003, typical of TTF radical cations.

[i] The IR spectrum is presented as a picture.

[j] Diffuse reflectance.

[k] Diastereo-isomers were isolated.

[l] Cr–S, M–O (M = Cu, Ag) isomer.

[m] Cr–O, M–S (M = Cu, Ag) isomer.

[n] Red needles from water; blue powder from water/ethanol–ether.

[o] In [70] a compound $[Mn(H_2O)_3][Mn(dto)_2]\cdot 4.5H_2O$ (?) is mentioned in a footnote.

[p] Measured at 7250 or 14 000 G, respectively.

[q] Published composition seems to be incorrect; most likely it concerns a metal(III) tris-complex.

[r] Very unstable.

[s] $NC_4H_4NH^+$ = pyrazinium, $C_5H_5NH^+$ = pyridinium, 3-Me-$C_5H_4NH^+$ = 3-methylpyridinium, 3-Et-$C_5H_4NH^+$ = 3-ethylpyridinium, 4-Me-$C_5H_4NH^+$ = 4-methylpyridinium, 4-Et-$C_5H_4NH^+$ = 4-ethylpyridinium, $C_{12}N_2H_{12}^{2+}$ = 6,7-dihydrodipyrido[1,2-*a*:2′1′-*c*]pyrazinium, TTF^+-tetrathiafulvalenium.

[t] The paramagnetic metal(I) species $[Ni(dto)(dtoSnF_4)]^{3-}$, $[M(dto)(dtoSnCl_4)]^{3-}$ and $[M(dtoSnCl_4]_2]^{3-}$ could be generated electrochemically in solution [28,107].

[u] In [108] reported without water.

[v] The first report [108] contains somewhat different spectroscopic data.

[w] The paramagnetic metal(I) species $[M(dto)(diphosphine)]^-$ or $[M(dto)(PR_3)_2]^-$ could be generated electrochemically in solution [46b,109].

[x] cdc = *N*-cyanodithiocarbimate, *i*-mnt = 1,1-dicyanoethene-2,2-dithiolate, cpd = 1-cyano-1-phenylethene-2,2-dithiolate, ned = 1-nitroethene-2,2-dithiolate, mnt = maleonitrile dithiolate.

[y] Subscripts: b = bridging ligand; t = terminal ligand.

In acetone, $K_2[Sn(dto)_3]$ reacts with $(Ph_3P)_3CuCl$ forming the complex $K\{Sn(dto)_2[(dto)Cu(PPh_3)_2]\}$, which can be transformed in CH_2Cl_2 by $(Ph_3P)_3CuX$ into $\{XSn[(dto)Cu(PPh_3)_2]_3\}$ (X = Cl, Br) [29]. A series $\{X_2Sn[(dto)Cu(PPh_3)_2]_2\}$ (X = Cl, Me) has been prepared starting with either Me_nSnCl_{4-n}, K_2dto and $(Ph_3P)_3CuCl$ in THF, water and CH_2Cl_2 or $\{Zn[(dto)Cu(PPh_3)_2]_2\}$ and Me_nSnCl_{4-n} in acetone. Obviously $\{MeSn[(dto)Cu(PPh_3)_2]_3\}$ can be prepared via $\{Me_2Sn[(dto)Cu(PPh_3)_2]_2\}$ using $[(PPh_3)_2Cu(dto)]^-$ [29].

A useful method for preparing binuclear compounds $\{(dto)[M(PPh_3)_2]_2\}$ (M = Cu, Ag) starts with a pyridine solution of $(Ph_3P)_3MCl$ in which K_2dto is suspended and subsequently dissolved by careful addition of water [45].

$Li_2[Ni(dto)_2]\cdot 2H_2O$ and $Na_2[Ni(dto)_2]\cdot 2H_2O$ are prepared from $K_2[Ni(dto)_2]$ using $LiClO_4$ or $NaClO_4$ in concentrated aqueous solutions [59]. The "black" form of $K_2[Ni(dto)_2]$ results from the "normal red" form by use of $K_2Cr_2O_7$ in aqueous solution [60] (see above).

Metal compounds MCl_2L_2 (M = Ni, Pd, Pt; L_2 = diphosphine or two phosphine ligands) react in suitable solvents, e.g. water, methanol or ethanol, to form mixed ligand species $[M(dto)L_2]$. It should be noted, however, that in the case of $[Ni(dto)(PMe_3)_2]$ this route is not successful because $[Ni(dto)_2]^{2-}$ is formed. Therefore the desired compound was synthesized via $[(CH_3OCH_2CH_2OCH_3)Ni(dto)]$ by ligand exchange using PMe_3. If the DMF solution of $[(PMe_3)_2Pd(dto)]$ is subjected to several heating and cooling cycles, thermolysis of the compound occurs and orange needles of $[Pd_3(\mu_3\text{-}S)_2(dto)(PMe_3)_4]$ can be separated [46(b)].

Usually, coordination polymers containing the nickel bis-dithio-oxalate unit $[Ni(dto)_2]^{2-}$ on the one hand and more or less "hard" coordination entities on the other crystallize when highly concentrated solutions of the water-soluble components are mixed; examples are: $[Ca(H_2O)_4]^{2+}$ [61], $[Ba(H_2O)_5]^{2+}$ [62], $[(RE)_2(H_2O)_{2n}]^{6+}$ with $n=5$ for Y, La, Ce, Nd, Sm, Eu and Gd and $n=4$ for Er and Yb [63,64], $[La(H_2O)_4(C_2O_4)]^+$ [65], $[La(H_2O)_4(^-O_2CCH_2NH_3{}^+]^{3+}$ [66], $[Yb(H_2O)_2(^-O_2CCH_2NH_3{}^+)_2]^{3+}$ [66], $[Ce_2(H_2O)_{10}(C_4O_4)]^{2+}$ [67], $\{[Ce(H_2O)_3(^-O_2CCH_2CH_2NH_3{}^+)]_2(C_2O_4)\}^{4+}$ (oxalate is formed by decomposition of dithio-oxalate during the reaction) [68], $[Yb(C_2O_4)]^+$ (also here oxalate is formed by decomposition of dithio-oxalate during preparation of the heterobimetallic compound in the presence of sodium maleate or maleic acid) [65], $[Th(H_2O)_6]^{4+}$ [69], $[Mn(H_2O)_3]^{2+}$ [53,70] (in this case the hard units can be linked also by the soft partner $[Pd(dto)_2]^{2-}$, $[Pt(dto)_2]^{2-}$ or $[Cu(dto)_2]^{2-}$ and $[Zn(H_2O)_2]^{2+}$ [72].

The compounds $(TTF)_m[M(dto)_2]$ ($m=1$, M = Cu, Ni; $m=2$, M = Pd, Pt; $m=3$, M = Pt), which are insoluble in common solvents, have been prepared by metathesis or slow interdiffusion of saturated acetonitrile solutions of $(TTF)_3(BF_4)_2$ and $A_2[M(dto)_2]$ (A = Ph_4As^+ or Et_4N^+) under inert conditions [77].

(c) *Magnetic properties; EPR and Mössbauer data*

The dto complexes behave as magnetically normal, i.e. they can be viewed as composed of innocent dto dianions and the metal ion in the corresponding electron configuration. Paramagnetic compounds are reported with V(IV) (as VO(II)), Cr(III), Tc(V) (as TcO(III) or TcN(II)), Re(V) (as ReO(III)), Fe(II) (as Fe(NO)(II)), Fe(III), Ru(III), Ni(II), Ni(I), Pd(I), Pt(I), Cu(II) and Cu(II)/Mn(II).

All chromium complexes show magnetic moments from 3.74 to 3.95 μ_B because of their three unpaired electrons, as expected [27,91].

$Bu_4N[TcO(dto)_2]$, $(Ph_4As)_2[TcN(dto)_2]$ and $Bu_4N[ReO(dto)_2]$ are weakly paramagnetic. The effective magnetic moments are field strength dependent (0.17–1.46 μ_B) and have been suggested to be due to temperature-independent paramagnetism, as found for some other d^2 configurations with local C_{4v} symmetry [56,95].

For iron(III) the question arises whether the compounds are high-spin, low-spin, medium-spin or spin-crossover systems. The magnetic moments of all Fe(III) tris-dithio-oxalate compounds containing different cations or solvate molecules fit more or less well the value expected for a low-spin complex (2.0–2.5 μ_B) [27,91,92,96,97,113] (presumably some workers had difficulties in obtaining pure samples of the complex salts [91]). The large negative Weiss constant for $KBa[Fe(dto)_3]\cdot 6H_2O$ (compare also $(Ph_4As)_3[Fe(dto)_3]\cdot CH_3NO_2$ [96]) first published by Carlin and Canziani [91] was confirmed later by other authors [97]. There is no evidence for spin-crossover behaviour. If, however, $[Fe(dto)_3]^{3-}$ was used as a "ligand" for the $[M(PPh_3)_2]^+$ cations (M = Cu, Ag), the high-spin compounds $\{Fe[(dto)M(PPh_3)_2]_3\}$ were formed. This is expected by analogy with the iron(III) oxalate complexes (which are high-spin) because the dto ligands flip from Fe—*S,S* chelation to Fe—*O,O* chelation (see above).

$(BzPh_3P)_2[Fe(dto)_2NO]$ exhibits a magnetic moment of 2.22 μ_B [96]. This suggests a structure similar to that known for the iron dithiocarbamate nitrosyl complexes having also one unpaired electron in the [Fe(NO)] core [114]. Analogies exist also between $[Fe(R_2dtc)_2X]$ compounds (X = halide ion) and $[Fe(dto)_2X]^{2-}$ ions [96,98]. The five-coordinated dithio-oxalate complex ions are paramagnetic down to 1.4 K, showing an intermediate spin of $S = 3/2$ as expected.

In contrast, the loosely bound dimer $\{K_2[Fe(dto)NO]\cdot H_2O\}_2$ exhibits strong intramolecular antiferrogmagnetic interactions via an unsymmetrical Fe_2S_2 unit (with two short and two rather long iron–sulphur distances) [57]. J was found to be $-23.8\ cm^{-1}$.

The magnetism of $(Ph_4As)_4[Fe_2(dto)_5]$ (3.5 μ_B) is rather surprising. One expects a strongly reduced amount because of antiferromagnetic interactions which should appear in the proposed bridging structure [96] (found for the indium compound $(Ph_4As)_4[In_2(dto)_5]$ [50]).

The polymeric mixed-metal copper–manganese complex $[CuMn(dto)_2(H_2O)_3]\cdot 4.5H_2O$, a quasi-one-dimensional compound, consists of chains $\cdots Cu(S_2C_2O_2)Mn(H_2O)_3(O_2C_2S_2)\cdots$, criss-crossing glide planes and stacking along these planes. Each layer of stacked chains is separated from the next one by intervening water molecules. The magnetic susceptibility of the compound shows a minimum at 130 K and a maximum at 7.5 K. The antiferromagnetic interaction between Cu(II) and Mn(II) through the dithio-oxalate bridges leads to "one-dimensional ferrimagnetism" ($J = -30.3$ cm^{-1}) [53,70,78,83].

The EPR spin Hamiltonian parameters of dithio-oxalate complexes are summarized in Table 8. The only single-crystal EPR studies on dto systems were carried out for $[Cu(dto)_2]^{2-}$ in different host lattices and for undiluted $\{Fe[(dto)Cu(PPh_3)_2]_3\}$. White and Belford studied the system $K_2[Cu/Ni(dto)_2]$ in the Q-band and analyzed the secondary ($\Delta m_I = 1$) transitions for the quadrupole coupling parameter which is $QD = 0.7 \times 10^{-4}$cm^{-1} [85]. The authors assign this small value (also found for other planar $Cu{-}S_4$ systems with the ligands isomaleonitriledithiolate and dithiocarbamate) to an effectively spherical symmetry caused by strong covalent nature of the Cu–S(σ) bond. In [117] the spin Hamiltonian parameters of $K_2[Cu/Ni(dto)_2]$ are compared with those of some other planar and tetrahedral CuS_4 species. As expected, the behaviour of $[Cu(dto)_2]^{2-}$ is markedly different in a $(Ph_4As)_2[Zn(dto)_2]$ single crystal with a tetrahedral ZnS_4 coordination sphere [54]. The copper guest, however, does not accept the structure of the host lattice completely [115]. The dihedral angle is found to be only about 10° ($(Ph_4As)_2[Zn(dto)_2]$: 86.8° [54]).

The EPR powder spectra of tetrathiafulvalenium salts $(TTF)_{1.0}[Cu(dto)_2]$, $(TTF)_2[M(dto)_2]$ (M = Pd, Pt) and $(TTF)_3[Pt(dto)_2]$ at room temperature show a weak, narrow signal with g values of about 2.003, typical for $TTF^{\cdot +}$ radical cations [77].

For $(Ph_4As)_3[Fe(dto)_3]\cdot 3CH_3NO_2$ no EPR spectra could be obtained, either at 300 or 78 K. However, at 1 K a strong signal has been observed for the $^2T_2$ ground state [96]. Later on the EPR spectrum could be obtained for $KBa[Fe(dto)_3]\cdot 3H_2O$ also at higher temperature [113]. The situation is similar for $[Ru(dto)_3]^{3-}$ [102]. Calculated resonance line positions and intensities are compared with the experimental EPR spectra of both isomorphic high-spin ($S = 5/2$) compounds $\{Fe[(dto)M(PPh_3)_2]_3\}$ (M = Cu as single crystal, M = Ag as powder) [101].

Five-coordinate iron(III) dithio-oxalato halides $(Ph_4P)_2[Fe(dto)_2X]$ show a behaviour expected for $S = 3/2$ with an axial character of the electronic spin Hamiltonian for X = I and increasing rhombicity for X = Br and Cl [98].

Compounds containing the anion $[Fe(dto)_2NO]^{2-}$ have been investigated in detail by EPR in liquid and rigid solution and as powder. The magnetic symmetry is axial. The spin Hamiltonian parameters are temperature- and solvent-dependent, indicating a vacant sixth site solvent coordination [99,100]. Addition of $SnCl_4$ under anhydrous conditions gives a ligand perturbation which shows that the unpaired electron is in an a_1 or a_2 type orbital (in C_{2v} symmetry, d_{z^2} or $d_{x^2-y^2}$).

Another five-coordinate complex containing one unpaired electron is $(Ph_4As)_2[VO(dto)_2]$ [90]. Its EPR parameters differ remarkably from those of other five-membered ring sulphur ligand (dithiolene) chelates. The differences could be caused by the nonrigidity of the dto ligands.

EPR is well suited to detect mixed-ligand species formed in solution [118] if

TABLE 8

EPR investigations of dithio-oxalate complexes (in the Q band)

Compound (system)	Solvent/state	Temperature (K)	Spin Hamiltonian parameters				Ref.
			g		A^a		
$K_2[Cu/Ni(dto)_2]$[b]	Single-crystal (and powder)	Ambient	g_z	2.0805(3)	A_z^{Cu}	−163.9(3)	85
			g_x	2.0197(3)	A_x	−42.4(3)	
			g_y	2.0191(3)	A_y	−41.6(3)	
$(Ph_4As)_2[^{63}Cu/Zn(dto)_2]$	Single-crystal	Ambient	g_1	2.086	A_1^{Cu}	−134.0	115
			g_2	2.021	A_2	−39.0	
			g_3	2.020	A_3	−29.0	
			g_{iso}	2.044	A_{iso}	−67.3	
$(Bu_4N)_2[Cu(dto)_2]$			g_0	2.043	a_0^{Cu}	76.7	116
$[Cu(dto)(n\text{-}bu_2btu)]^-$ [c]			g_0	2.060	a_0^{Cu}	77.6	116
$[Cu(dto)(i\text{-}bu_2bsu)]^-$ [c]			g_0	2.063	a_0^{Cu}	78.3	116
$(Ph_4As)_2[VO(dto)_2]$	Acetone	295	g_0	1.987(2)	a_0^V	75.9(1.0)	90
		133	g_z	1.982(2)	A_z	137.4(1.0)	
			g_y	1.985(3)	A_y	48.3(2.0)	
			g_x	1.990(3)	A_x	46.7(2.0)	
$[Ni(Ph_2PCH_2CH_2PPh_2)(dto)]^-$ [d]	CH_2Cl_2	233	g_0	2.091	a_0^P	90.8	109
		113	g_1	2.187	A_1	81.7	
			g_2	2.047	A_2	83.6	
			g_3	2.038	A_3	97.5	
$[Ni(dto)(dtoSnCl_4)]^{3-}$ [d]	CH_2Cl_2	293	g_0	2.0065	a_0^{Sn}	5.6	107
$[Ni(dtoSnCl_4)_2]^{3-}$ [d]	CH_2Cl_2	293	g_0	2.0010	a_0^{Sn}	4.6	107
$[Pd(dto)(dtoSnCl_4)]^{3-}$ [d]	CH_2Cl_2	293	g_0	2.0039	a_0^{Sn}	10.8	107
		113	g_1	1.994	A_1^{Sn}	9	
			g_2	2.006	A_2	14	
			g_3	2.011	A_3	9.5	
$[Pd(dtoSnCl_4)_2]^{3-}$ [d]	CH_2Cl_2	293	g_0	2.0032	a_0^{Sn}	5.1	107
$[Pt(dto)(dtoSnCl_4)]^{3-}$ [d]	CH_2Cl_2	293	g_0	2.007	a_0^e	11.0	107
		113	g_1	1.973	A_1	−13	
			g_2	2.011	A_2	23	
			g_3	2.016	A_3	23	
$[Pt(dtoSnCl_4)_2]^{3-}$ [d]	CH_2Cl_2	293	g_0	1.9982	a_0^e	12.7	107
$(Ph_4As)_3[Fe(dto)_3]\cdot 3CH_3NO_2$	Powder	1	one line (no data)				96
$KBa[Fe(dto)_3]\cdot H_2O$	Powder		$g_\parallel$	1.99			113

$\{Fe[(dto)Cu(PPh_3)_2]_3\}$	Single-crystal		**Line shape analysis**				**101**
$\{Fe[(dto)Ag(PPh_3)_2]_3\}$	Powder		**Line shape analysis**				**101**
$\{Fe[(dto)Ag(PPh_3)_2]_3\}$	Powder		**g**	**2.000(2)**			**96**
$(Ph_4P)_2[Fe(dto)_2Cl]$	Powder		g^f	2.06(1)			98
$(Ph_4P)_2[Fe(dto)_2Br]$	Powder		g^f	2.04(1)			98
$(Ph_4P)_2[Fe(dto)_2I]$	Powder		g^f	2.04(1)			98
$(BzPh_3P)_2[Fe(dto)_2NO]$	Frozen solution	193	g	2.0332(5)	A^N	14.3(1)	96
$(BzPh_3P)_2[Fe(dto)_2NO]$	[g]	ambient	g_0	2.0329– 2.0336	a_0^N	12.90– 13.27	100
$[Fe(dto)_2NO]^{2-}$	Methanol–glycerol (1:1)	298	g_0	2.0333(10)	a_0^N	12.6(1)	99
		113	$g_{\parallel}$	2.0162(5)	$A_{\parallel}$	15.6(1)	
			$g_{\perp}$	2.0345(15)	$A_{\perp}$	12.7(1)	
			g_{iso}	2.0284(10)	A_{iso}	13.7(1)	
	CH_2Cl_2	298	g_0	2.0337(10)	a_0^N	12.8(1)	
		223	g_0	2.0322(10)	a_0^N	13.2(1)	
$\{K_2[Fe(dto)_2NO]\cdot H_2O\}_2$	Powder	5–300	g^h	2.061			57
$(BzPh_3P)_2[Fe(dtoSnCl_4)_2NO]$	CH_2Cl_2	298	g_0	2.0359(10)	a_0	11.6(1)	99
		113	$g_{\parallel}$	2.0150(5)	$A_{\parallel}$	14.0(1)	
			$g_{\perp}$	2.0383(15)	$A_{\perp}$	10.9(1)	
			g_{iso}	2.0305(10)	A_{iso}	11.9(1)	
$[TcN(dto)_2]^{-}$ [i]	$CHCl_3$	130	$g_{\parallel}$	2.037(3)	$A_{\parallel}$	206.0(1.5)	56
$(Ph_4As)_3[Ru(dto)_3]$	$CHCl_3$–toluene	77	g_1	2.04			102
			g_2	2.04			
			g_3	1.98			

ccr121874L/14-10-92 13:11:03

---

[a] A values in 10^{-4} cm^{-1}.

[b] Quadrupole coupling constant $QD = 0.7 \times 10^{-4}$ cm^{-1}.

[c] n-bu$_2$btu = di-n-butylbenzoylthiourea; i-bu$_2$bsu = di-isobutylbenzoylselenourea.

[d] Electrochemically generated.

[e] Probably ^{195}Pt coupling.

[f] Determined by susceptibility data.

[g] 16 different solvents: methanol, HCONHMe, ethanol, n-propanol, n-butanol, tetrahydrothiophen-1,1-dioxide, $MeNO_2$, Me_2SO, propylene carbonate, MeCN, DMF, $PhNO_2$, acetone, pyridine, CH_2Cl_2, $CHCl_3$.

[h] Broad line.

[i] Generated by bromine oxidation; paramagnetic mixed-ligand (dto/bromide) compounds showing S_3Br, S_2Br_2 and SBr_3 coordination spheres are also detected.

the spin Hamiltonian parameters are changed strongly on moving from the starting complexes to mixed-ligand systems. $[Cu(dto)_2]^{2-}$, for example, reacts with copper(II) benzoylthioureas (e.g. 1,1-di-*n*-butyl-3-benzoylthiourea (*n*-bu)$_2$btu) or benzoylselenoureas (e.g. (*i*-bu)$_2$bsu) giving mixed-ligand chelates containing a five-membered (dto) and a six-membered ring [116].

Oxidation of $[TcN(dto)_2]^{2-}$ with Cl_2 or Br_2 yields paramagnetic (Tc(VI)) mixed ligand compounds which contain dto as well as the corresponding halide, detected by EPR [56].

A reversible one-step reduction (−1.19 V) of $[(Ph_2PCH_2CH_2PPh_2)Ni(dto)]$ in CH_2Cl_2 gives the corresponding paramagnetic anion with a d^9 configuration, giving rise to an EPR spectrum with the expected ^{31}P superhyperfine structure [109].

Unlike dithio-oxalato complexes, the $SnCl_4$ "adducts" also undergo well-defined reversible electrochemical reduction to d^9 species [107]. EPR spectra could be taken from the products obtained by in situ electrolysis. They consist of intense central lines with *g* values close to the free electron value and satellite lines due to hyperfine coupling with magnetic isotopes of tin. The closeness of the *g* values to the free electron value and the small degree of anisotropy in the *g* values for the frozen solutions are indicative of an essentially ligand-based orbital for the unpaired electron. The reason for the stabilization effect of $SnCl_4$ on the one-electron reduction products is a lowering of the energy of a π-antibonding orbital on the dto ligand. In $[(dto)M(dtoSnCl_4)]^{3-}$ the unpaired electron could be expected to reside mainly on the dto which is coordinated to the $SnCl_4$ unit. In $[M(dtoSnCl_4)_2]^{3-}$ (the π^* orbitals of both dto ligands are lowered! See Fig. 20 [28,108]), on the other hand, the electron should be delocalized over both dto ligands. Thus the spin density near the Sn nuclei is expected to be higher in the 1:1 than in the 1:2 complexes. This fact is reflected by a decrease in the Sn coupling constants on going from $[M(dto)(dtoSnCl_4)]^{3-}$ to $[M(dtoSnCl_4)_2]^{3-}$ (see Table 8).

As can be seen from Table 9, the shift values in the Mössbauer spectra of all Fe(III) dithio-oxalates lie in the expected range found also for 1,2-dithiolenes or dithiocarbamates, indicating that the extent of delocalization is similar in these systems [97]. Lower shift values are normally associated with low-spin configurations. $\{Fe[(dto)M(PPh_3)_2]_3\}$ complexes (*O,O*-chelation), however, formed by ligand flips from $[Fe(dto)_3]^{3-}$ (*S,S*-chelation) have the lowest values for Fe(III) dithio-oxalates despite their high-spin character. On the other hand, the expected lower isomer shift values for $[Fe(dto)_2NO]^{2-}$ could be verified, reflecting the powerful π-bonding character of the NO^+ group. The relatively large quadrupole splitting (≈ 1 mm s^{-1}) observed for $\{Fe[(dto)M(PPh_3)_2]_3\}$ (unexpected for spherically symmetric $^6A_1$ systems) confirms a considerable distortion from O_h symmetry [32].

Because the Fe(III) tris-dithio-oxalates exhibit no spin-crossover behaviour different quadrupole splittings (varying from 0.3 to 1.7 mm s^{-1}) should be the result of different degrees of distortion from octahedral symmetry in all cases.

The isomer shifts found for the complexes $(Ph_4P)_2[Fe(dto)_2X]$ (X = Cl, Br, I)

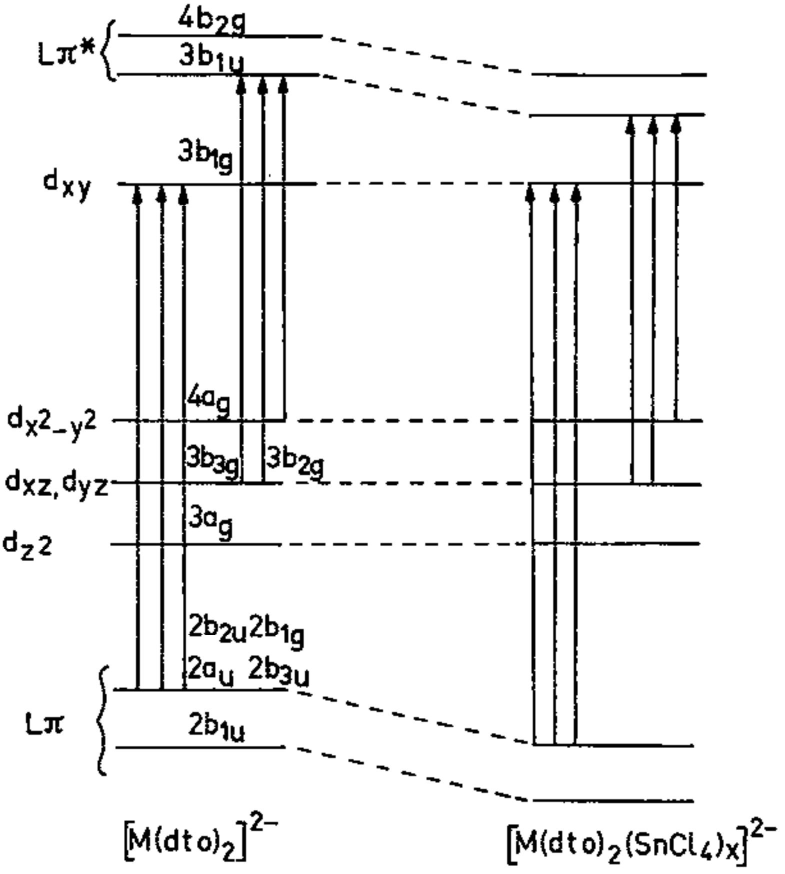

Fig. 20. Energy level diagram for $[M(dto)_2]^{2-}$ and $[M(dto)_2(SnCl_4)_x]^{2-}$ ($x=1,2$) [108].

lie between 0.25 and 0.30 mm s^{-1} (relative to metallic iron). They agree very well with those published for analogous five-membered chelate ring Fe(III) dithiolenes having $S=3/2$ (four-membered chelate ring compounds, e.g. $Fe(R_2dtc)_2X$, where R_2dtc signifies dithiocarbamate, show isomer shifts in the region of 0.5 mm s^{-1}), indicating substantial d electron delocalization in the ligand systems. The observed quadrupole splittings between 3.25 and 3.6 mm s^{-1} are the highest reported for intermediate spin complexes [98].

A mixture of ferric nitrate and potassium dithio-oxalate in aqueous solution at 77 K gives more than one iron species, the relative intensities of which vary with the Fe^{3+}/dto^{2-} ratio. The Mössbauer signals have been attributed to low-spin Fe(III) and also high-spin Fe(II) [97].

(d) Electronic spectra

Qualitative spectroscopic data of $[M(dto)_2]^{2-}$ chelates were first published by Cox et al. in 1935 [3]. The next paper did not follow until 1951. Its authors studied

TABLE 9

Mössbauer data of dithio-oxalate complexes

Compound	Temperature (K)	δ (mm s^{-1}) (vs. metallic iron)	ΔE_Q (mm s^{-1})	Ref.
$KBa[Fe(dto)_3]\cdot 6H_2O$	77	0.37	0.42	97
	196	0.33	0.35	
	298	0.27	0.31	
$KSr[Fe(dto)_3]\cdot H_2O$	4	0.37	1.06	97
	77	0.36	1.09	
	298	0.26	0.68	
$[Co(en)_3][Fe(dto)_3]\cdot H_2O$	77	0.40	1.68	97
	298	0.32	1.36	
	330	0.28	1.05	
$(PhNH_3)_3[Fe(dto)_3]\cdot H_2O$	4	0.40	1.27	97
	77	0.38	1.12	
	123	0.40	1.01	
	173	0.38	0.93	
	223	0.36	0.81	
	298	0.29	0.64	
$(PhNH_3)_3[Fe(dto)_3]\cdot H_2O$[a]	77	0.38	1.14	97
	298	0.29	0.64	
$(Ph_4As)_3[Fe(dto)_3]\cdot 3CH_3NO_2$	77	0.53	0.90	97
	298	0.43	0.95	
$\{Fe[(dto)Ag(PPh_3)_2]_3\}$	77	0.42	0.99	97
	298	0.24	0.87	
$\{Fe[(dto)Cu(PPh_3)_2]_3\}$	77	0.33	1.18	97
	298	0.24	1.17	
$(Et_4N)_2[Fe(dto)_2NO]$	77	0.29	1.04	97
$(Bu_4N)_2[Fe(dto)_2NO]$	4	0.29	1.05	97
	196	0.26	1.04	
	298	0.36	0.67	
$(Bu_4N)_2[Fe(dto)_2NO]$[a]	77	0.28	1.03	97
	298	0.35	0.68	
$(Ph_4P)_2[Fe(dto)_2Cl]$	4.2–77	0.25(5)	3.60(1)	98
$(Ph_4P)_2[Fe(dto)_2Br]$	4.2–77	0.29(2)	3.25(2)	98
$(Ph_4P)_2[Fe(dto)_2I]$	4.2–77	0.30(2)	3.33(2)	98

[a] Prepared from ferrous salt.

the absorption spectra of $K_2[M(dto)_2]$ (M = Ni, Pd, Pt) in solution and in the crystalline state [105].

Deskin compared the nickel complexes of dithio-oxalate, dithiomalonate and trithiocarbonate by UV–VIS spectroscopy and evaluated the formation constants $\log K_f$ in aqueous solution (total ionic strength 0.1), which gave a series: dto > dithiomalonate > trithiocarbonate. The $\log K_f$ of $[Ni(dto)_2]^{2-}$ (9.43) is also found to be markedly higher than that of $[Ni(ox)_2]^{2-}$ (6.51) [119], indicating that oxalate is a rather weaker ligand for Ni(II) than is dithio-oxalate. Deskin's value of the formation constant of $[Ni(dto)_2]^{2-}$ has been doubted by Pearson and Sweigart, who found a much higher value (16.1 ± 0.2) determined using three different methods in aqueous solution [86]. The formation of mixed ligand complexes containing the dto ligand has been followed spectrophotometrically, as well as the kinetics and mechanisms of the formation of $[Ni(dto)_2]^{2-}$. Ligand exchange reactions were also studied spectrophotometrically involving dto as nucleophile, as leaving group and as *trans* group in Ni(II), Pd(II) and Cu(II) complexes [17,86,110,112].

In 1964, Latham et al. came up with a detailed interpretation of the electronic spectra of the planar $(Bu_4N)_n[M(dto)_2]$ ($n=2$: M = Ni, Pd, Pt; $n=1$: M = Au) on the basis of a molecular orbital (MO) theory treatment [89]. Figure 20 shows the relative energies of the most important levels of $[Ni(dto)_2]^{2-}$ with an interchange of both $4a_g(d_{x^2y^2})$ and $3b_{3g}(d_{yz})$ metal orbitals proposed by Coucouvanis and co-workers [28]. The bands in the absorption spectrum (taken in acetonitrile) were assigned as follows: 44 400 cm^{-1} ($\varepsilon = 16\,700$) $L(\sigma) \rightarrow M$; 38 600 cm^{-1} (18 800) $L(\pi) \rightarrow L(\pi^*)$; 33 400 cm^{-1} (24 000) $L(\pi) \rightarrow M$; 19 900 cm^{-1} (3700) $M \rightarrow L(\pi^*)$ and a shoulder at 17 700 cm^{-1} (1300) $M \rightarrow L(\pi^*)$ and/or $d_{x^2-y^2} \rightarrow d_{xy}$ (see also assignments made in [74] for pyridinium salts of $[Ni(dto)_2]^{2-}$). The spectra of $[Pd(dto)_2]^{2-}$, $[Pt(dto)_2]^{2-}$ and $[Au(dto)_2]^{-}$ are similar. The assignments were used to place dto in the spectrochemical series and to compare its position with those of other bidentate (geminal or vicinal) sulphur-donor ligands. The position of dto is consistently highest in the Ni(II), Pd(II) and Pt(II) complexes containing dithio ligands, and maleonitriledithiolate (mnt), another well-investigated 1,2-dithiolate ligand, is consistently lowest.

Carlin and Canziani estimated the octahedral splitting parameter D_q from the transition ${}^4A_{2g} \rightarrow {}^4T_{2g}$ in $[Cr(dto)_3]^{3-}$ [91]. They found a value of 1700 cm^{-1} (oxalate 1754 cm^{-1}) and a Racah parameter $B = 406$ cm^{-1} (oxalate 522 cm^{-1}), supporting the theory that dithio-oxalate is actually a weaker field ligand than is oxalate. The sulphur ligator atoms, on the other hand, cause a reduction in the B parameter, i.e. in the electron–electron repulsion (compared with the free Cr^{3+}) because of higher covalency. The absorption spectra, including circular dichroism studies, of $[Co(dto)_3]^{3-}$, $[Cr(dto)_3]^{3-}$, $[Co(en)_2(dto)]^{+}$, $[Co(en)_3]^{3+}$ and dto^{2-}, are compared by Hidaka and Douglas to figure out the origin of the individual bands [93]. The absorption bands of $[Co(en)_3]^{3+}$ are shifted towards lower frequencies and have increased intensities when en is replaced by dto to give $[Co(en)_2(dto)]^{+}$ and $[Co(dto)_3]^{3-}$. The bands assigned to d→d transitions gain intensity through Co–S bonding. Kanamori et al. could show by a resonance Raman study [103] that in $[Co(dto)_3]^{3-}$ a charge-transfer (CT) transition situated at about 20 000 cm^{-1} overlaps with two d–d transitions producing two shoulders at 17 000 and 21 800 cm^{-1} [93].

The position of dto in the spectrochemical series is mentioned also by Jørgensen [120] and by Lockyer and Martin [121].

The reaction of $[M(dto)_2]^{2-}$ with R_xSnCl_{4-x} [28,108] introduces a bathochromic shift of the M→L CT bands (assigned by Gray and co-workers), as can be seen from Fig. 20. Possible interchange of the $4a_g$ ($d_{x^2-y^2}$) and $3b_{3g}$ (d_{yz}) orbitals [28,30,107,108] has no fundamental influence on this statement.

The question whether the reaction of $[M(dto)_3]^{3-}$ (M = Cr, Co) with $[M'(PPh_3)_2]^+$ (M' = Cu, Ag) (yielding $\{M[(dto)M'(PPh_3)_2]_3\}$) causes an increase of the ligand field strength cannot be answered directly. However, the 10Dq transitions (17 000 cm^{-1} for Co(III) and 17 700 cm^{-1} for Cr(III)) in the spectra of the "parent" complexes are not observed in the spectra of the "adducts". This is presumably because of a hypsochromic shift as the result of increasing ligand field strength (*S,S*-chelation→*O,O*-chelation) which moves the d→d bands below the intense charge-transfer absorption [27].

As shown first by Dwyer and Sargeson, $[M(dto)_3]^{3-}$ (M = Cr, Co and Rh, but not Fe) are stable and sufficiently inert to be separated enantioselectively via $Ca[Co(en)_2(NO_2)_2][M(dto)_3]$ [92]. Using also (−)-*cis*$[Co(en)_2(NO_2)_2]Cl$, Hidaka and Douglas [93] prepared (+)-$KBa[M(dto)_3]$ for circular dichroism studies and found an absolute configuration which was checked and verified later by X-ray structure analysis on (+)-$KCa[Co(dto)_3]\cdot 4H_2O$ by Butler and Snow [58] as the Λ-configuration (according to the IUPAC Information Bulletin 1968). This is the same configuration as found for the oxalate complex (−)-$[Co(ox)_3]^{3-}$. Both the oxalate and the dithio-oxalate compound have a dominant positive circular dichroism in the region of the $^1A_{1g}\rightarrow{}^1T_{1g}$ transition. The correlation between two observed circular dichroism bands and the stereochemical chirality was investigated by McCaffery et al., including (−)-$[Co(dto)_3]^{3-}$ and (+)-$[Rh(dto)_3]^{3-}$. For the latter two complexes a right-handed helical stereochemistry was found [122].

(e) IR, Raman and resonance Raman spectra

The classical IR treatment of dto complexes (Ni, Pd, Pt, Co) was made by Fujita and Nakamoto in 1964 [106] and accepted by most subsequent authors. They interpreted the IR spectra of $K_2[Pt(dto)_2]$ on the basis of a normal coordinate analysis. Because the spectra are little sensitive to the nature of the metal, the IR spectra of the other dto complexes are very similar. A band near 1600 cm^{-1} has been assigned to the C−O stretching vibrations, a band at about 1080 cm^{-1} to a combination of the C−C and C−S stretching vibrations, a band around 940 cm^{-1} to a combination of C−O and C−S stretching vibrations, and a band at 570 cm^{-1} to the C−S stretching vibration. Absorptions at 436, 422 and 322 cm^{-1} were attributed to Pt−S vibrations.

Later on Czernuszewicz et al. measured the IR and Raman spectra of both the "red" and the "black" form of $K_2[Ni(dto)_2]$ and made complete vibrational assignments on the basis of ^{58}Ni, ^{62}Ni isotope data and a thorough normal coordinate calculation for "red" $K_2[Ni(dto)_2]$ [31]. The calculated frequencies were in excellent agreement with the observed values with an average error of less than 1%. The assignments above 500 cm^{-1} are close to those reported for $[Pt(dto)_2]^{2-}$ (1602, 1585 cm^{-1}: ν_{C-O}; 1084 cm^{-1}: ν_{C-C} coupled with ν_{C-S}; 933 cm^{-1}: ν_{C-S} coupled with $\delta_{O=C-S}$; 615 cm^{-1}: ν_{C-S} coupled with ν_{C-C}, ν_{C-O}). In contrast to Coucouvanis et al. [28], who found only one band (360 cm^{-1}) shifted by ^{58}Ni–^{62}Ni isotope substitution, Czernuszewicz et al. reported that three far-IR bands showed significant isotopic shifts at 362.0, 352.6 and 435.0 cm^{-1}. The former two are dominated by Ni–S stretching coordinates and the last contains also a significant Ni–S stretching contribution (32%).

The IR and resonance Raman spectra of the "red" and the "black" form of $K_2[Ni(dto)_2]$ differ mainly in the position of three band sets: in the "black" compound the ν_{C-O} vibrations occur at lower frequencies (1500 and 1488 cm^{-1}), whereas the band due to the coupled $\nu_{C-C}+\nu_{C-S}$ is found at higher frequency (1144 cm^{-1}). These observed frequency shifts are completely consistent with the bond length changes reported for the X-ray structures (see Table 6). Increasing C–O bond distances cause decreasing frequencies of those modes which involve C–O stretching, and the opposite change is found in the C–S stretching region. Drastic changes of the vibrational frequencies in the third spectral region where the Ni–S stetching vibrations are expected show that force constants and thus vibrational frequencies are obviously rather more sensitive measures of bond lengths than are X-ray data, because Ni–S bond lengths in both X-ray structures are found to be nearly identical [28,60].

The IR and Raman spectra of the non-coordinated dithio-oxalate ion (K_2dto, as well as Cs_2*i*-dto, K_2*i*-dto, K_2trto·KCl and K_2mto·H_2O) in the solid state and in solution were published by Mattes et al. in 1977. The fundamentals were also assigned on the basis of a normal coordinate analysis and Raman polarization data [43]. Taking into account the differences between a coordinated and a non-coordinated dto ligand, these results support the assignments for $[M(dto)_2]^{2-}$ very well.

As already mentioned in Sect. C, vibrational spectroscopy is especially useful to detect the mode of coordination of the dto ligand and ligand "flipping" from *S,S*- to *O,O*-chelation, which can be followed sometimes in solution [27,29].

Also, when going from the "parent" complex $K_2[Ni(dto)_2]$ to the trinuclear heterobimetallic complex $(BzPh_3P)_2[Ni(dtoSnCl_4)_2]$, containing two dto bridges *S,S*-chelated to Ni(II) and *O,O*-chelated to Sn(IV), the IR and Raman spectra are changed dramatically: $\bar{\nu}_{C-S}$ drops by more than 100 cm^{-1} while the coupled $\nu_{C-C}+\nu_{C-S}$ shifts upward by 70 cm^{-1} and $\bar{\nu}_{Ni-S}$ jumps 17 cm^{-1}. The ground-state MO involves overlap of the Ni(4s) and S(σ) orbitals as well as the metal d_{xz} (d_{yz}) with a π orbital located at the S atom. As electron density is moved toward the oxygen parts of the dto ligands the $S\rightarrow Ni(\sigma)$ bonding is expected to decrease, but apparently $d_{xz}\rightarrow\pi$ back donation increases, thus stabilizing the Ni–S bond length. This interpretation agrees very well with decreasing C–C and C–S bond lengths [28] (see also Table 6).

In the binuclear complexes $(BzPh_3P)_2[(dto)Ni(dtoSnX_4)]$, containing only one dto bridge, the perturbation for this bridging dto is even greater than that observed for dto in the trinuclear compounds. It should also be mentioned that the highenergy ν_{C-O} (1640 cm^{-1}) in the terminal dto is appreciably different from that of the same vibration in the spectrum of $[Ni(dto)_2]^{2-}$ [28].

There is IR evidence that dto is thermally and photolytically degraded, producing COS gas [46,51,88,104] (see above).

Resonance Raman spectroscopy is very useful and selective in cases of more than one chromophore in the molecule. Nakamoto and co-workers investigated the trinuclear heterometal complex $(BzPh_3P)_2[Ni(dtoSnI_4)_2]$, which has two different chromophoric groups (NiS_4 and SnO_2I_4) [30]. Four electronic transitions are observed at 15.9, 18.5, 27.9 and 30.0×10^3 cm^{-1}. Using 611.4, 514.5, 457.5 and 488.0 nm for the excitation energies, the authors showed that two electronic bands at 15.9 and 18.5×10^3 cm^{-1} are due to the Ni→dto charge transfer transitions as assigned earlier by Coucouvanis et al. [28]. The third band at 27.9×10^3 cm^{-1} is due to the charge transfer within the SnO_2I_4 unit, and the last one at 33.0×10^3 cm^{-1} must be due to a $\pi \rightarrow \pi^*$ transition of the $Ni(dto)_2$ moiety, since the parent complex exhibits a similar absorption.

Nakamoto and his group also used excitation profile studies of two totally symmetric vibrations (ν_1 and ν_4(Ni–S stretch)) of both forms of $[Ni(dto)_2]^{2-}$ ("red" and "black") to reveal the presence of three transitions lying underneath the visible absorption envelope [31], as claimed by Latham et al. [89] on the basis of MO calculations. The unusual nature of the excitation profiles of the "red" $[Ni(dto)_2]^{2-}$ gives a useful restriction of the order of the highest occupied molecular orbitals (HOMO) and supports the order published in ref. 89.

A resonance Raman study on the visible absorption spectrum of tris(dithio-oxalato)cobaltate(III) was carried out by Kanamori et al. [103]. They found that the Raman bands due to the totally symmetric coupled $\nu_{C-C} + \nu_{C-S}$ (113 cm^{-1}) and ν_{Co-S} (349 cm^{-1}) exhibit resonance enhancements with excitation lines in the visible region. The resonance Raman excitation profiles of these two modes reveal the presence of a charge-transfer transition in the visible absorption spectrum (see also the previous chapter).

(f) ESCA spectra

The only two reports concerning X-ray photoelectron spectra on dithio-oxalate complexes are by Folkesson and Jonson in 1984 [87] and Bellitto et al. in 1989 [77(a)]. Findings for the potassium and Ph_4P^+ salts of the Fe, Co, Ni, Pd, Pt, and Cu complexes (the Co complexes are described as Co(II) bis-chelates; however, they are probably Co(III) tris-chelates) are presented in the first paper.

The effective charges have been calculated from the measured binding energies (see Table 10) using the following relations for the ligand atoms

$$E_b(\mathrm{S\ 2p}) = 3.38 q_S + 163.8$$

$$E_b(\mathrm{C\ 1s}) = 11.5 q_C + 284.8$$

$$E_b(\mathrm{O\ 1s}) = 6.04 q_O + 535.6$$

TABLE 10

Binding energies (eV) of dithio-oxalate and tetrathio-oxalate complexes

Compound	S 2p	O 1s	C 1s	P 2p	M $2p_{1/2}$	M $2p_{3/2}$	M $3d_{5/2}$	M $4f_{7/2}$	Ref.
$K_3[Fe(dto)_3]$	163.3	531.0	287.9			708.6			87[a]
$K_2[Co(dto)_2]$[b]	162.2	530.8	287.6			778.8			87[a]
$K_2[Ni(dto)_2]$	162.1	530.4	286.3			852.8			87[a]
$K_2[Pd(dto)_2]$	162.3	530.5	286.5				336.9		87[a]
	162.4					342.7	337.4		77(a)[c]
$K_2[Pt(dto)_2]$	162.4	530.6	286.3					72.1	87[a]
$K_2[Cu(dto)_2]$[d]	162.6	530.7	286.6			931.3			87[a]
$(Et_4N)_2[Pt(dto)_2]$	162.8						75.6	72.2	77(a)[e]
$(Ph_4P)_3[Fe(dto)_3]$	163.1	531.4	288.0	133.5		708.3			87[f]
$(Ph_4P)_2[Co(dto)_2]$[g]	162.8	531.4	288.2	133.3		779.3			87[f]
$(Ph_4P)_2[Ni(dto)_2]$	162.9	531.3	287.1	133.5		853.6			87[f]
$(Ph_4P)_2[Pd(dto)_2]$	163.1	531.2	287.2	133.6			337.4		87[f]
$(Ph_4P)_2[Pt(dto)_2]$	163.4	531.3	287.1	133.5				72.9	87[f]
$(Ph_4P)_2[Cu(dto)_2]$[d]	163.1	531.3	287.2	133.6		931.9			87[f]
$(TTF)_2[Pt(dto)_2]$[i]	161.8 164.0[h]					342.2	337.4		77(a)[e]

TABLE 10 (*continued*)

Compound	S 2p	O 1s	C 1s	P 2p	M $2p_{1/2}$	M $2p_{3/2}$	M $3d_{5/2}$	M $4f_{7/2}$	Ref.
$(TTF)_2[Pt(dto)_2]$	162.6 164.7[h]						75.5	72.3	77(a)[e]
$(TTF)_3[Pt(dto)_2]$	162.5 163.8[i] 164.8[h]						75.4	72.1	77(a)[e]
$TTF[Cu(dto)_2]$[d]	162.1 164.0[h]				955.8	935.6			77(a)[e]
$\{[(Ph_3P)_2Cu]_2(tto)\}$	162.6			131.7		932.4			177
$\{Cu[(tto)Cu(PPh_3)_2]_2\}$	163.1			131.9		932.4			177
$\{Pd[(tto)Cu(PPh_3)_2]_2\}$	162.7			131.8		932.6	337.6		177

[a] Referred to $E_b(K\ 2p_{3/2})=292.2$ eV.
[b] More likely $K_3[Co(dto)_3]$.
[c] Referred to $E_b\ (K\ 2p_{3/2})=292.9$ eV.
[d] Obviously reduction to Cu(I) upon irradiation during measurements.
[e] Referred to $E_b(C\ 1s)=285.0$ eV.
[f] Referred to $E_b(C\ 1s)=285.5$ eV.
[g] More likely $(Ph_4P)_3[Co(dto)_3]$.
[h] $TTF^{\cdot +}$.
[i] TTF^0.

Table 11 summarizes all estimated effective charges. As shown, the charge at the oxygen atoms is nearly the same in all dto complexes. A similar situation occurs for the dto carbons (exceptions are found, however, for the tris-chelates $[M(dto)_3]^{3-}$, M = Fe, Co). The largest variation in charge is estimated for the sulphur ligator atoms. Taking into account that no charge transfer takes place between the cation and the complex anion, the charge at the central metal ion (q_M) could be calculated from the charges on the ligand atoms, giving the following series: q_{Fe}, $q_{Co} < q_{Ni}$ and $q_{Ni} > q_{Pd} > q_{Pt}$. The first-row trend implies a general increase of covalence in the M–S bond as the d orbitals are gradually filled. The trend in the nickel triad is expected from the increased softness of the metal ions: the greater the tendency towards a $S \rightarrow M(\sigma)$ bonding, the smaller q_M will be. This effect is also reflected by the decreasing negative charges on the sulphur donor atoms.

The authors could show that the copper(II) in $[Cu(dto)_2]^{2-}$ is actually reduced during X-ray bombardment.

In the second paper the ESCA data are used to confirm the oxidation state of the metal ions in the donor–acceptor systems $(TTF)_m[M(dto)_2]$, $(TTF)_2[Pt(dto)_2]$, $(TTF)_3[Pt(dto)_2]$ and $(TTF)_2[Pd(dto)_2]$. They contain the metal ions in the oxidation state +2. The S 2p peak analysis obtained by deconvolution gave three values (162.5, 163.8 and 164.8 eV) in the case of $(TTF)_3[Pt(dto)_2]$ attributed to the S 2p orbitals of the anion sulphur, of the $(TTF^{\cdot +})_2$ cation and the neutral TTF molecule found by crystal structure analysis. $(TTF)_{1.0}[Cu(dto)_2]$ does not show shake-up satellites (expected for a paramagnetic Cu(II) compound). It seems that the initial Cu(III) complex is reduced at its surface to a Cu(I) compound during X-ray exposure, accompanied by elimination of gaseous COS.

(g) Redox behaviour

Although the $[M(dto)_2]^{2-}$ complexes can be formally classified as 1,2-dithiolene complexes, they do not exhibit the extensively studied electron transfer behaviour

TABLE 11

Estimated effective charges on the atoms in various dithio-oxalate complexes [87][a]

Compound	q_S	q_C	q_O	q_M
$(Ph_4P)_3[Fe(dto)_3]$	−0.29	+0.28	−0.70	+0.8(2)
$(Ph_4P)_2[Co(dto)_2]$[b]	−0.29	+0.30	−0.70	+0.8(2)
$(Ph_4P)_2[Ni(dto)_2]$	−0.26	+0.20	−0.71	+1.1(2)
$(Ph_4P)_2[Pd(dto)_2]$	−0.21	+0.21	−0.73	+0.9(2)
$(Ph_4P)_2[Pt(dto)_2]$	−0.12	+0.20	−0.71	+0.5(2)
$(Ph_4P)_2[Cu(dto)_2]$[c]	−0.21	+0.21	−0.71	+0.8(2)

[a] The electronic charge is used as a unit.

[b] More likely $(Ph_4P)_3[Co(dto)_3]$.

[c] Obviously reduction to Cu(I) upon irradiation during measurements.

typical of the latter [123,124]. Copper bis-dithio-oxalate is the only binary dithiooxalate complex which undergoes a reversible one-electron transition

$$[\mathrm{Cu(dto)_2}]^{2-} \rightleftharpoons [\mathrm{Cu(dto)_2}]^{-} + \mathrm{e}^{-} \tag{3}$$

The electrochemical oxidation occurs for example in CH_2Cl_2 (at scan rates between 0.02 and 20 V s^{-1}), at a potential $E_{1/2} = +0.128(3)$ V vs. the SCE. The electrochemical reduction process of $[Cu(dto)_2]^-$ is also reversible over the same scan rate scale: $E_{1/2} = +0.135(2)$ V [51]. The "oxidation product" $[Cu(dto)_2]^-$ was described originally as $[Cu(dto)(SCO)_2]^-$ because addition of PPh_3 splits off COS gas ([88], see Sect. D (iii)(b)). The reason is the redox–substitution reaction

$$[\mathrm{Cu(dto)_2}]^{-} + 2\mathrm{PPh_3} \rightarrow [\mathrm{Cu(dto)(PPh_3)_2}]^{-} + 2\mathrm{COS}\uparrow \tag{4}$$

Thus, even in the presence of a low concentration of PPh_3 the cathodic peak disappears and the anodic peak shifts to more negative values.

The oxidation of $[Cu(dto)_2]^{2-}$ can also be effected chemically in DMF or CH_2Cl_2 by either Cu(II) or Fe(III) ions [88]. Kinetic studies were carried out using major changes in the absorption spectra of $(Bu_4N)_2[Cu(dto)_2]$ (2.54×10^{-4} M solution) after adding $Bu_4N(FeCl_4)$ ($4.36 \times 10^{-3}\ \mathrm{M} > [Bu_4N(FeCl_4)]_0 \geqslant 0$) solutions. The reaction proceeds in a 1:1 molar ratio. Kinetic measurements were also carried out for the $(Ph_4P)_2[Cu(dto)_2]$–$Bu_4N(FeCl_4)$ and $(Bu_4N)_2[Cu(dto)_2]$–$(Bu_4N)_2(CuCl_4)$ systems. The higher (by more than 10 times) second-order rate constant in the case of Cu(II) oxidation suggests that the metal ion of the oxidant markedly influences the rate-determining step [51].

A compound TTF$[Ni(dto)_2]$ is mentioned in [77(b)]. The details given, however, do not give sufficient confirmation for a Ni(III) species.

The only reversible one-electron reduction is reported for $Bu_4N[TcO(dto)_2]$ (voltammetry at Hg pool or rotating Pt electrode; SCE; acetonitrile; 0.1 M tetrabutylammonium perchlorate (TBAP); −0.75 V). A second irreversible step follows at −1.56 V. The analogous Re compound exhibits two irreversible reduction steps (−0.94 and −1.35 V). None of the reduction products is accessible by conventional chemical techniques [95].

Unlike the strongly irreversible reductions of the parent bis(dithiooxalato)metalates $[M(dto)_2]^{2-}$ (M = Ni: −2.03; Pd: −2.05; Pt: < −2.05 V), the 1:1 "adducts" $[(dto)M(dtoSnCl_4)]^{2-}$ undergo a single reversible one-electron reduction (cyclovoltammetric data taken in CH_2Cl_2; 0.1 M LiCl; Ag/AgCl; M = Ni: −0.53; Pd: −0.54; Pt: −0.15 V) whereas the 2:1 compounds $[M(dtoSnCl_4)_2]^{2-}$ undergo reversible reduction in two steps (M = Ni: −0.15, −0.51; Pd: −0.23, −0.52; Pt: −0.15, −0.54 V) [107] (see also ref. 108). Using other Sn(IV) halides, only the compound $[(dto)Ni(dtoSnF_4)]^{2-}$ shows a reversible reduction (cyclovoltammetry in CH_2Cl_2; TBAP; Ag/AgI: −0.99 V). Under similar conditions the bromides and iodides $[M(dtoSnX_4)_2]^{2-}$ gave irreversible reductions (Ni/$SnBr_4$: −0.55; Ni/SnI_4: −0.42; Pd/$SnBr_4$: −0.63; Pd/SnI_4: −0.37 V) [28].

It has been suggested that the (reversible) reductions are ligand rather than transition metal based, where a ligand antibonding orbital (b_{1u}) takes the added electrons whose energy is lowered relatively to that in the parent bis(dithio-oxalato)metalates by coordination of SnX_4 to the "diketone ends" of the dto ligands (see Fig. 20) [28,108].

Cyclovoltammetric measurements on mixed ligand compounds $[L_2M(dto)]$ (M = Ni, Pd, Pt; L_2 = 1,2-bis(diphenylphosphino)ethane, 1,2-bis(diethylphosphino)-ethane or two PMe_3) also revealed chemically reversible reductions for all Pt compounds. Most of the Ni and Pd complexes containing the bisphosphine ligands show some degree of chemical reversibility. The ease of reduction follows the order Ni > Pd > Pt, as a result of the increasing stability of d^8 square-planar structures by increasing crystal field strength on descending the metal triad. Controlled potential coulometry investigations for $[(Ph_2PCH_2CH_2PPh_2)Pt(dto)]$ showed 0.95(1) electron transferred in the reduction [46(b),109].

$[Ni(dto)_2]^{2-}$ is reduced irreversibly at the dropping mercury electrode in two steps (aqueous solution, supporting electrolyte KCl), whereas $[Ni(CN)_4]^{2-}$ exhibits under similar conditions only one irreversible reduction. All three original steps disappeared when a mixture of both complexes was investigated by polarography. A new well-defined step was described as proof for the formation of the mixed ligand complex $[(dto)Ni(CN)_2]^{2-}$ [111].

In contrast to, for example, platinum bis-oxalate $[Pt(ox)_2]^{2-}$, which can be partially oxidized to form a highly one-dimensional conducting system [125,126], attempts to synthesize similar dto systems failed. However, oxidation of "red" $K_2[Ni(dto)_2]$ by iodine in acetone or acetonitrile (see above) yielded a blue "adduct" (formulated as $K_2[Ni(dto)_2I]$) which obviously exists in equilibrium with $K_2[Ni(dto)_2]$. The blue compound could not be isolated in the solid state. The "oxidation" using $K_2Cr_2O_7$ resulted in a blend of the parent "red" form and a polymorphic "black" form, both, however, containing nickel(II) (see above).

(h) Photo- and thermochemical behaviour

Most information concerning the behaviour of dithio-oxalate complexes towards light and heat is qualitative. $K[Au(dto)_2]$ was found to be unstable to heat and light [89]. Also, tris-chelates $[M(dto)_3]^{3-}$ (M = Cr, Fe, Co) are reported to decompose very fast in the presence of light [92]. As already mentioned (see Sect. D (iii)(f)), the copper ions in $[Cu(dto)_2]^{2-}$ and $[Cu(dto)_2]^{-}$ are actually reduced to Cu(I) during X-ray bombardment in ESCA experiments [77(a),87]. It seems, however, that the Cu(III) complex $[Cu(dto)_2]^{-}$ is appreciably more light-sensitive than the Cu(II) complex. Thus the cleavage of the C—C bond in one of the coordinated dto ligands of this compound is light-induced. Recording the IR spectra, the first rapid scan in the narrow IR region 2020–2060 cm^{-1} showed no evidence of absorption at 2055 cm^{-1} (COS). However, subsequent repetitive scans over the same region produced a band appearing at 2055 cm^{-1}, which increased in intensity as a function of exposure time to the IR light source. It appears, therefore, that light, including the visible light component of the IR light source, promotes an intramolecular two-electron dto→Cu(III) transfer in $[Cu(dto)_2]^-$ with cleavage of the C–C bond and generation of COS [51,88].

The photochemistry of $[M(dto)L_2]$ (L = phosphines) was investigated in detail [46]. All compounds (M = Ni, Pd, Pt) are slightly light-sensitive in the solid state and thermally stable only below 50°C. The thermal and photochemical sensitivity decreases in the sequence Ni > Pd > Pt. After the discovery of light-induced C–C bond splitting in dto complexes, attempts were made to generate COS in this way within the coordination sphere of coordinatively unsaturated zero-valent metals. However, the electronic spectra of the nickel and palladium species show only a decrease in the initial absorbing complex concentration on UV photolysis. The platinum complexes show isosbestic behaviour which varies with the solvent used (in CH_3CN, isosbestic behaviour is observed even with extended photolysis times; in CH_2Cl_2 there is initially an isosbestic point which disappears on continued irradiation). Secondary photolysis or thermal decomposition according to the equation

$$[M(dto)L_2] \xrightarrow[CH_2Cl_2]{h\nu \text{ or } \Delta} [MCl_2L_2] + 2COS\uparrow \qquad (M = Pd, Pt) \tag{5}$$

occurs in halogenated solvents (e.g. CH_2Cl_2) when a solution of $[Ni(dto)L_2]$ ($L_2 = R_2PCH_2CH_2PR_2$, with R = Et or Ph) is irradiated; IR absorption at 2030 cm^{-1} attributed to free COS starts growing immediately. This peak is soon followed by new absorptions attributable to nickel carbonyls resulting from the carbonylating ability of COS. Two of the photolysis products in CH_3CN were identified as $[Ni(CO)_2(Ph_2PCH_2CH_2PPh_2)]$ and $[Ni(\eta^2\text{-}COS)(Ph_2PCH_2CH_2PPh_2)]$. The same metal species are formed in the photochemical and thermal reactions. Therefore one can suggest that the photochemistry of these metal bis(phosphine)dithio-oxalates proceeds through a coordinatively unsaturated zero-valent species which reacts with available COS.

Some bis- and tris-dithio-oxalato complexes are patented as photosensitive components in photoimaging materials [127,128].

(i) Ligand exchange reactions and mixed ligand complexes

The formation of $[Ni(dto)(CN)_2]^{2-}$ in water according to the equation

$$[Ni(dto)_2]^{2-} + [Ni(CN)_4]^{2-} \rightleftharpoons 2[Ni(dto)(CN)_2]^{2-} \tag{6}$$

was detected polarographically in 1959 [111]. This reaction was also confirmed spectrophotometrically [110]. However, using identical conditions, it was impossible to extend the reaction to Pd(II) and Pt(II) complexes.

Also in solution, a large number of mixed ligand complexes of Ni(II), Pd(II) and Cu(II) containing the dto ligand have been generated and investigated by Pearson et al. [17,86,112]. They studied the kinetics of ligand exchange reactions of bis(dithiolato)metalate(II) complexes with dithiolates or cyanide as the nucleophiles mainly in aqueous solution at 25°C using a stopped-flow technique. The reactions in which dto is involved either as the nucleophile, as the leaving group or as the *trans* group are summarized in Table 12 (abbreviations of the ligands are listed in a footnote to the table). Most experiments have been carried out with Ni(II). The following conclusions were drawn.

The stability constant of $[Ni(dto)_2]^{2-}$ (16.1) fits better in a series of constants of 1,1-dithiolato complexes (cpd: 20.3, ned: 14.4, cdc: 13.7, *i*-mnt: 12.2) than of 1,2-dithiolato (dithiolene) compounds (tfd = 1,2-trifluoromethylethylene-1,2-dithiolate: >36, and mnt: <25). This is somewhat surprising because dto forms five-membered chelate rings like dithiolenes which are considerably more stable than the analogous four-membered rings formed by the 1,1-dithiolates.

Keeping the *trans* group and the nucleophile constant, the ease of displacement of the leaving group decreases in the series *i*-mnt, ned > cds > dto > cpd > mnt, following (with the exception of ned) the inverted series of stability constants.

The general order for the dithiolato nucleophiles, keeping the leaving group and the *trans* group constant, is mnt > ned > cpd > cdc > dto, which only very roughly parallels the stability series.

It was proposed that substitution mechanisms both with bidentate and CN^- nucleophiles follow an associative path. This means that the first step should in all cases be the rapid formation of a five-coordinate adduct. Considering the reactions

$$[Ni(mnt)L]^{2-} + CN^- \rightleftharpoons [Ni(mnt)L(CN)]^{3-} \qquad (7)$$

the stability of the cyanide adducts decreases as L is changed: *i*-mnt (k (M^{-1}) > 1000) > cdc (850) > ned (160) > dto (< 50). The adduct constants agree with the assumption that the larger the π density in the $4p_z$, the smaller is the tendency for a nucleophile to form a bond along the z direction.

The effect of the *trans* group, keeping the nucleophile and the leaving group constant, on the kinetics of nickel(II) dithiolate substitution reactions decreases in the order *i*-mnt > cdc > dto > cpd > mnt and ned > cpd, agreeing nicely with the stability series of the five-coordinate adducts. This leads to the suggestions that the rate of ligand exchange reactions increases as the adduct stability increases and that the major part of the *trans* influence operates via the stability of the five-coordinate adduct which must form before substitution can occur.

The exchange behaviour of palladium(II) complexes largely parallels the behaviour of nickel(II) complexes. The fact that only one reaction is observed when $[Pd(dto)_2]^{2-}$ reacts with cyanide is probably due to the apparent instability of $[Pd(dto)(CN)_2]^{2-}$. The reaction sequence appears to be as shown in the equations

$$[Pd(dto)_2]^{2-} + 2CN^- \xrightarrow{K} [Pd(dto)(CN)_2]^{2-} + dto^{2-} \qquad (8)$$

TABLE 12

Second-order rate constants for ligand exchange reactions of Ni(II), Pd(II) and Cu(II) complexes with bidentate (or tridentate) ligands including dithio-oxalate as ligand and/or nucleophile and first-order rate constants with cyanide, determined in aqueous solution at 25°C[a]

Reactant[b]	Nucleophile[b]	Product	k_{obsd} (10^{-3} M^{-1} s^{-1})	k_{obsd} (s^{-1})[c]	Ref.
$[Ni(dto)_2]^{2-}$	mnt^{2-}	$[Ni(dto)(mnt)]^{2-}$	0.33		86
$[Ni(dto)(mnt)]^{2-}$	mnt^{2-}	$[Ni(mnt)_2]^{2-}$	0.019		86
$[Ni(dto)(cpd)]^{2-}$	mnt^{2-}	$[Ni(cpd)(mnt)]^{2-}$	0.11		86
$[Ni(dto)(cdc)]^{2-}$	mnt^{2-}	$[Ni(dto)(mnt)]^{2-}$	23		86
$[Ni(dto)(i\text{-}mnt)]^{2-}$	mnt^{2-}	$[Ni(dto)(mnt)]^{2-}$	53		86
$[Ni(cdc)_2]^{2-}$	dto^{2-}	$[Ni(dto)(cdc)]^{2-}$	6.0		86
$[Ni(dto)(cdc)]^{2-}$	dto^{2-}	$[Ni(dto)_2]^{2-}$	0.55		86
$[Ni(cdc)(mnt)]^{2-}$	dto^{2-}	$[Ni(dto)(mnt)]^{2-}$	0.0057		86
$[Ni(cdc)(CN)_2]^{2-}$	dto^{2-}	$[Ni(dto)(CN)_2]^{2-}$	0.25		86
$[Ni(i\text{-}mnt)_2]^{2-}$	dto^{2-}	$[Ni(dto)(i\text{-}mnt)]^{2-}$	28		86
$[Ni(dto)(i\text{-}mnt)]^{2-}$	dto^{2-}	$[Ni(dto)_2]^{2-}$	1.6		86
$[Ni(i\text{-}mnt)(mnt)]^{2-}$	dto^{2-}	$[Ni(dto)(mnt)]^{2-}$	0.025		86
$[Ni(i\text{-}mnt)(CN)_2]^{2-}$	dto^{2-}	$[Ni(dto)(CN)_2]^{2-}$	0.80		86

$[Ni(i\text{-}mnt)(cpd)]^{2-}$	dto^{2-}	$[Ni(dto)(cpd)]^{2-}$	0.52		86
$[Ni(cpd)_2]^{2-}$	dto^{2-}	$[Ni(dto)(cpd)]^{2-}$	0.00087		86
$[Ni(dto)(i\text{-}mnt)]^{2-}$	cdc^{2-}	$[Ni(dto)(cdc)]^{2-}$	≈10		86
$[Ni(dto)(mnt)]^{2-}$	cpd^{2-}	$[Ni(mnt)(cpd)]^{2-}$	0.0049		86
$[Ni(dto)_2]^{2-}$	en	$[Ni(en)_3]^{2+}$	0.15		86
$[Ni(dto)_2]^{2-}$	dien	$[Ni(dien)_2]^{2+}$	0.10		86
$[Pd(i\text{-}mnt)_2]^{2-}$	dto^{2-}	$[Pd(dto)(i\text{-}mnt)]^{2-}$	0.0125		112
$[Pd(ned)_2]^{2-}$	dto^{2-}	$[Pd(dto)(ned)]^{2-}$	0.197		112
$[Pd(dto)(ned)]^{2-}$	dto^{2-}	$[Pd(dto)_2]^{2-}$	0.0038		112
$[Cu(dto)(mnt)]^{2-}$	mnt^{2-}	$[Cu(mnt)_2]^{2-}$	≈140		86
$[Ni(dto)_2]^{2-}$	CN^-	$[Ni(dto)(CN)_2]^{2-}$		$40 \times 10^6[CN^-]^2$	86
$[Ni(dto)(CN)_2]^{2-}$	CN^-	$[Ni(CN)_4]^{2-}$		$12 \times 10^6[CN^-]^2$	86
$[Ni(dto)(mnt)]^{2-}$	CN^-	$[Ni(mnt)(CN)_2]^{2-}$		$3.1 \times 10^4[CN^-]^2$	86
$[Pd(dto)_2]^{2-}$	CN^-	$[Pd(CN)_4]^{2-}$		$2.7 \times 10^4[CN^-]^2$	112

---

[a] Ionic strength 0.2 M ($NaClO_4$) for nickel complexes and 0.1 M for palladium complexes.

[b] Abbreviations: mnt = maleonitriledithiolate, cpd = 1-cyano-1-phenylethylene-2,2-dithiolate, cdc = *N*-cyanodithiocarbimate, *i*-mnt = 1,1-dicyanoethylene-2,2-dithiolate, ned = 1-nitroethylene-2,2-dithiolate, en = ethylenediamine, dien = diethylenetriamine.

[c] k_{obsd} is the pseudo-first-order rate constant obtained with cyanide in excess.

$$[\mathrm{Pd(dto)(CN)_2}]^{2-} + 2\mathrm{CN}^- \xrightarrow{\text{fast}} [\mathrm{Pd(CN)_4}]^{2-} + \mathrm{dto}^{2-} \tag{9}$$

Comparing the rate of the first reaction with the rate of the corresponding reaction of $[\mathrm{Ni(dto)_2}]^{2-}$, a ratio $K_{\mathrm{Ni}}/K_{\mathrm{Pd}} = 1470$ has been found. This rate increase on going from palladium to nickel is unusually large, because ratios of the order of 10 are expected [129].

The species $[\mathrm{Cu(dto)_2}]^{2-}$ reacts with mnt^{2-} according to the equations

$$[\mathrm{Cu(dto)_2}]^{2-} + \mathrm{mnt}^{2-} \xrightarrow{\text{fast}} [\mathrm{Cu(dto)(mnt)}]^{2-} + \mathrm{dto}^{2-} \tag{10}$$

$$[\mathrm{Cu(dto)(mnt)}]^{2-} + \mathrm{mnt}^{2-} \xrightarrow{K} [\mathrm{Cu(mnt)_2}]^{2-} + \mathrm{dto}^{2-} \tag{11}$$

The reaction is very fast with an approximate second-order rate constant $k \approx 1.4 \times 10^5\ \mathrm{M}^{-1}\ \mathrm{s}^{-1}$, indicating that copper(II) dithio-oxalate reacts, as expected, more than 7000 times faster than nickel(II) dithio-oxalate with mnt^{2-} (see Table 12).

In addition to UV–VIS spectroscopy, EPR is suitable for detecting copper(II) mixed ligand systems, as mentioned before [118]. In solution, $[\mathrm{Cu(dto)_2}]^{2-}$ reacts with Cu(II) benzoylthio- or selenoureas forming mixed ligand species which contain a five-membered (dto) and a six-membered (urea ligand) chelate ring [116].

Some mixed ligand Co(III) complexes containing dto and a nitrogen donor ligand have been reported [36,93,104]. Obviously the $\mathrm{N_4S_2}$ donor atom set in $[\mathrm{Co(en)_2(dto)}]\mathrm{X}$ and $[\mathrm{Co(phen)_2(dto)}]\mathrm{X}$ is particularly stable and forms easily. A special case of a mixed ligand complex is found in $[\mathrm{In_2(dto)_5}]^{4-}$, in which two different terminal "*cis*-dtos" and a planar *trans* bridging dto were detected by X-ray structure analysis [41]. There is also a huge number of dto complexes containing additional halogenides, methyl, carbonyl, phosphines, oxygen, sulphur, nitrogen or nitrosyl as ligands: $\{\mathrm{XSn[(dto)Cu(PPh_3)_2]_3}\}$ (X = Cl, Br, Me) [29], $\{\mathrm{X_2Sn[(dto)Cu(PPh_3)_2]_2}\}$ (X = Cl and/or Me) [29], $\{\mathrm{X_2Cl_2Sn[(dto)Cu(PPh_3)_2]}\}^-$ (X = Cl and/or Me) [29], $\{\mathrm{Sn_3Cl_4[(dto)Cu(PPh_3)_2]_2}\}$ [29], $[\mathrm{Cu(dtoSnCl_4)_2Cl}]^{3-}$ [88], $\{[\mathrm{Mn(CO)_5}]_2(\mathrm{dto})\}$ [25], $\{[(\mathrm{Co})_3\mathrm{Re(dto)}]_2(\mathrm{dto})\}$ [26], $[\mathrm{Mo_2O_2S_2(dto)_2}]^{2-}$ [21,94], $[(\mathrm{S_2})\mathrm{MoO}(\mu\text{-S})_2\mathrm{MoO(dto)}]^{2-}$ [94], $[\mathrm{MA(dto)_2}]^{n}$ (M = Mo, A = O, $n = 2$ [39]; M = Tc, Re, A = O, $n = 1$ [26,55,95]; M = Tc, A = N, $n = 2$ [55,56]; M = Fe, A = Cl, Br, I, NO, $n = 2$ [96–99]), $[(\mathrm{PMe_3})_2\mathrm{M(dto)}]$ (M = Ni, Pd, Pt) [46(b)], $[(\mathrm{PPh_3})_2\mathrm{Cu(dto)}]^-$ [29,51], $[(\mathrm{R_2PCH_2CH_2PR_2})\mathrm{M(dto)}]$ (M = Ni, Pd, Pt, R = Et, Ph) [46(b),109], $[(\mathrm{CH_3OCH_2CH_2OCH_3})\mathrm{Ni(dto)}]$ [46(b)], $[\mathrm{Pd_3}(\mu_3\text{-S})_2(\mathrm{dto})(\mathrm{PMe_3})_4]$ [46(b)]. Mixed ligand systems are also formed when only one of two or three dto ligands present reacts with coordinatively unsaturated metal complex species. Thereby ligand scrambling reactions (*S,S* to *O,O* coordination) can occur depending on the relative softness of the metal species: $[(\mathrm{dto})\mathrm{M(S_2C_2O_2SnX_4)}]^{2-}$ (M = Ni; X = F, Cl or M = Pd, Pt; X = Cl) [28,107,108] and $\{(\mathrm{dto})_2\mathrm{Sn[(O_2C_2S_2)Cu(PR_3)_2]}\}^-$ (R = Ph, Tol) [29,33].

(j) Analytical use of dto complexes

In their classical paper in 1909, Jones and Tasker already pointed to the analytical usefulness of dithio-oxalate for determining Ni, Co and Fe ions [2]. In the 1920s, techniques were developed to determine nickel colorimetrically in neutral or acidic aqueous solution (also in tissues, excreta and foodstuffs) with dithio-oxalate [130,131]. The complex composition depending on the relative concentrations of Ni^{2+} and dto^{2-} in aqueous solution (Job's method) and the validity of Beer's law were checked and formation constants were evaluated (necessary for unambiguous analytical use) [86,119]. Welcher devotes a separate chapter in his reference book [132] to dithio-oxalate. Besides a procedure to synthesize potassium dithio-oxalate, he describes reactions of this reagent with metal ions, especially nickel, cobalt and iron. The colour of nickel dithio-oxalate is approximately three times more intense than that of the permanganate ion, thus producing a sensitivity for nickel of up to $1:4\times10^7$. The colour reaction with cobalt is as intense as that of nickel and may therefore interfere. The sensitivity of the iron reaction, however, is only about $1:10^5$.

In 1982, two papers were published dealing with ion-pair extraction of $[M(dto)_2]^{2-}$ complexes from aqueous solution into chloroform by use of bulky organic cations Q, forming 1:2 ion pairs $Q_2[M(dto)_2]$ [133,134]. The extraction constants $K_{ex}=[Q_2[Ni(dto)_2]]$ (in $CHCl_3$)/$[Q^+]^2[[Ni(dto)_2]^{2-}]$ (in H_2O) were determined for dodecyltrimethylammonium ($\log K_{ex}=8.97$), tetrabutylammonium (9.38), *N*-dodecylpyridinium (11.37), hexadecyltrimethylammonium (12.88), benzyldimethyldodecylammonium (14.75), *N*-hexadecylpyridinium (14.82), benzyldimethyltetradecyclammonium (16.46), and tetrahexylammonium (18.05) at ionic strength 0.3 and 25°C. A linear correlation was obtained between $\log K_{ex}$ and the number of carbon atoms constituting the Q^+ ions. However, the data for cations with an aromatic group and those without follow two independent lines. Empirical parameters for estimating extraction constants have been deduced: the values $\Delta \log K_{ex}$ (the contribution of the functional group to $\log K_{ex}$) were 0.47 for the methylene group, 0.82 for the methyl group, 3.18 for the phenyl group, 0.95 for the ammonium ion, 4.52 for the pyridinium ion, and -9.79 for the $[Ni(dto)_2]^{2-}$ anion.

The simultaneous spectrophotometric determination of palladium(II) and platinum(II) can be carried out after ion-pair extraction of $[Pd,Pt(dto)_2]^{2-}$ from water into chloroform using benzyldimethyltetradecylammonium perchlorate as a quaternary ammonium ion buffer (the concentration of the benzyldimethyltetradecylammonium ion Q^+ in the aqueous phase is controlled by the combined use of the $Q^+ClO_4{}^-$ ion pair in the chloroform phase and the perchlorate ion in the aqueous phase). The extraction constants are 12.15 for Q_2dto, 16.69 for $Q_2[Pd(dto)_2]$, and 16.83 for $Q_2[Pt(dto)_2]$ at ionic strength 0.3 (Na_2SO_4) and 25°C. Possible interfering metal ions can be masked by use of ethylenediaminetetraacetic acid [134].

(iv) Trithio-oxalate $[SOC{-}CS_2]^{2-}$, trto

Trithio-oxalate has the inverted O/S topology of monothio-oxalate. Therefore, in contrast to mto, the soft parts of the ligand should govern the coordination modes.

Potassium trithio-oxalate seems to be the most unstable mixed-chalcogen potassium thio-oxalate. Although the synthesis of potassium trithio-oxalate, its vibrational spectra and the X-ray structure of K_2trto KCl had already been published by Mattes and co-workers by the middle seventies [9,15,43], the coordination chemistry of trto was started only in 1988 [19,135], when the first bi-, tri- and tetranuclear complexes were isolated with trithio-oxalate as bridging ligand (see Table 13).

The reaction of trithio-oxalate (potassium, Ph_4As^+ or $BzPh_3P^+$ salt) with coordinatively unsaturated species such as $(Ph_3P)_2M^+$ (M = Cu, Ag, Rh) results in the formation of binuclear homometal compounds of the type $\{[(Ph_3P)_2M]_2(\text{trto})\}$. Tri- or tetranuclear heterometal complexes of the general formula $\{[(Ph_3P)_2Cu(\text{trto})]_nM\}$ can be obtained by reaction of trithio-oxalate with the corresponding metal salt followed by extraction of the resulting complex solution with $(Ph_3P)_3CuCl$ in dichloromethane. The formal composition does not differ from that of compounds containing monothio-, 1,2-dithio- or tetrathio-oxalate as bridging ligands linking identical or different metal ions. The IR spectra, however, are more complicated. A band at 1530 cm^{-1} (potassium salt [43]) or 1520 cm^{-1} (Ph_4As^+ salt [135]) has been assigned to the C—O stretching vibration. This absorption was found, e.g., in $\{[(Ph_3P)_2Ag]_2(\text{trto})\}$ at a higher frequency (1563 cm^{-1}), unexpected for a bridging ligand. Surprisingly, the homologous copper complex shows a bathochromically shifted C—O stretching mode (1475 cm^{-1}).

Until now only the X-ray structure of the binuclear silver complex is known (see Fig. 21) [19(d),(e)], exhibiting an unexpected result: whereas one silver ion is

TABLE 13

Trithio-oxalate complexes [19(b),135]

Compound	M.p. (°C)	Colour (solid state)	IR spectra $\bar{\nu}_{C-O}$ (cm^{-1})	Electronic spectra $\bar{\nu}_{max}$ (10^3 cm^{-1}) (ε_0)
$\{[(Ph_3P)_2M]_2(\text{trto})\}$				
M = Cu	206–8	Violet	1475s	13.5 (8700)
				22.0 (2100)
Ag	167	Olive-green	1563s	21.0 (3300)
				27.0 (2000)
Rh	162–4	Brown	1610br	
$\{M'[(\text{trto})Cu(PPh_3)_2]_2\}$				
M′ = Cu	125–7	Violet	1583s	13.0 (16200)
			1520s	25.5 (300)
Ni	165	Green	1570s	13.2 (13500)
			1520s	29.3 (23400)
Pd	160–2	Blue–violet	1580s	12.9 (12600)
			1528s	23.8 (7800)
$\{Fe[(\text{trto})Cu(PPh_3)_2]_3\}$	164–6	Violet	1600br	13.0 (22400)
				27.0 (40700)

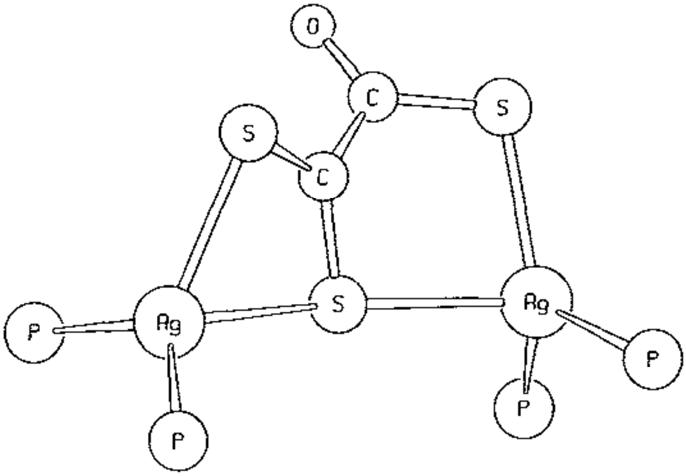

Fig. 21. Molecular structure of $[(Ph_3P)_2Ag(trto)Ag(PPh_3)_2]$ (phenyl rings omitted) [19(e)].

bound "normally", i.e. side-on, to two sulphur atoms of trto, the other is bound end-on to two sulphur atoms. The latter coordination mode has been detected for the first time for thio-oxalate ligands. The bridging trithio-oxalate ligand is far from being planar. The dihedral angle between the COS and the CS_2 group is 50(1)°. The C–O bond length (1.25(2) Å) is markedly longer than those of the non-coordinated C–O entities in monothio-oxalate complexes (1.09(!)–1.23 Å) [21,36–38]. There are numerous complexes where sulphur ligator atoms of unsaturated dithio ligands are bound to more than one metal ion in oligonuclear species. Examples are $\{[(Ph_3P)_2Ag]_2(mnt)\}$ [136,137], $Ni(i\text{-}mnt)_2[Ag(PPh_3)_2]_2\}$, $\{Ni(mnt)_2[Ag(PPh_3)_2]_2\}$ and $[Ni(mnt)_2[Ag(PPh_2Et)_2]_2\}$ [138,139] with Ag–S (mean 2.808 Å) and C–S distances (mean 1.77 Å) somewhat longer than those found for $\{[(Ph_3P)_2Ag]_2(trto)\}$ (Ag–S, with S bound to two Ag: 2.680(2) and 2.725(2) Å and C–S 1.68(1) Å) (see also Table 15). On the other hand, the Ag–P bond lengths are almost identical (mean values 2.474 and 2.477(2) Å, respectively).

The anion $MoOS_3^{2-}$, tetrahedrally configured but formally comparable with trto, forms a compound $\{[(Ph_3P)Au](MoOS_3)[Au(PPh_3)_2\}$ with an $(MoOS_3)$ bridge using also exclusively the three sulphur atoms, i.e. a similar arrangement to that found in $\{[(Ph_3P)_2Ag]_2(trto)\}$ with non-coordinated oxygen [140].

One argument that the C=O of the trto ligand remains uncoordinated follows from the shape of the highest occupied molecular orbitals (HOMOs). MO calculations (ab initio self-consistent field (SCF)) for trithio- and tetrathio-oxalate [19(e)] show, in agreement with the extended Hückel calculations for the C_2S_4 unit [141], four in-plane σ donor orbitals (see Fig. 22). In trto a group of three donor orbitals, mainly localized at the sulphur atoms, is significantly separated from one low lying orbital localized at the oxygen. This indicates that the donor ability via the sulphur atoms is dominant.

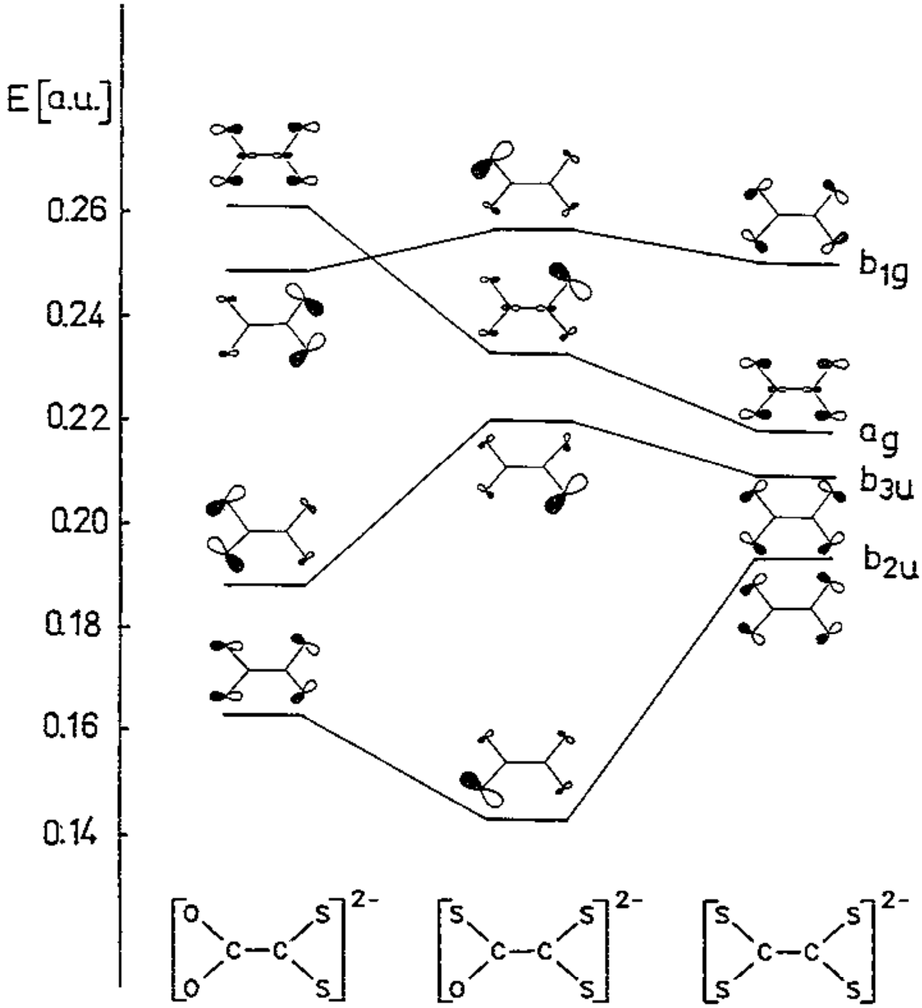

Fig. 22. In-plane σ donor orbitals of *i*-dto, trto and tto [19(e)].

(v) *Tetrathio-oxalate* $[S_2C{-}CS_2]^{2-}$, *tto*

The discovery of the first solely sulphur-compound-based superconductor bis(ethylenedithio)tetrathiafulvalene (BEDT-TTF or in short "ET") and its radical cation salts has prompted several laboratories to start synthetic programmes for new extended multisulphur π donors and to investigate their inorganic complexes [142].

Obviously the C_2S_4 subunits in TTF, BEDT-TTF and related compounds are fundamentally important for that class of "organic metals" and lead directly to the simple tetrathio-oxalate ligands. A rising interest in developing new transition metal tetrathio-oxalates and in understanding their structural and electronic relationship is also motivated by their possible use in syntheses of extended low-dimensional metal tetrathiolene arrays with metallic or semiconducting properties [141].

Tetrathio-oxalate is unique among all thio-oxalates with respect to its highly symmetrical topology and, in connection with this, to the chemical consequences of its "all sulphur" constitution. All four sulphurs can serve as effective donor sites and the C_2S_4 unit can formally or really accept or release electrons, and does so especially when switched in tune with the electronic system of a transition metal in an appropriate symmetry. It is also unique with respect to the manifold chemical individuals which contain the C_2S_4 entity in the same topology as in the free ligand, (i.e. $S_2C_2S_2$) regardless of its overall charge. Moreover, there is also a huge number of compounds which have the same net content (C_2S_4) but different connectivity.

Examples of "non-tetrathio-oxalate C_2S_4" are:

(1) Metal promoted head-to-tail dimerization of two coordinated CS_2 molecules, see Fig. 23 [143–146], where subsequent splitting into coordinated "C_2S_3" and S has been observed [147]. Dimerization of [Pt(η^2-CS_2)(dppe)] (dppe = 1,2-bis(diphenylphosphino)ethane) in the presence of excess methyl iodide also forms a dimethylated "C_2S_4" unit [148]. Even pseudo-trimerization exists with dual head-to-tail linking of three CS_2 molecules with central sp^3 carbon [149], in contrast to the

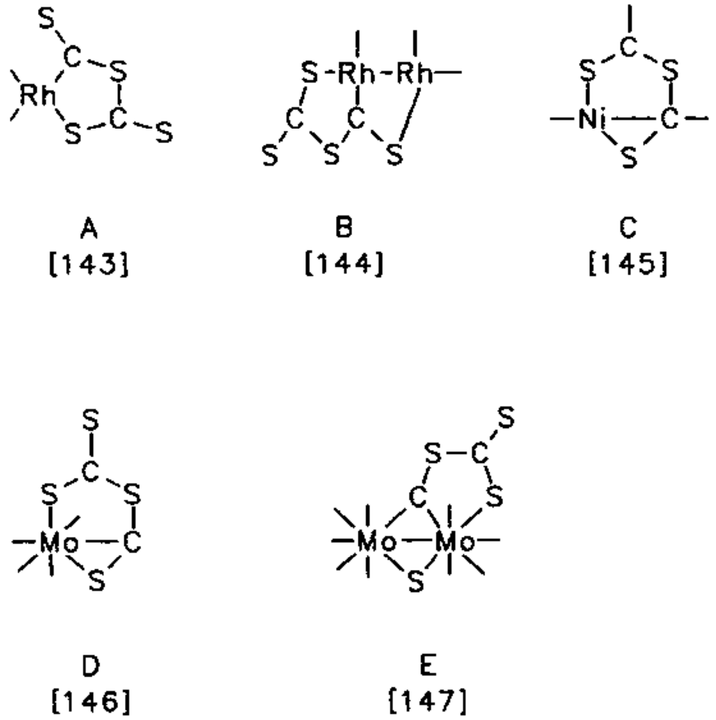
A [143]
B [144]
C [145]
D [146]
E [147]

Fig. 23. Selection of head-to-tail coupled "$(CS_2)_2$" ligands.

formal trimerization of CS_2 giving a C–C–C connection [150]. Head-to-tail linking at metal centres was also found for CSSe [151] and CSe_2 by Werner and co-workers [151,152]. Tributylphosphine reacts with CSe_2 yielding n-$Bu_3P{=}C_3Se_4$ with a head-to-tail coupled C_2Se_4 moiety [153].

(2) Linking of two metal ions by two non-coupled CS_2 bridges [154,155]. Trimeric or polymeric species are postulated [156].

(a) Metal-promoted head-to-head dimerizations of CS_2

The first authentic and structurally proven example of coordinated C_2S_4 was realized by Maj et al. [157] (see Fig. 24). The condensation proceeded through activation of CS_2 coordinated at electron rich nickel pentamethylcyclopentadienyldicarbonyl $[Cp'Ni(CO)_2]_2$, which leads to a side-on bridging C_2S_4 linking with Cp'Ni fragments. After reaction of CS_2 with oligonuclear cluster carbonyls like $Fe_2(CO)_9$, Broadhurst et al. identified, among many other products, a tetranuclear iron complex in low yield, in which the central μ-C_2S_4 unit links, end-on-like, two Fe_2 fragments [158] (Fig. 25). A titanium(II)-activated carbon–carbon bond forma-

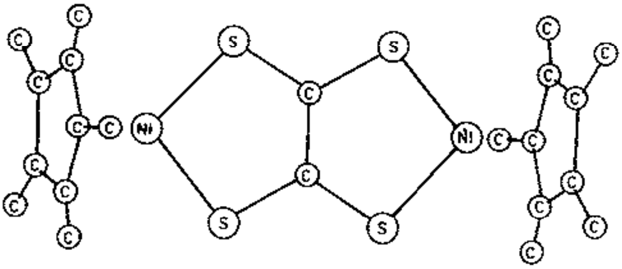

Fig. 24. Molecular structure of $[(\eta^5\text{-}Me_5C_5)Ni(C_2S_4)Ni(\eta^5\text{-}Me_5C_5)]$ [157].

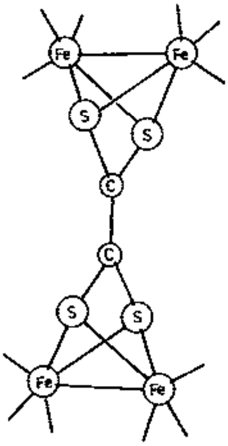

Fig. 25. Molecular structure of $[(CO)_6Fe_2(C_2S_4)Fe_2(CO)_6]$ [158].

tion by reductive head-to-head coupling of CS_2 is reported by Harris et al. [159]. Starting from $[(\eta^5\text{-}C_5H_5)_2Ti(CO)_2]$ in CS_2 solution, dark purple $\{[(\eta^5\text{-}C_5H_5)_2Ti]_2(\mu\text{-}C_2S_4)\}$ is formed at room temperature after about one day (see Fig. 26). The C_2S_4 core is described by the authors as "tetrathio-oxalate (or ethylene tetrathiolate)". C–C bond formation to a tetrathiolate moiety also occurs by reduction of cationic η^2-coordinated methyldithioformate with borohydride [160,161]. The reaction yields the coordinated dimethyl ester of tetrathio-oxalate. The remarkably short C–C bond length of 1.390(15) Å shows, however, that the ligand coordinates as a 1,2-dimercaptoethylene derivative rather than as tetrathio-oxalate (see the following chapter). The formation of $[(\text{triphos})Rh(\mu\text{-}C_2S_4)Rh(\text{triphos})](BPh_4)_2\cdot CH_2Cl_2$ (triphos = $MeC(CH_2PPh_2)_3$) by addition of CS_2 to $[RhCl(C_2H_4)_2]_2$ and triphos in THF–benzene in the presence of $NaBPh_4$, is comparable with the previous reaction [162,163]. The C_2S_4 unit is planar (see Fig. 27), but the $Rh(\mu\text{-}C_2S_4)Rh$ core is not completely planar, each Rh atom being about 0.3 Å out of the C_2S_4 plane. According

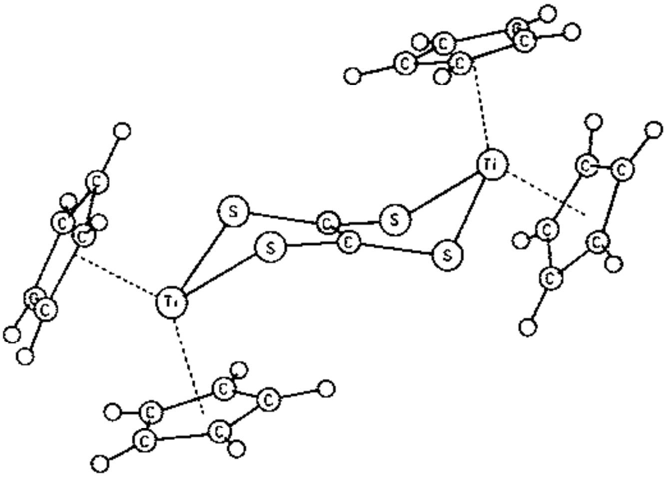

Fig. 26. Molecular structure of $[(\eta^5\text{-}C_5H_5)_2Ti(C_2S_4)Ti(\eta^5\text{-}C_5H_5)_2]$ [159].

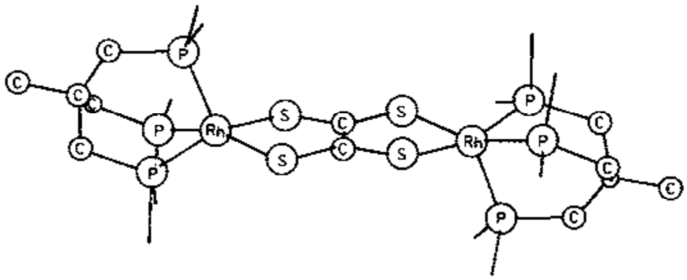

Fig. 27. Structure of the cation in $[(\text{triphos})Rh(C_2S_4)Rh(\text{triphos})](BPh_4)_2\cdot CH_2Cl_2$ [162].

to chemical behaviour, these authors also claim the analogous ethenetetrathiolate-bridged binuclear Ir compound $[(\text{triphos})\text{Ir}(\mu\text{-C}_2\text{S}_4)\text{Ir}(\text{triphos})]^{2+}$ [163].

Metal-promoted head-to-head coupling is also reported for CSe_2, from the same laboratory, yielding $[(\text{triphos})\text{Rh}(\mu\text{-CSe}_2)_2\text{Rh}(\text{triphos})]^{2+}$ [163,164]. However, Jensen and Huge-Jensen in 1973 had already reported two compounds ($[(Ph_3P)_2Ni(CSe_2)_2]$ and $[(Ph_3P)_2RhCl(CSe_2)_2]$) with possibly coupled CSe_2 moieties [165]. The description of coordinated C_2S_4 units is often not clear. Some so-called thio-oxalate compounds should rather be interpreted as ethenetetrathiolate (ett) derivatives. The C—C bond length is a suitable indicator as to whether there is oxalate or ethenetetrathiolate behaviour; see Tables 14 and 15.

(b) Dimethyl tetrathio-oxalate, ttoMe$_2$, and dimethyl ethenetetrathiolate, ettMe$_2$ complexes

The first authentic tetrathio-oxalic acid derivative, namely the dimethyl ester, was isolated in 1976 by Kissel et al. by photolytic decarbonylation of the heterocycle 4,5-bis(methylthio)-1,3-dithiole-2-one [166] (see Fig. 28). Surprisingly, all attempts to prepare higher esters have so far failed [4]. Dimethyl tetrathio-oxalate reacts with electron rich metal centres forming neutral chelates, for example $[Ni(ettMe_2)_2]$ or $[Mo(ettMe_2)_3]$, or mixed ligand chelates such as $[Pd(PPh_3)_2(ettMe_2)]$ [167,168] (see Fig. 29). However, in all attempts to coordinate the $ttoMe_2$ ligand, a thermal or photochemical redox reaction takes place, where the destiny of the ligand is to be transformed into an ethenetetrathiolate derivative ($ettMe_2$) indicated by short C—C bonds with typical dithiolene behaviour (intense absorptions in low energy visible and near IR region, reversible one-electron transitions).

TABLE 14

Coordination modes of C_2S_4 species

Compound	Bond distance (Å)		Mode[a]	Ref.
	C–C	C–S		
1 $(Ph_4P)_2(C_2S_4)\cdot 6H_2O$	1.46(2)	1.713(9) 1.691(10)	tto	10
2 $\{[(CO)_6Fe_2]_2(C_2S_4)\}$	1.332	1.775	ett/end-on	158
3 $\{[\eta^5\text{-Cp})Ni]_2(C_2S_4)\}$	1.36(1)	1.718(2)	ett/side-on	157
4 $\{[(\text{triphos})Rh]_2(C_2S_4)\}^{2+}$	1.36(3)	1.76(2) 1.73(2)	ett/side-on	163
5 $\{[(Ph_3P)_2Cu]_2(C_2S_4)\}$	1.53(8)	1.668(6) 1.689(6)	tto/side-on	188
6 $\{[(C_3OS_4)Cu]_2(C_2S_4)\}^{2-}$	1.467(10)	1.673(5) 1.678(5)	tto(?)/side-on	189(b)
7 $\{[(\eta^5\text{-Cp})Ti]_2(C_2S_4)\}$	1.41	1.736	ett/side-on	159

[a] tto = tetrathio-oxalate-like; ett = ethenetetrathiolate-like.

TABLE 15

Selected bond distances (Å) and angles (°) of *i*-dto, trto and tto complexes

Compound	Bond distances					Angles			Coord. mode	Ref.
	M–S	M–O	C–S	C–O	C–C	Intraligand		Torsion		
						SMS	SMO			
1 $[Ph_3P)_2Cu(i\text{-dto})Cu(PPh_3)_2]^a$	2.323(4) 2.307(5)	2.05(1) 2.105(9)	1.65(2)	1.28(2) 1.27(2)	1.52(2)		85.2(3) 84.3(3)	18.5(2)	Side-on	19(e)
2 $[(Ph_3P)_2Ag(trto)Ag(PPh_3)_2]$	2.680(2) 2.545(3) $2.725(2)^b$ $2.645(3)^b$		1.683(10) 1.696(8) 1.688(10)	1.25(2)	1.52(2)	81.82(9) 66.87(8)		50(1)	Side-on/ end-on	19(e)
3 $[(Ph_3P)_2Cu(tto)Cu(PPh_3)_2]$	2.308(2) 2.275(2)		1.668(6) 1.689(6)		1.531(8)	89.18(7)		Planar	Side-on	188
4 $[(C_3OS_4)Cu(tto)Cu(C_3OS_4)]^{2-}$	2.258(2) 2.245(2)		1.673(5) 1.678(5)		1.467(10)	89.0(1)		Planar	Side-on	189

[a] The analogous Ag complex $[(Ph_3P)_2Ag(i\text{-dto})Ag(PPh_3)_2]$ is isostructural.

[b] End-on coordination.

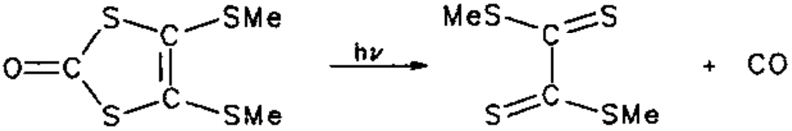

Fig. 28. Photolytic synthesis of tetrathio-oxalate dimethyl ester [166].

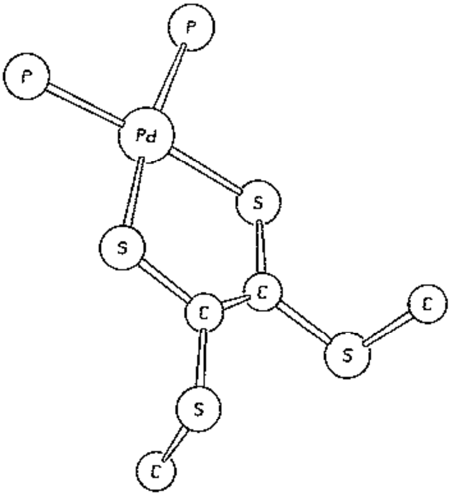

Fig. 29. Molecular structure of $[(PPh_3)_2Pd(ettMe_2)]$ (phenyl rings omitted) [168].

The synthesis of $ettMe_2$ complexes from the components is more versatile, especially for mixed ligand chelates, than the in situ preparation starting with 4,5-bis(methylthio)-1,3-dithiole-2-one [169].

The monoanionic species with, formally, Ni(III) or Pd(III) can also be reached by hydrolytic cleavage of 4,5-bis(methylthio)-1,3-dithiole-2-one and subsequent reaction of the generated 1,2-bis(methylthio)ethene-1,2-dithiolate with an appropriate M(II) starting material (for example $NiCl_2 \cdot 6H_2O$) [170]. The conversion of $ttoMe_2$ into $ettMe_2$ during coordination to metal centres is comparable with the formation of Diels–Alder-like [4+2]-cycloaddition products, where the $ttoMe_2$ behaves as a dithiabutadiene [171].

(c) *Authentic tetrathio-oxalate — synthesis and complex behaviour*

There have been several claims for tetrathio-oxalate. The first goes back to 1927 [172]. 4,5-Dimethylthio-1,3-dithiole-2-thione (Me_2dmit), which is formed by chemical reduction of CS_2 and subsequent methylation, was wrongly seen as the dimethyl ester of tetrathio-oxalic acid because of similar elemental analyses. There is even a patent in 1973 which claims the preparation of tetrathio-oxalate [173]. The reduction was repeated using different reductants and media (e.g. electrochemically in DMF [174]). In all these cases, the dimethylthioether Me_2dmit was formed instead of ttoMe$_2$. In 1981 Lodmell et al. proved by HPLC that tto is indeed formed during the electroreduction of CS$_2$ [175]. The preparation is surprisingly simple: the important factors are the solvent, the CS$_2$ concentration, the supporting electrolyte and the cathode material. Use acetonitrile instead of the commonly used DMF, Et$_4$NBr or KI instead of Bu$_4$NX, and a mercury pool electrode, and it can be prepared. After applying a potential slightly more negative than the reduction potential of CS$_2$ (−1.15 V vs. SCE) the corresponding $C_2S_4^{2-}$ salt is formed and precipitates, thus possibly preventing undesired follow-up reactions. The Et$_4$N$^+$ salt can be purified by reprecipitation from concentrated aqueous solution by acetone. The orange crystals can be stored for a long time if moisture is excluded [5,10,176]. For organic follow-up reactions see, e.g., [5]. The X-ray structure of $(Ph_4P)_2C_2S_4 \cdot 6H_2O$ (crystallized from water) shows that the dianion of tto is far from being planar [10]. The dihedral angle between the two CS$_2$ units is 79.5° (±1.0°). This is analogous to potassium 1,2-dithio-oxalate (76.5°). The C—C bond length (1.46 Å) is noticeably shorter than in the other thio-oxalates and oxalate (1.55–1.58 Å) (see Table 1). Tetrathio-oxalate can act as a multisulphur bridging ligand with electron delocalization capacity. So far, five types of tetrathio-oxalate complexes are known (see Table 16).

Polymeric complexes. Deeply coloured precipitates are formed from aqueous solutions of $(Et_4N)_2C_2S_4$ after adding heavy metal ions. With M^{2+} ions, the materials obtained are insoluble in common solvents, non-melting up to 300°C and obviously polymeric. Their metal-to-ligand ratio roughly corresponds to a 1:1 composition [177–181]. Obtained from aqueous solutions [182], or from methanol or methanol–DMF solutions under anaerobic conditions [183,184], polymeric (or oligomeric) tetrathio-oxalates [M(tto)]$_n$ (M = Cu, Ni, Pd, Pt) and {A[M(tto)]}$_n$ (M = Cu(I); A = Na$^+$, Et$_4$N$^+$) display typical semiconducting behaviour with pressed-pellet conduc-

TABLE 16

Tetrathio-oxalate complexes

Compound	M.p. (°C)	Colour	Electronic spectra $\bar{\nu}_{max}$ (10^{-3} cm^{-1}) (ε_0)	Ref.
$[(Ph_3P)_2Cu]_2(tto)$	212–215	Blue	15.9 (11700)	177,178,188
$[(Ph_3P)_2Ag]_2(tto)$	115–118	Red–brown	20.8 (9000)	177,178
$[(Ph_3P)_2Au]_2(tto)$	157–160	Light brown		177,178
$[(Ph_3P)_2Rh]_2(tto)$	142–143	Dark brown		44
$\{Cu[(tto)Cu(PPh_3)_2]_2\}$	184–187	Blue	15.5 (5500)	177,178,191
$\{Ni[(tto)Cu(PPh_3)_2]_2\}$	162–165	Violet	18.7 (18600)	177,178,191
$\{Zn[(tto)Cu(PPh_3)_2]_2\}$	181–184	Blue		177,178,191
$\{Pd[(tto)Cu(PPh_3)_2]_2\}$	203–207	Black	25.1 (16800)	177,178,191
$\{VO[(tto)Cu(PPh_3)_2]_2\}$	145–147	Blue–black		44
$\{Ni[(tto)Ag(PPh_3)_2]_2\}$	125–128	Dark brown		190
$\{Fe[(tto)Cu(PPh_3)_2]_3\}$	173–176	Blue	16.5 (15000)	177,178,191

tivities in the 10^{-1}–10^{2} Ω^{-1} cm^{-1} range. Recently, Jolly and Reynolds published the preparation of the first semiconducting and optically polarizing poly(nickel tetrathio-oxalate)/poly(vinyl alcohol) composites made by the reaction of tetrathio-oxalate with nickel ions in a poly(vinyl alcohol) matrix [185]. Structural data on the $[M(tto)]_n$ powders have been obtained by the large angle X-ray scattering technique (LAXS) [184]. Polymeric ethenetetrathiolates have been prepared and found to be non-stoichiometric [186].

Mononuclear complexes. In the presence of a large excess of precipitating cation and with very slow addition of metal salt solution, mononuclear anionic complexes can be isolated [187].

Binuclear complexes. By treating aqueous solutions of tto with dichloromethane, solutions of $(Ph_3P)_3MCl$ (M = Cu, Ag, Rh) deeply coloured tto-bridged binuclear metal(I) neutral chelates are formed in the organic phase, from which they can be isolated after concentration and subsequent addition of 2-propanol [177–180]. The X-ray structure of $\{[(Ph_3P)_2Cu]_2(C_2S_4)\}$ revealed the first authentic coordination compound containing a real tetrathio-oxalate (C–C bond length 1.531(8) Å) [188] (see Fig. 30).

Coordinatively halfside-saturated $(Ph_3P)_2M^+$ moieties act as "lids", which prevent the formation of polymeric compounds. Starting from tetrathiapentalene-dione (TPD), by incomplete basic hydrolysis in the presence of Cu(II) the compound $(Ph_4As)_2[(C_3OS_4)Cu(\mu\text{-}C_2S_4)Cu(C_3OS_4)]$ can be isolated (see Fig. 31). The C–C bond length of the bridging C_2S_4 unit (1.467(10) Å) [189] does not alone allow a clear decision as to whether the bridging ligand is tto- or ett-like: it is very close to

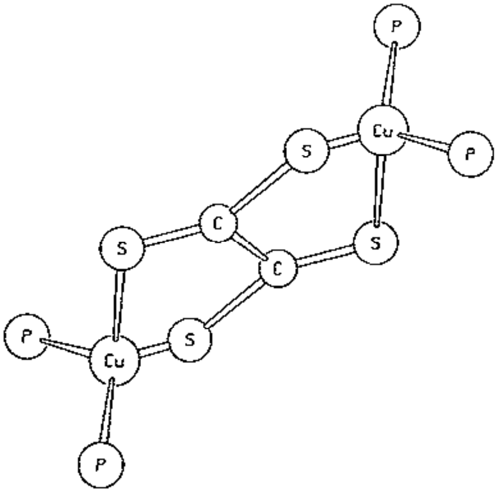

Fig. 30. Molecular structure of $[(Ph_3P)_2Cu(C_2S_4)Cu(PPh_3)_2]$ (phenyl rings omitted) [188].

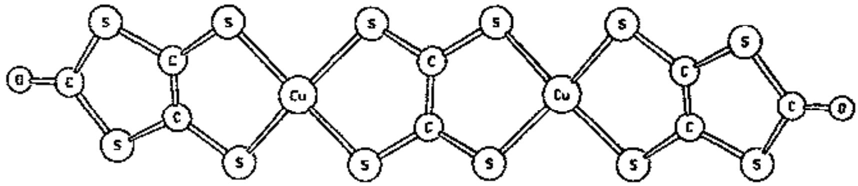

Fig. 31. Structure of the anion in $(Ph_4As)_2[(C_3OS_4)Cu(C_2S_4)Cu(C_3OS_4)]$ [189(b)].

that in $(Ph_4P)_2$(tto) (1.46(2) Å) but markedly shorter than in $\{[(Ph_3P)_2Cu]_2(tto)\}$ (1.53(8) Å) (see Table 15).

Tri- and tetranuclear complexes. Treating the mononuclear complexes with a CH_2Cl_2 solution of $(Ph_3P)_3CuCl$ [178] or $(Ph_3P)_3AgCl$ [190], intensely coloured trinuclear complexes $\{M^{II}[(tto)M^{I}(PPh_3)_2]_2\}$ are formed. The reactive extraction of the wet insoluble material obtained by the reaction between tto and metal ions with solutions of $(Ph_3P)_3MCl$ (in, e.g., CH_2Cl_2) gives complexes identical to those from the previous procedure. $(Ph_3P)_2M^+$ cations probably act not only as "chain-stoppers" but also as "chain-breakers".

Starting with trivalent metal ions (e.g. Fe(III)), tetranuclear complexes $\{M^{III}[(tto)M^{I}(PPh_3)_2]_3\}$ can also be isolated [178]. The tetrathiolate units C_2S_4 (also C_2Se_4) were thoroughly analyzed by several groups from a theoretical MO calculation point of view also including isolobal analogies for the extended system [141,163,164]. Tetrathio-oxalate complexes are intensely coloured with extinction coefficients of the order of 10^4 mol^{-1} cm^{-1} in the visible region, independently of whether they are mono- or oligonuclear or which central metal ion they contain. Many are light-sensitive. Obviously the unit L_2M^I(tto) is responsible for the transition. For instance, $[(PPh_3)_2Cu^I(C_2S_4)Cu^I(PPh_3)_2]$ is deep blue with an absorption band at about 1.5×10^4 cm^{-1}, which is typical of all tto systems with a terminating L_2Cu^+ fragment linked to tto. The results of an extended Hückel calculation for the entity are shown in Fig. 32 [191]. The tto is linked to the CuL_2 fragment via the a_1 and b_2 orbitals. Interaction of the occupied fragment orbital $b_1(d_{xz})$ with the tto lowest unoccupied molecular orbital (LUMO) yields the bonding b_1 MO with mainly metal character. The remaining four d orbitals of the metal interact only weakly with the occupied tto orbitals and are, therefore, only slightly destabilized. The typical absorption mentioned above is thus caused by a transition from the d block to the b_1 LUMO and is of metal-to-tto charge-transfer type.

(d) Related ligand systems containing the C_2S_4 core

Apart from tetrathio-oxalate and its dimethyl ester, several other sulphur ligands have a C_2S_4 building block. The coordination chemistry of these ligand systems would require at least one review to itself. There are close relations as well

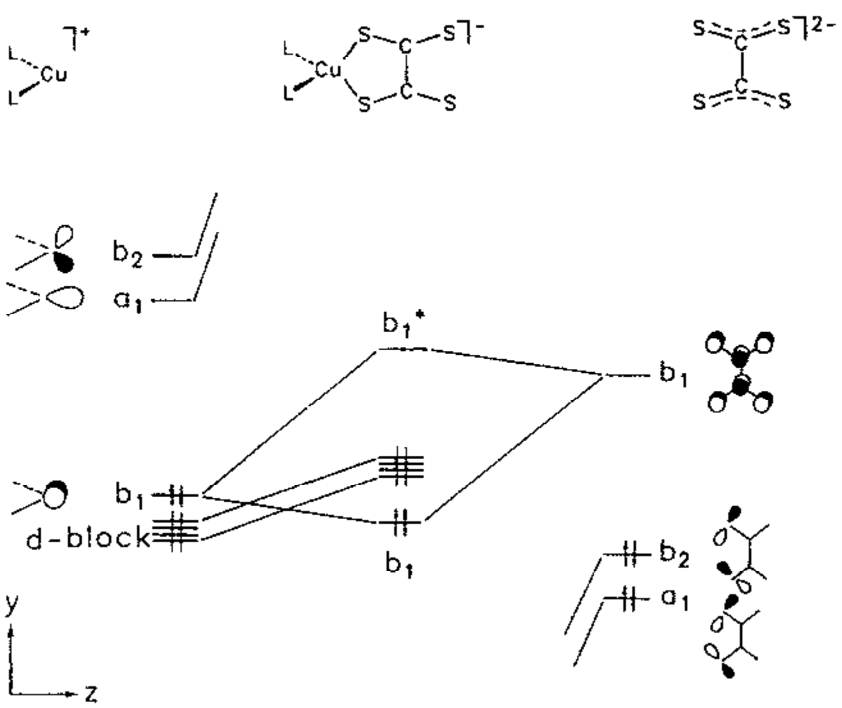

Fig. 32. Qualitative orbital interaction diagram of d^{10}-ML_2 fragments with $C_2S_4^{2-}$ (C_{2v} symmetry) [191].

as significant differences in structure and topology between these “non-oxalate” systems and tetrathio-oxalate. Therefore some characteristic compounds should be mentioned, without any claim of completeness.

Ethenetetrathiolate (ett), the reduced tetrathio-oxalate, has a coordination chemistry very close to that of tetrathio-oxalate and its esters. Obviously, sharp differentiation between tto and ett is difficult. Most of the published complexes containing a bridging head-to-head coupled C_2S_4 ligand are in fact ett complexes with a formal $C_2S_4^{4-}$ moiety and an unambiguous C—C double bond (see Table 14) [157–164, 167–170, 186,189,192]. Lappert and co-workers [193,194] and Abel et al. [195] reported a series of compounds with ethenetetrathiolate derivatives as ligands.

The dianions 1,4-dithiin-2,3-dithiolate (DDT) [196,197] and 5,6-dihydro-1,4-dithiin-2,3-dithiolate (DDDT) [198–210], which are cyclic analogues of Me_2ett, and a follow-up product of tetrathio-oxalate during the reductive dimerization of excess CS_2, 1,3-dithiole-2-thione-4,5-dithiolate (dmit) [211], also contain a C_2S_4 unit with a C—C double bond. All these ligands show typical dithiolene behaviour and an extensive coordination chemistry, and have attracted the attention of numerous laboratories by virtue of their solid state properties.

Tetrathiofulvalene (TTF), as part of the classic organic superconductor TTF–TCNQ, stimulated this development of chalcogen rich (S, Se, Te) systems, but its ligand behaviour is far from that of tetrathio-oxalate (see, e.g., [212] and references therein).

Finally, the coordination chemistry of the thio-oxalates is related to that of thiosquarates [213–229] and tetrachalcogeno metalates [230–232], with a more or less rigid planar or tetrahedral arrangement, respectively, preventing the flexibility found for thio-oxalates in their complexes.

ACKNOWLEDGEMENTS

We thank Mrs. Hannelore Morgner, Mrs. Ingeborg Krüger and Dr. Rhett Kempe for their help in the preparation of the manuscript.

REFERENCES

1 H. Kolbe and E. Drechsel, Justus Liebigs Ann. Chem., 146 (1868) 140.
2 H.O. Jones and H.S. Tasker, J. Chem. Soc., 95 (1909) 1904.
3 E.G. Cox, W. Wardlaw and K.C. Webster, J. Chem. Soc., (1935) 1475.
4 W. Thiel and R. Mayer, Sulfur Rep., 8 (1988) 1.
5 P. Jeroschewski and P. Hansen, Sulfur Rep., 7 (1986) 1.
6 D.J. Hodgson and J.A. Ibers, Acta Crystallogr. Sect. B, 25 (1969) 469; see also H. Küppers, Acta Crystallogr. Sect. B, 29 (1973) 318.
7 R. Mattes and W. Meschede, Chem. Ber., 109 (1976) 1832.
8 R. Mattes, W. Meschede and W. Stork, Chem. Ber., 108 (1975) 1.
9 W. Meschede and R. Mattes, Chem. Ber., 109 (1976) 2510.
10 H. Lund, E. Hoyer and R. Grønbaek-Hazell, Acta Chem. Scand. Ser. B, 36 (1982) 207.
11 U. Niemer and R. Mattes, Chem. Ber., 111 (1978) 2118.
12 R. Mattes, W. Meschede and U. Niemer, Chem. Ber., 110 (1977) 2584.
13 C. Matz and R. Mattes, Z. Naturforsch. Teil B, 33 (1978) 461.
14 (a) R.G. Delaplane and J.A. Ibers, Acta Crystallogr. Sect. B, 25 (1969) 2423.
(b) T.M. Sabine, G.W. Cox and B.M. Craven, Acta Crystallogr. Sect. B, 25 (1969) 2437.
15 W. Stork and R. Mattes, Angew. Chem., 87 (1975) 452.
16 M. Leitheiser and D. Coucouvanis, J. Inorg. Nucl. Chem., 39 (1977) 811.
17 R.G. Pearson and P. Ellgen, Inorg. Chem., 6 (1967) 1379.
18 P. Jeroschewski, Z. Chem., 21 (1981) 412.
19 (a) W. Dietzsch, A. Mewes and E. Hoyer, Z. Chem., 28 (1988) 341.
(b) W. Dietzsch, L. Golič, A. Mewes and E. Hoyer, Proc. Conf. Coord. Chem., 12th, Smolenice, Bratislava, 1989, p. 85
(c) R.-M. Olk, W. Dietzsch, L. Golič, R. Kirmse, J. Reinhold, J. Sieler, P. Strauch and E. Hoyer, Proc. Int. Conf. Coord. Chem., 26th, Porto, 1988, Poster B127.
(d) P. Strauch, W. Dietzsch, K. Trübenbach, L. Golič, A. Franke and E. Hoyer, Proc. Int. Conf. Coord. Chem., 28th, 1990, Gera, P 6–30.
(e) P. Strauch, W. Dietzsch, L. Golič, J. Sieler, A. Franke, I. Münzberg, K. Trübenbach, R. Kirmse, J. Reinhold and E. Hoyer, manuscript in preparation.
(f) I. Münzberg, Diploma work, University of Leipzig, 1990.
(g) P. Strauch, I. Münzberg, W. Dietzsch and R. Kirmse, Z. Anorg. Allg. Chem., 613 (1992) 119.
20 A.E. Martell and R.J. Motekaitis, J. Am. Chem. Soc., 110 (1988) 8059.

21 K. Mennemann and R. Mattes, J. Chem. Res., Miniprint, (1979) 1343.
22 T. Shibahara, S. Ooi and H. Kuroya, Bull. Chem. Soc. Jpn., 55 (1982) 3742.
23 G.J. Kruger, E.L.J. Breet and R. van Eldik, Inorg. Chim. Acta, 19 (1976) 151.
24 K. Zhou, J. Huang and J. Lu, Jiegou Huaxue (Struct. Chem.), 2 (1983) 269.
25 H. Weber and R. Mattes, Chem. Ber., 112 (1979) 95.
26 R. Mattes and H. Weber, Z. Anorg. Allg. Chem., 474 (1981) 216.
27 D. Coucouvanis and D. Piltingsrud, J. Am. Chem. Soc., 95 (1973) 5556.
28 D. Coucouvanis, N.C. Baenziger and S.M. Johnson, J. Am. Chem. Soc., 95 (1973) 3875.
29 M. Leitheiser and D. Coucouvanis, Inorg. Chem., 16 (1977) 1611.
30 R. Czernuszewicz, D.P. Strommen and K. Nakamoto, Inorg. Chim. Acta, 34 (1979) L211.
31 R.S. Czernuszewicz, K. Nakamoto and D.P. Strommen, J. Am. Chem. Soc., 104 (1982) 1515.
32 F.J. Hollander and D. Coucouvanis, Inorg. Chem., 13 (1974) 2381.
33 F.J. Hollander, M. Leitheiser and D. Coucouvanis, Inorg. Chem., 16 (1977) 1615.
34 C.J. Weschler, J.C. Sullivan and E. Deutsch, J. Am. Chem. Soc., 95 (1973) 2720.
35 C.J. Weschler, J.C. Sullivan and E. Deutsch, Inorg. Chem., 13 (1974) 2360.
36 J.D. Lydon, K.J. Mulligan, R.C. Elder and E. Deutsch, Inorg. Chem., 19 (1980) 2083.
37 G.J. Gainsford, W.G. Jackson and A.M. Sargeson, Aust. J. Chem., 33 (1980) 707.
38 K. Mennemann and R. Mattes, Angew. Chem., 89 (1977) 269.
39 K. Mennemann and R. Mattes, J. Chem. Res., Miniprint, (1979) 1372.
40 Z. Chen, J.Z. Zhang, J.M. Shen and S.L. Ding, Proc. Int. Conf. Coord. Chem., 25th, Nanjing, 1987, p. 338.
41 W. Dietzsch, N. Bulc, L. Golič and J. Šiftar, Z. Chem., 21 (1981) 269.
42 N.B. Kalinichenko, L.E. Kordonskij, V.K. Belyaeva, I.N. Marov, E. Hoyer and W. Dietzsch, Zh. Neorg. Khim., 35 (1990) 1237.
43 R. Mattes, W. Stork and J. Kahlenberg, Spectrochim. Acta Part A, 33 (1977) 643.
44 A. Müller, Diploma work, University of Leipzig, 1985.
45 L. Golič, N. Bulc and W. Dietzsch, Polyhedron, 2 (1983) 1201.
46 (a) W.C. Trogler, in A.B.P. Lever (Ed.), Excited States and Reactive Intermediates — Photochemistry, Photophysics and Electrochemistry, ACS Symp. Ser. 307, Washington, DC, 1986, pp. 177–196.
(b) R.L. Cowan, D.B. Pourreau, A.L. Rheingold, S.J. Geib and W.C. Trogler, Inorg. Chem., 26 (1987) 259.
47 D. Coucouvanis, in A. Müller and E. Diemann (Eds.), Transition Met. Chem., Proc. Workshop, 1980, Verlag Chemie, Weinheim, 1981, pp. 59–87.
48 G. Kiel, M. Dräger and U. Reuter, Chem. Ber., 107 (1974) 1483.
49 M.A. Pellinghelli, A. Tiripicchio and M. Tiripicchio Camellini, Cryst. Struct. Commun., 3 (1974) 159.
50 L. Golič, N. Bulc and W. Dietzsch, Inorg. Chem., 21 (1982) 3560.
51 T. Imamura, M. Ryan, G. Gordon and D. Coucouvanis, J. Am. Chem. Soc., 106 (1984) 984.
52 M.G. Kanatzidis, N.C. Baenziger and D. Coucouvanis, Inorg. Chem., 24 (1985) 2680.
53 A. Gleizes and M. Verdaguer, J. Am. Chem. Soc., 106 (1984) 3727.
54 L. Golič, N. Bulc and W. Dietzsch, Acta Crystallogr. Sect. C, 42 (1986) 811.
55 S.F. Colmanet and M.F. Mackay, Inorg. Chim. Acta, 147 (1988) 173.
56 U. Abram, R. Münze, R. Kirmse, K. Köhler, W. Dietzsch and L. Golič, Inorg. Chim. Acta, 169 (1990) 49.
57 L. Qian, P. Singh, H.K. Ro and W.E. Hatfield, Inorg. Chem., 29 (1990) 761.
58 K.R. Butler and M.R. Snow, Inorg. Nucl. Chem. Lett., 8 (1972) 541; Acta Crystallogr. Sect. B, 31 (1975) 354.

59 F. Maury and A. Gleizes, Inorg. Chim. Acta, 41 (1980) 185.

60 A. Gleizes, F. Clery, M.F. Bruniquel and P. Cassoux, Inorg. Chim. Acta, 37 (1979) 19.

61 A. Gleizes, F. Maury and J. Galy, Nouv. J. Chim., 8 (1984) 521.

62 A. Gleizes, F. Maury, P. Cassoux and J. Galy, Z. Kristallogr., 155 (1981) 293.

63 J.C. Trombe, A. Gleizes and J. Galy, C. R. Acad. Sci., 294–II (1982) 1369.

64 J.C. Trombe, A. Gleizes and J. Galy, Inorg. Chim. Acta, 87 (1984) 129.

65 C. Frasse, J.C. Trombe, A. Gleizes and J. Galy, C. R. Acad. Sci., 300–II (1985) 403.

66 J.C. Trombe, C. Frasse and A. Gleizes, C. R. Acad. Sci., 301–II (1985) 483.

67 J.C. Trombe, A. Gleizes and J. Galy, C. R. Acad. Sci., 302–II (1986) 21.

68 J.C. Trombe, A. Gleizes, F. Dahan and J. Galy, C. R. Acad. Sci., 303–II (1986) 907.

69 J.C. Trombe, A. Gleizes and J. Galy, Nouv. J. Chim., 9 (1985) 55; see also GIT Fachz. Lab., 31 (1987) 89.

70 A. Gleizes and M. Verdaguer, J. Am. Chem. Soc., 103 (1981) 7373.

71 P.D.W. Boyd, J. Hope, C.L. Raston and A.H. White, Aust. J. Chem., 43 (1990) 601.

72 F. Maury, A. Gleizes and J. Galy, C. R. Acad. Sci., Ser. C, 291 (1980) 49.

73 R. Enjalbert, A. Gleizes, J.C. Trombe, M.L. Gutiérrez-Campo and P. Román, J. Mol. Struct., 131 (1985) 1.

74 (a) P. Román, C. Bao, J.M. Gutiérrez-Zorilla and A. Vegas, J. Crystallogr. Spectrosc. Res., 18 (1988) 207.
(b) P. Román, J.M. Gutiérrez-Zorilla, A. Luque, J.I. Beitia, C. Guzmán-Miralles and M. Martinez-Ripoll, Acta Crystallogr. Sect. C, 47 (1991) 48.

75 J.C. Trombe, A. Gleizes and J. Galy, C. R. Acad. Sci., 300-II (1985) 5.

76 J.M. Gutiérrez-Zorilla López, P. Román and A. Gleizes, C. R. Acad. Sci., 305-II (1987) 1353.

77 (a) C. Bellitto, M. Bonamico, V. Fares, P. Imperatori and S. Patrizio, J. Chem. Soc. Dalton Trans., (1989) 719.
(b) P. Delhaes and M. Drillon (Eds.), Organic and Inorganic Low-Dimensional Crystalline Materials, NATO Adv. Study Inst. Ser. Ser. B, Vol. 168, Plenum, New York, 1987, p. 337.

78 M. Verdaguer, A. Gleizes, J.P. Renard and J. Seiden, Phys. Rev. B, 29 (1984) 5144.

79 J.D. Forrester, A. Zalkin and D.H. Templeton, Inorg. Chem., 3 (1964) 1507.

80 D. Coucouvanis, F.J. Hollander and M.L. Caffery, Inorg. Chem., 15 (1976) 1853.

81 R. Eisenberg, Prog. Inorg. Chem., 12 (1970) 295.

82 C. Mahadevan, J. Crystallogr. Spectrosc. Res., 16 (1986) 347.

83 O. Kahn, Proc. Indian Acad. Sci. Chem. Sci., 98 (1987) 33.

84 C.S. Robinson and H.O. Jones, J. Chem. Soc., 101 (1912) 62.

85 L.K. White and R.L. Belford, J. Am. Chem. Soc., 98 (1976) 4428.

86 R.G. Pearson and D.A. Sweigart, Inorg. Chem., 9 (1970) 1167.

87 B. Folkesson and B. Jonson, J. Electron Spectrosc. Relat. Phenom., 34 (1984) 319.

88 D. Coucouvanis, J. Am. Chem. Soc., 93 (1971) 1786.

89 A.R. Latham, V.C. Hascall and H.B. Gray, Inorg. Chem., 4 (1965) 788.

90 R. Kirmse, W. Dietzsch, J. Stach, R.-M. Olk and E. Hoyer, Z. Anorg. Allg. Chem., 548 (1987) 133.

91 R.L. Carlin and F. Canziani, J. Chem. Phys., 40 (1964) 371.

92 F.P. Dwyer and A.M. Sargeson, J. Am. Chem. Soc., 81 (1959) 2335.

93 J. Hidaka and B.E. Douglas, Inorg. Chem., 3 (1964) 1724.

94 (a) D. Coucouvanis, A. Toupadakis and A. Hadjikyriacou, Inorg. Chem., 27 (1988) 3272.
(b) D. Coucouvanis, A. Toupadakis, Sang-Man Koo and A. Hadjikyriacou, Polyhedron, 8 (1989) 1705.

95 A. Davison, C. Orvig, H.S. Trop, M. Sohn, B.V. DePamphilis and A.G. Jones, Inorg. Chem., 19 (1980) 1988.

96 D. Coucouvanis, R.E. Coffman and D. Piltingsrud, J. Am. Chem. Soc., 92 (1970) 5004.
97 T. Birchall and K.M. Tun, Inorg. Chem., 15 (1976) 376.
98 D. Niarchos, A. Kostikas, A. Simopoulus, D. Coucouvanis, D. Piltingsrud and R.E. Coffman, J. Chem. Phys., 69 (1978) 4411.
99 W.V. Sweeney and R.E. Coffman, J. Phys. Chem., 76 (1972) 49.
100 R.G. Kooser, J. Phys. Chem., 80 (1976) 1601.
101 W.V. Sweeney, D. Coucouvanis and R.E. Coffman, J. Chem. Phys., 59 (1973) 369.
102 R.E. DeSimone, J. Am. Chem. Soc., 95 (1973) 6238.
103 K. Kanamori, A. Ono, S. Ino, I. Kanesaka, K. Kawai and J. Hidaka, Bull. Chem. Soc. Jpn., 62 (1989) 2720.
104 H. Hennig, W. Kumpf, K. Jurdeczka and R. Benedix, J. Prakt. Chem., 319 (1977) 444.
105 S. Kida, K. Nakamoto and R. Tsuchida, Nippon Kagaku Zasshi, 72 (1951) 749.
106 J. Fujita and K. Nakamoto, Bull. Chem. Soc. Jpn., 37 (1964) 528.
107 G.A. Bowmaker, P.D.W. Boyd and G.K. Campbell, Inorg. Chem., 21 (1982) 3565.
108 D. Coucouvanis, J. Am. Chem. Soc., 92 (1970) 707.
109 G.A. Bowmaker, P.D.W. Boyd and G.K. Campbell, Inorg. Chem., 21 (1982) 2403.
110 S. Kida, Bull. Chem. Soc. Jpn., 33 (1960) 1204.
111 N. Maki, S. Kida and R. Tsuchida, Bull. Chem. Soc. Jpn., 32 (1959) 573.
112 R.G. Pearson and M.J. Hynes, J. Coord. Chem., 1 (1971) 245.
113 S.A. Cotton and J.F. Gibson, J. Chem. Soc. A, (1971) 803.
114 (a) A.R. Butler, C. Glidewell and M.-H. Li, Adv. Inorg. Chem., 32 (1988) 335.
(b) J.A. McCleverty, N.M. Atherton, J. Locke, E.J. Wharton and C.J. Winscom, J. Am. Chem. Soc., 89 (1967) 6082.
(c) G.R. Davies, J.A.J. Jarvis, B.T. Kilbourn, R.H.B. Mais and P.G. Owston, J. Chem. Soc. A, (1970) 1275.
115 J. Stach, R. Kirmse, W. Dietzsch, R.-M. Olk, L. Golič and N. Bulc, manuscript in preparation.
116 J. Stach, R. Kirmse, A. Heinrich, W. Dietzsch, J. Hartung and L. Beyer, Z. Chem., 23 (1983) 453.
117 S. Sakaguchi and A.W. Addison, J. Am. Chem. Soc., 99 (1977) 5189.
118 W. Dietzsch, J. Reinhold, R. Kirmse, E. Hoyer, I.N. Marov and V.K. Belyaeva, J. Inorg. Nucl. Chem., 39 (1977) 1377.
119 W.A. Deskin, J. Am. Chem. Soc., 80 (1958) 5680.
120 C.K. Jørgensen, J. Inorg. Nucl. Chem., 24 (1962) 1571.
121 T.N. Lockyer and R.L. Martin, Prog. Inorg. Chem., 27 (1980) 223.
122 A.J. McCaffery, S.F. Mason and R.E. Ballard, J. Chem. Soc., (1965) 2883.
123 J.A. McCleverty, Prog. Inorg. Chem., 10 (1968) 49.
124 E. Hoyer, W. Dietzsch and W. Schroth, Z. Chem., 11 (1971) 41.
125 F.N. Lecrone, M.J. Minot and J.H. Perlstein, Inorg. Nucl. Chem. Lett., 8 (1972) 173.
126 T.W. Thomas, C. Hsu, M.M. Labes, P.S. Gomm, A.E. Underhill and D.M. Watkins, J. Chem. Soc. Dalton Trans., (1972) 2050.
127 Agency of Industrial Sciences and Technology, Jpn. Kokai Tokkyo Koho, JP 57 154 239 [82 154 239]; Chem. Abstr., 99 (1983) 203 629d.
128 Agency of Industrial Sciences and Technology, Jpn. Kokai Tokkyo Koho, JP 58 200 234 [83 200 234]; Chem. Abstr., 100 (1984) 148 635q.
129 (a) F. Basolo, Adv. Chem. Ser., 49 (1965) 81.
(b) R.G. Pearson and M.J. Hynes, K. Tek. Hoegsk. Handl., (248–296) (1972) 459.
130 L.T. Fairhall, J. Ind. Hyg., 8 (1926) 528.
131 J.H. Yoe and F.H. Wirsing, J. Am. Chem. Soc., 54 (1932) 1866.

132 F.J. Welcher, Organic Analytical Reagents, Vol. IV, Van Nostrand, New York, 1955, p. 142.

133 H. Matsunaga and T. Yotsuyanagi, Nippon Kagaku Kaishi, (1982) 785.

134 H. Matsunaga and T. Yotsuyanagi, Bunseki Kagaku, 31 (1982) 289.

135 A. Mewes, Diploma work, University of Leipzig, 1988.

136 F. Estevan, P. Lahuerta and I. Solana, Polyhedron, 4 (1985) 1965.

137 D.D. Heinrich, J.P. Fackler, Jr. and P. Lahuerta, Inorg. Chim. Acta, 116 (1986) 15.

138 D. Coucouvanis, N.C. Baenziger and S.M. Johnson, Inorg. Chem., 13 (1974) 1191.

139 F.J. Hollander, Y.L. Ip and D. Coucouvanis, Inorg. Chem., 15 (1976) 2230.

140 J.M. Charnock, S. Bristow, J.R. Nicholson, C.D. Garner and W. Clegg, J. Chem. Soc. Dalton Trans., (1987) 303.

141 S. Alvarez, R. Vicente and R. Hoffmann, J. Am. Chem. Soc., 107 (1985) 6253.

142 (a) J.M. Williams, H.H. Wang, T.J. Emge, U. Geiser, M.A. Beno, P.C.W. Leung, K.D. Carlson, R.J. Thorn, A.J. Schultz and M.-H. Whangbo, Prog. Inorg. Chem., 35 (1987) 51.
(b) P. Cassoux, L. Valade, H. Kobayashi, A. Kobayashi, R.A. Clark and A.E. Underhill, Coord. Chem. Rev., 110 (1991) 115.

143 H. Werner, O. Kolb, R. Feser and U. Schubert, J. Organomet. Chem., 191 (1980) 283.

144 M. Cowie and S.K. Dwight, J. Organomet. Chem., 214 (1981) 233.

145 (a) J.A. Ibers, Chem. Soc. Rev., 11 (1982) 57.
(b) M.G. Mason, P.N. Swepston and J.A. Ibers, Inorg. Chem., 22 (1983) 411.

146 (a) E. Carmona, J. Organomet. Chem., 358 (1988) 283.
(b) E. Carmona, J. Cámpora, M.A. Muñoz, M. Paneque and M.L. Poveda, Pure Appl. Chem., 61 (1989) 1701.
(c) E. Carmona, A. Galindo, A. Monge, M.A. Muñoz, M.L. Poveda and C. Ruiz, Inorg. Chem., 29 (1990) 5074.

147 S.J.N. Burgmayer and J.L. Templeton, Inorg. Chem., 24 (1985) 3939.

148 S. Myrvold, O.A. Nassif, G. Semelhago, A. Walker and D.H. Farrar, Inorg. Chim. Acta, 117 (1986) 17.

149 C. Bianchini, C.A. Ghilardi, A. Meli, S. Midollini and A. Orlandini, J. Chem. Soc. Chem. Commun., (1983) 545.

150 (a) H.G. Raubenheimer, J.C. Viljoen, S. Lotz, A. Lombard and G. Kruger, J. Chem. Soc. Chem. Commun., (1981) 749.
(b) H.G. Raubenheimer, S. Lotz, G.J. Kruger, A. van A. Lombard and J.C. Viljoen, J. Organomet. Chem., 336 (1987) 349.

151 O. Kolb and H. Werner, J. Organomet. Chem., 268 (1984) 49.

152 M. Ebner and H. Werner, Chem. Ber., 119 (1986) 482.

153 H.P. Fritz, G. Müller, G. Reber and M. Weis, Angew. Chem., 97 (1985) 1057.

154 C. Bianchini, C.A. Ghilardi, A. Meli, S. Midollini and A. Orlandini, J. Chem. Soc. Chem. Commun., (1983) 753.

155 D.H. Farrar, R.R. Gukathasan and S.A. Morris, Inorg. Chem., 23 (1984) 3258.

156 M.C. Zonnevylle, R. Hoffmann, C. Mealli and C. Bianchini, Gazz. Chim. Ital., 117 (1987) 117.

157 J.J. Maj, A.D. Rae and L.F. Dahl, J. Am. Chem. Soc., 104 (1982) 4278.

158 P.V. Broadhurst, B.F.G. Johnson, J. Lewis and P.R. Raithby, J. Chem. Soc. Chem. Commun., (1982) 140.

159 H.A. Harris, A.D. Rae and L.F. Dahl, J. Am. Chem. Soc., 109 (1987) 4739.

160 D. Touchard, J.-L. Fillaut, P. Dixneuf, C. Mealli, M. Sabat and L. Toupet, Organometallics, 4 (1985) 1684.

161 D. Touchard, J.-L. Fillaut, D.V. Khasnis, P. Dixneuf, C. Mealli, D. Masi and L. Toupet, Organometallics, 7 (1988) 67.

162 C. Bianchini, C. Mealli, A. Meli and M. Sabat, Inorg. Chem., 23 (1984) 4125.

163 C. Bianchini, C. Mealli, A. Meli, M. Sabat and P. Zanello, J. Am. Chem. Soc., 109 (1987) 185.

164 C. Bianchini, C. Mealli, A. Meli and M. Sabat, J. Chem. Soc. Chem. Commun., (1984) 1647.

165 K.A. Jensen and E. Huge-Jensen, Acta Chem. Scand., 27 (1973) 3605.

166 (a) T. Kissel, R. Matusch and K. Hartke, Z. Chem., 16 (1976) 318.
(b) T. Kissel, Ph.D Thesis, Marburg University, 1976.

167 C. Keller, D. Walther, J. Reinhold and E. Hoyer, Z. Chem., 28 (1988) 410.

168 C. Kraffert, D. Walther, K. Peters, O. Lindqvist, V. Langer, J. Sieler, J. Reinhold and E. Hoyer, Z. Anorg. Allg. Chem., 588 (1990) 167.

169 E. Fanghänel and H. Poleschner, J. Prakt. Chem., 323 (1981) 1.

170 C.T. Vance and R.D. Bereman, Inorg. Chim. Acta, 149 (1988) 229.

171 (a) K. Hartke, T. Kissel, J. Quante and G. Henssen, Angew. Chem., 90 (1978) 1016.
(b) K. Hartke, J. Quante and T. Kämpchen, Justus Liebigs Ann. Chem., (1980) 1482.
(c) K. Hartke, T. Kissel, J. Quante and R. Matusch, Chem. Ber., 113 (1980) 1898.

172 B. Fetkenheuer, H. Fetkenheuer and H. Lecus, Chem. Ber., 60 (1927) 2528.

173 H.D. Hartzler, U.S. Pat. 3,717,619; Chem. Abstr., 78 (1973) 137 673b.

174 S. Wawzonek and S.M. Heilmann, J. Org. Chem., 39 (1974) 511.

175 J.C. Lodmell, W.C. Anderson, M.F. Hurley and J.Q. Chambers, Anal. Chim. Acta, 129 (1981) 49.

176 P. Jeroschewski, Z. Chem., 21 (1981) 412.

177 P. Strauch, Diploma work, Leipzig University, 1983.

178 P. Strauch, W. Dietzsch and E. Hoyer, Z. Chem., 23 (1983) 448.

179 E. Hoyer, Comments Inorg. Chem., 2 (1983) 261.

180 E. Hoyer, R.-M. Olk and P. Strauch, in J.J. Ziolkowski (Ed.), Coordination Chemistry and Catalysis, World Scientific, Singapore, 1988, pp. 337–368.

181 J.R. Reynolds, F.E. Karasz, C.P. Lillya and J.C.W. Chien, J. Chem. Soc. Chem. Commun., (1985) 268.

182 P. Jeroschewski, D.Sc. Thesis, Rostock University, 1984.

183 J.R. Reynolds, J.C.W. Chien and C.P. Lillya, Macromolecules, 20 (1987) 1184.

184 (a) T. Vogt, C. Faulmann, R. Soules, P. Lecante, A. Mosset, P. Castan, P. Cassoux and J. Galy, J. Am. Chem. Soc., 110 (1988) 1833.
(b) C.A. Jolly, F. Wang, S. Krichene, J.R. Reynolds, P. Cassoux and C. Faulmann, Synth. Met., 29 (1989) F189.
(c) J.R. Reynolds, C.A. Jolly, S. Krichene, P. Cassoux and C. Faulmann, Synth. Met., 31 (1989) 109.

185 C.A. Jolly and J.R. Reynolds, Chem. Mater., 2 (1990) 479.

186 H. Polescher, W. John, F. Hoppe, E. Fanghänel and S. Roth, J. Prakt. Chem., 325 (1983) 957.

187 P. Strauch, M. Friese and E. Hoyer, Ger. Pat. DD249 908; Chem. Abstr., 108 (1988) 230989g.

188 L.K. Hansen, J. Sieler, P. Strauch, W. Dietzsch and E. Hoyer, Acta Chem. Scand. Ser. A, 39 (1985) 571.

189 (a) J. Ribas, R. Vicente, X. Solans and M. Verdaguer, Proc. Int. Conf. Coord. Chem., 24th, Athens, 1986, p. 436.
(b) R. Vicente, J. Ribas, S. Alvarez, A. Segui, X. Solans and M. Verdaguer, Inorg. Chem., 26 (1987) 4004.

190 P. Strauch, M. Friese, E. Hoyer, Ger. Pat. DD236 089; Chem. Abstr., 106 (1987) 20655c.

191 J. Reinhold, G. Stich, P. Strauch, R. Benedix, J. Sieler and E. Hoyer, Z. Chem., 27 (1987) 29.

192 S. Alvarez, M. Julve and M. Verdaguer, Inorg. Chem., 29 (1990) 4500.

193 (a) B. Cetinkaya, P.B. Hitchcock, M.F. Lappert and P.L. Pye, J. Chem. Soc. Chem. Commun., (1975) 683.
(b) B. Cetinkaya, P.B. Hitchcock, M.F. Lappert, P.L. Pye and D.B. Shaw, J. Chem. Soc. Dalton Trans., (1979) 434.

194 M.F. Lappert, D.B. Shaw and G.M. McLaughlin, J. Chem. Soc. Dalton Trans., (1979) 427.

195 E.W. Abel, K. Kite and B.L. Williams, J. Chem. Soc. Dalton Trans., (1983) 1017.

196 T. Nakamura, T. Nogami and Y. Shirota, Bull. Chem. Soc. Jpn., 60 (1987) 3447.

197 H. Kim, A. Kobayashi, Y. Sasaki, R. Kato, H. Kobayashi, T. Nakamura, T. Nogami and Y. Shirota, Bull. Chem. Soc. Jpn., 61 (1988) 2559.

198 C.T. Vance, R.D. Bereman, J. Bordner, W.E. Hatfield and J.H. Helms, Inorg. Chem., 24 (1985) 2905.

199 H.J. Keller, R. Niebl, D. Nöthe, D. Schweitzer and A. Weber, Physica B, 143 (1986) 301.

200 R. Kato, H. Kobayashi, A. Kobayashi and Y. Sasaki, Bull. Chem. Soc. Jpn., 59 (1986) 627.

201 H. Kim, A. Kobayashi, Y. Sasaki, R. Kato and H. Kobayashi, Bull. Chem. Soc. Jpn., 61 (1988) 579.

202 A.J. Schultz, H.H. Wang, L.C. Soderholm, T.L. Sifter, J.M. Williams, K. Bechgaard and M.-H. Wangbo, Inorg. Chem., 26 (1987) 3757.

203 U. Geiser, A.J. Schultz, H.H. Wang, M.A. Beno and J.M. Williams, Acta Crystallogr. Sect. C, 44 (1988) 259.

204 C.T. Vance and R.D. Bereman, Inorg. Chim. Acta, 149 (1988) 229.

205 J.H. Welch, R.D. Bereman and P. Singh, Inorg. Chem., 27 (1988) 3680.

206 J.H. Welch, R.D. Bereman, P. Singh and C. Moreland, Inorg. Chim. Acta, 158 (1989) 17.

207 J.H. Welch, R.D. Bereman, P. Singh, D. Haase, W.E. Hatfield and M.L. Kirk, Inorg. Chim. Acta, 162 (1989) 89.

208 J.H. Welch, R.D. Bereman and P. Singh, Inorg. Chim. Acta, 163 (1989) 93.

209 C.T. Vance, J.H. Welch and R.D. Bereman, Inorg. Chim. Acta, 164 (1989) 191.

210 (a) S.S. Nagapetyan, V.E. Shklover, L.V. Vetoshkina, A.I. Kotov, L.Yu. Ukhin, Yu.T. Struchkov and E.B. Yagubskii, Mater. Sci., 14 (1988) 5.
(b) E.B. Yagubskii, A.I. Kotov, L.I. Buravov, A.G. Khomenko, V.E. Shklover, S.S. Nahapetyan, Yu.T. Struchkov, L.V. Vetoshkina and L.Yu. Ukhin, Synth. Met., 35 (1990) 271.

211 R.-M. Olk, B. Olk, W. Dietzsch, R. Kirmse and E. Hoyer, Coord. Chem. Rev., 117 (1992) 99.

212 A.R. Siedle, T.J. Kistenmacher, R.M. Metzger, Chiun-Shiung Kuo, R.P. van Duyne and T. Cape, Inorg. Chem., 19 (1980) 2048.

213 D. Coucouvanis, F.J. Hollander, R. West and D. Eggerding, J. Am. Chem. Soc., 96 (1974) 3006.

214 (a) F.J. Hollander and D. Coucouvanis, J. Am. Chem. Soc., 96 (1974) 5646.
(b) F.J. Hollander and D. Coucouvanis, J. Am. Chem. Soc., 99 (1977) 6268.

215 D. Coucouvanis, D.G. Holah and F.J. Hollander, Inorg. Chem., 14 (1975) 2657.

216 D. Coucouvanis, D. Swenson, N.C. Baenziger, D.G. Holah, A. Kostikas, A. Simopoulos and V. Petrouleas, J. Am. Chem. Soc., 98 (1976) 5721.

217 A. Avdeef and J.P. Fackler, Jr., Inorg. Chem., 17 (1978) 2182.

218 D. Altmeppen and R. Mattes, Acta Crystallogr. Sect. B, 36 (1980) 1942.

219 D. Coucouvanis, D. Swenson, N.C. Baenziger, C. Murphy, D.G. Holah, N. Sfarnas, A. Simopoulos and A. Kostikas, J. Am. Chem. Soc., 103 (1981) 3350.

220 P. Arrizabalaga, G. Bernardinelli, P. Castan, M. Geoffroy and R. Soules, C. R. Acad. Sci., 304-II (1987) 559.

221 J.-F. Petit, J.C. Trombe, A. Gleizes and J. Galy, C. R. Acad. Sci., 304-II (1987) 1117.

222 J.-J. Bonnet, P. Cassoux, P. Castan, J.-P. Laurent and R. Soules, Mol. Cryst. Liq. Cryst., 142 (1987) 113.

223 P. Arrizabalaga, G. Bernardinelli, M. Geoffroy and P. Castan, Inorg. Chim. Acta, 154 (1988) 35.

224 R. Krause and R. Mattes, Z. Naturforsch. Teil B, 45 (1990) 490.

225 R. Krause and R. Mattes, Z. Naturforsch. Teil B, 45 (1990) 1457.

226 F. Götzfried, W. Beck, A. Lerf and A. Sebald, Angew. Chem., 91 (1979) 499.

227 P.G. Jones, G.M. Sheldrick, A. Fügner, F. Götzfried and W. Beck, Chem. Ber., 114 (1981) 1413.

228 F. Götzfried, R. Grenz, G. Urban and W. Beck, Chem. Ber., 118 (1985) 4179.

229 R. Grenz, F. Götzfried, U. Nagel and W. Beck, Chem. Ber., 119 (1986) 1217.

230 D. Coucouvanis, Acc. Chem. Res., 14 (1981) 201.

231 A. Müller, E. Diemann, R. Jostes and H. Bögge, Angew. Chem., 93 (1981) 957.

232 A. Müller, H. Bögge, U. Schimanski, M. Penk, K. Nieradzik, M. Dartmann, E. Krickemeyer, J. Schimanski, C. Römer, M. Römer, H. Dornfeld, U. Wienböker, W. Hellmann and M. Zimmermann, Monatsh. Chem., 120 (1989) 367.